



Project Number: DE-FE-0011194

Research Area:

Topic B: High Performance Materials for Long-Term Fossil Energy Applications

SERRATION BEHAVIOR OF HIGH-ENTROPY ALLOYS (HEAs)

Principal Investigator (PI):

Professor Karin A. Dahmen

Department of Physics, University of Illinois at Urbana-Champaign (UIUC)

Co-Principal Investigator (Co-PI):

Professor Peter K. Liaw

Department of Materials Science & Engineering, The University of Tennessee, Knoxville (UTK)

Ph.D. Students: Shuying Chen and Michael LeBlanc

Undergraduate student: Robert Carroll

Research Associate: Drs. Gongyao Wang and Xie Xie

Collaborators: Mingwei Chen¹, Junwei Qiao², Jien Wei Yeh³, Chao-Wei Tsai³, Yong Zhang⁴, M. Laktionova⁵, E.Tabachnikova⁵, Oleg N. Senkov⁶, Michael C. Gao^{7, 8}, Shizhong Yang⁹, and Jonathan T. Uhl¹⁰

1. WPI Advanced Institute for Materials Research, Tohoku University
2. College of Materials Science and Engineering, Taiyuan University of Technology, China
3. Department of Materials Science and Engineering, National Tsing Hua University, Taiwan
4. State Key Laboratory for Advanced Metals and Materials, University of Science and Technology Beijing, 100083, China
5. B.I. Verkin Institute for Low Temperature Physics and Engineering of National Academy of Sciences of Ukraine, Kharkiv 61103, Ukraine
6. Air Force Research Laboratory, Materials and Manufacturing Directorate, OH 45433, USA
7. National Energy Technology Laboratory, Albany, OR 97321, USA
8. USR Corporation, 1450 Queen Ave SW, Albany, OR 97321, USA
- Southern University and A&M College, Baton Rouge LA 70807
10. Private

Acknowledgements

We are very grateful to

- (1) **Jessica Mullen**
- (2) **Steven R. Markovich**
- (3) **Patricia Rawls**
- (4) **Vito Cedro**
- (5) **Richard Dunst**
- (6) **Susan Maley**
- (7) **Robert Romanosky**
- (8) **Conrad Regis**
- (9) **National Energy Technology Laboratory (NETL)**

for sponsoring this project

Outline of Presentation

- **Objectives**
- **Introduction of high-entropy alloys (HEAs) and mean field theory (MFT)**
- **MFT applications and predictions**
- **Experimental results**
- **Conclusions**
- **Published papers and presentations**

Objectives

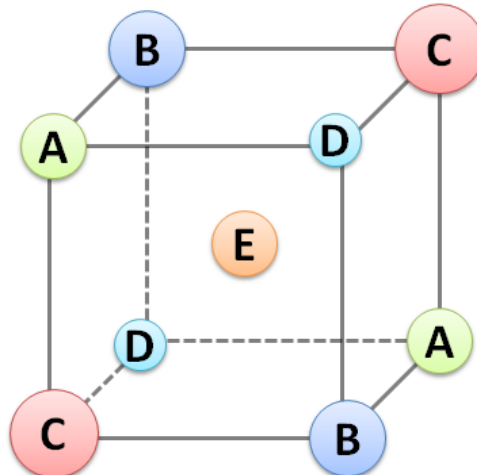
- To provide a fundamental understanding of the serration behavior of high-entropy alloys (HEAs) through
 - ❖ Slip-avalanche modeling
 - ❖ Theoretical analyses
 - ❖ Mechanical experiments
- To reveal the deformation mechanisms of HEAs
- To develop and test serration-based models to predict the mechanical performance and creep behavior for long-term fossil-energy applications of HEAs

Introduction: High-entropy alloys

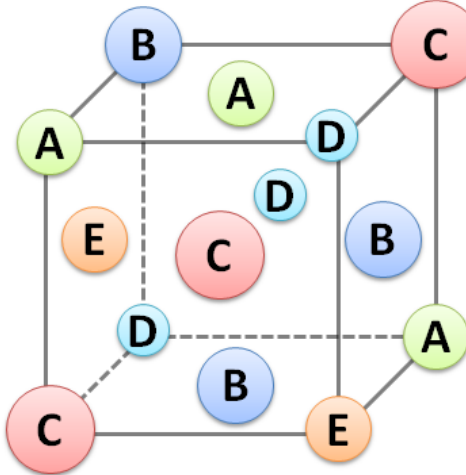
HEAs: typically defined as the alloys that contain five or more principal elements with each element of 5 to 35 atomic percentage or in near-equimolar ratios, possessing a single structure, such as face-centered cubic (FCC), body-centered cubic (BCC), and hexagonal- close-packed (HCP) phase.

$$\text{The Gibbs free energy: } \Delta G_{\text{mix}} = \Delta H_{\text{mix}} - T\Delta S_{\text{mix}}$$

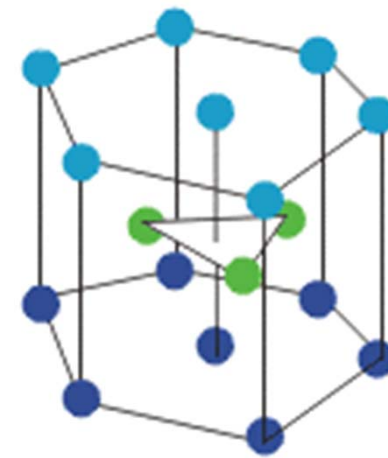
(A) BCC: five principal elements



(B) FCC: five principal elements

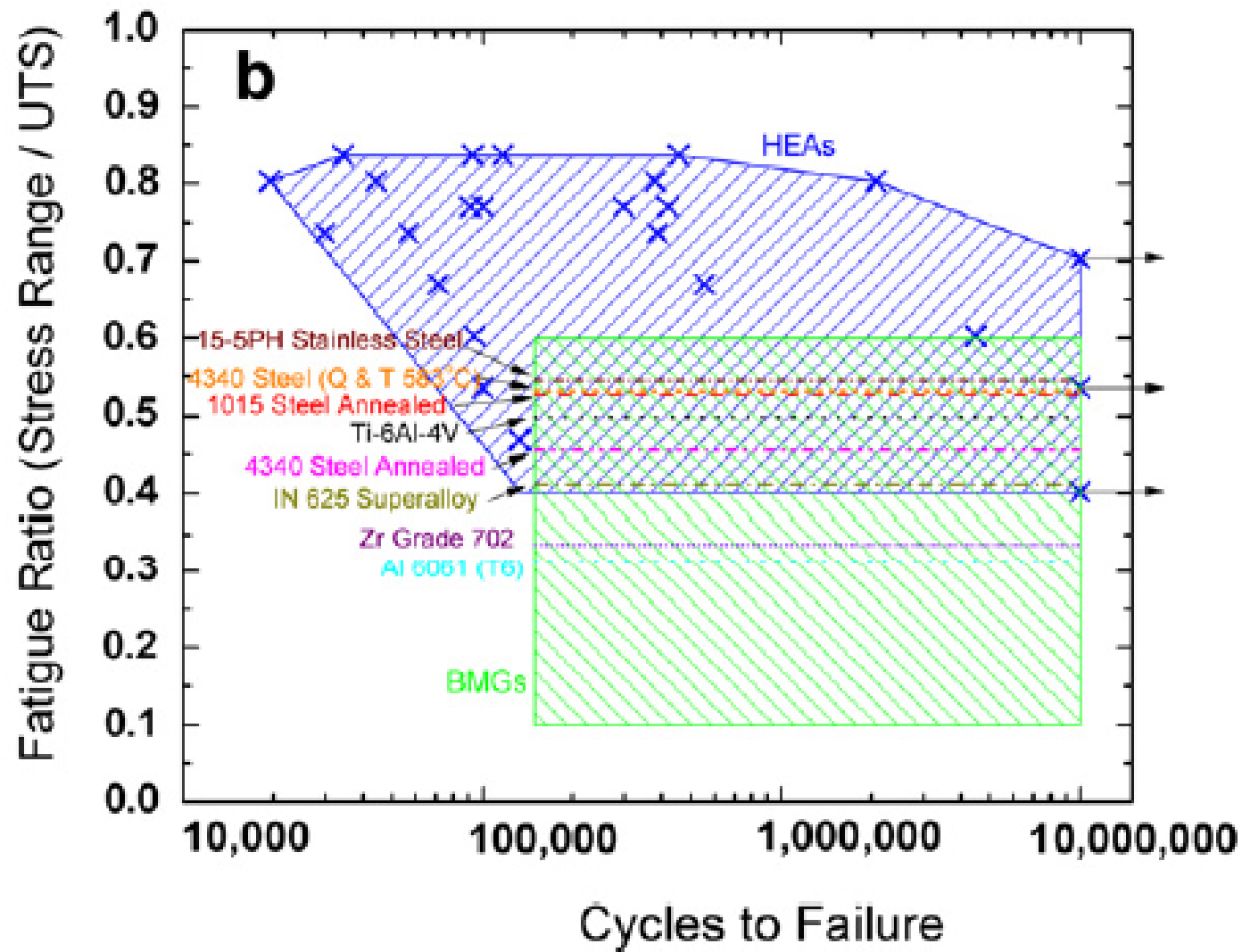


(C) HCP



1. J. W. Yeh, S. Y. Chang, Y. D. Hong, S. K. Chen, S. J. Lin, *Materials Chemistry and Physics* 103 (2007) 41–46.
2. M. C. Gao & D. E. Alman. Searching for Next Single-Phase High-Entropy Alloy Compositions. *Entropy* 15, 4504-4519 (2013).
3. Y. Zhang, T. T. Zuo, Tang, M.C. Gao, K. A. Dahmen, P. K. Liaw, Z. P. Lu, *Progress in Materials Science* 61 (2014) 1–93.
4. L.J. Santodonato, Y. Zhang, M. Feygenson, C. Parish, J. Neuefeind, R.J.R. Weber, M.C. Gao, Z. Tang, P.K. Liaw, *Nature Communications*. 2015, 6: 5964 .
5. B. Cantor, I. T. H. Chang, P. Knight, and A. J. B. Vincent, *Materials Science and Engineering A*, 2004, 375-377, pp. 213-218.
6. K. M. Youssef, A. J. Zaddach, C. Niu, D. L. Irving, and C. C. Koch, *Materials Research Letters*, 2014, pp. 1-5.

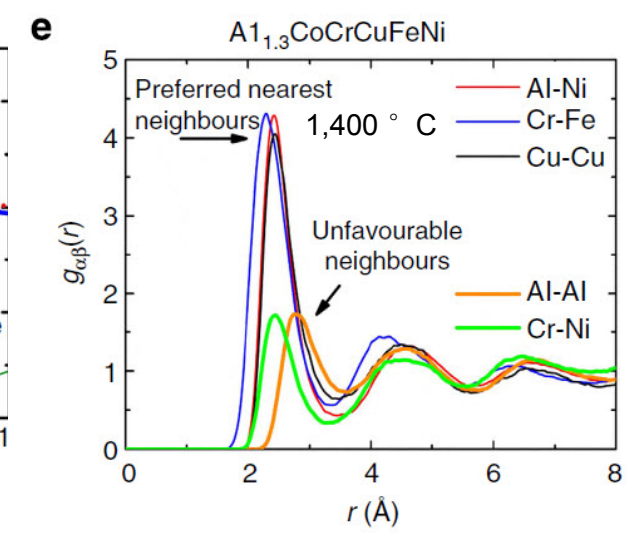
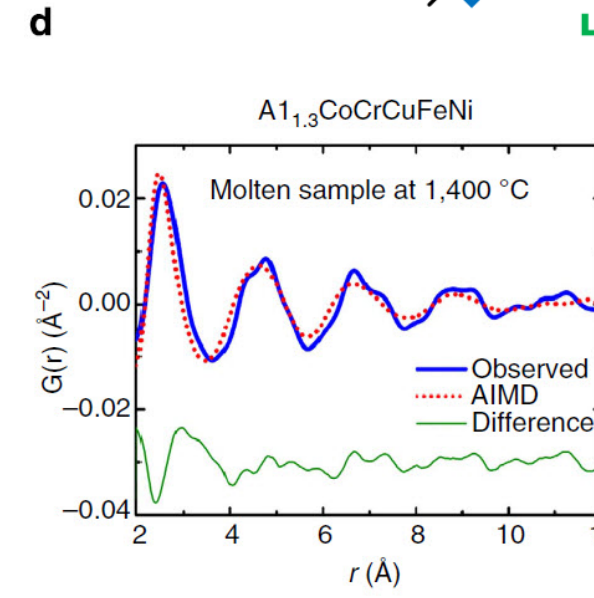
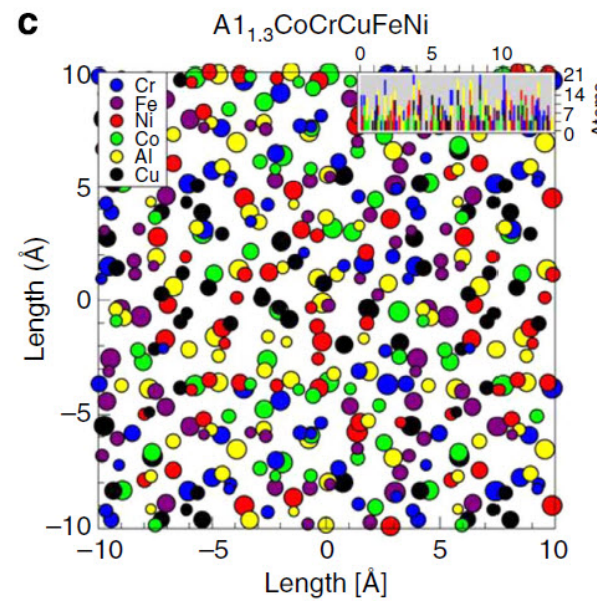
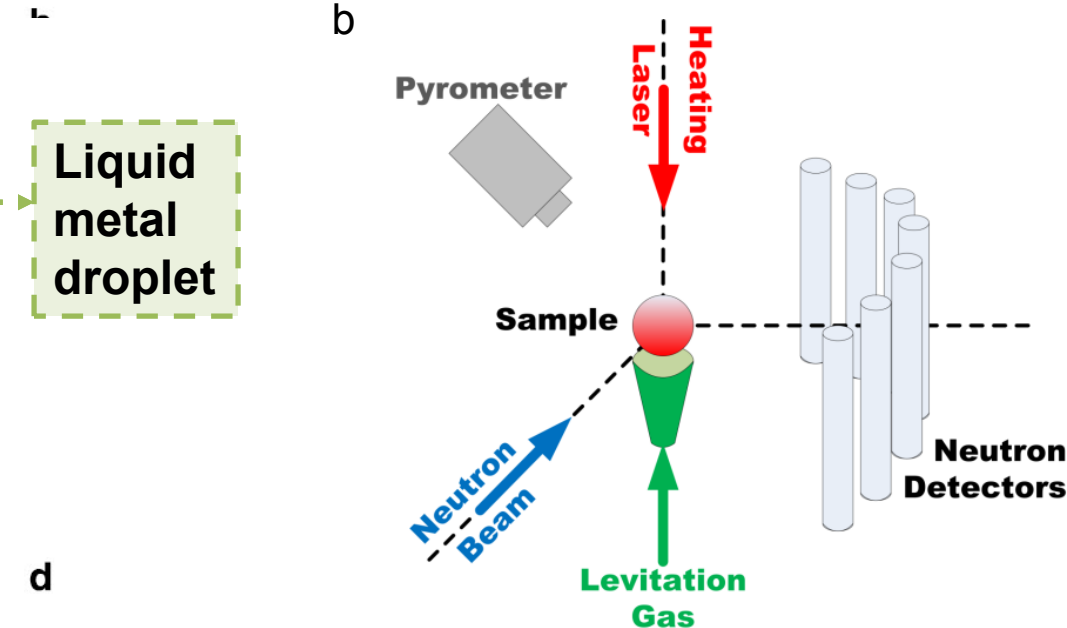
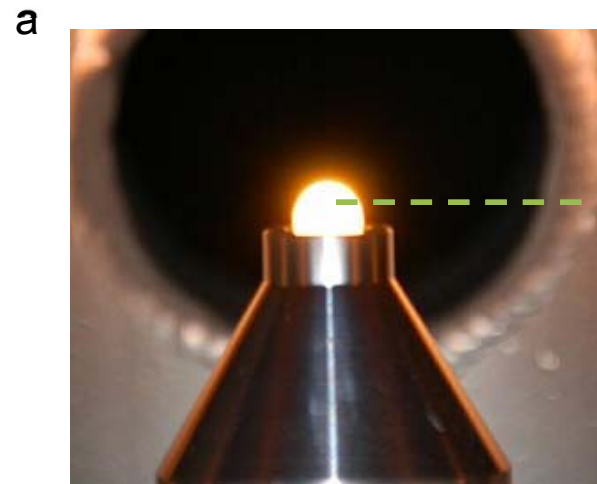
Fatigue properties of HEA



S-N curves comparing the fatigue ratios of the $\text{Al}_{0.5}\text{CoCrCuFeNi}$ HEA, other conventional alloys, and BMGs

1. M. A. Hemphill, T. Yuan, G. Y. Wang, J. W. Yeh, C. W. Tsai, A. Chuang, and P. K. Liaw, "Fatigue behavior of $\text{Al}_{0.5}\text{CoCrCuFeNi}$ high entropy alloys", *Acta Materialia*, 2012, 60(16), pp. 5723-5734.

Local Structure of $\text{Al}_{1.3}\text{CoCrCuFeNi}$ (SNS, ORNL)



1. L. J. Santodonato, Y. Zhang, M. Feygenson, C. M. Parish, M. C. Gao, R. J. K. Weber, J. C. Neufeind, Z. T  ng, and P. K. Liaw, *Nature Communications*, 2015, 6, p. 5964.

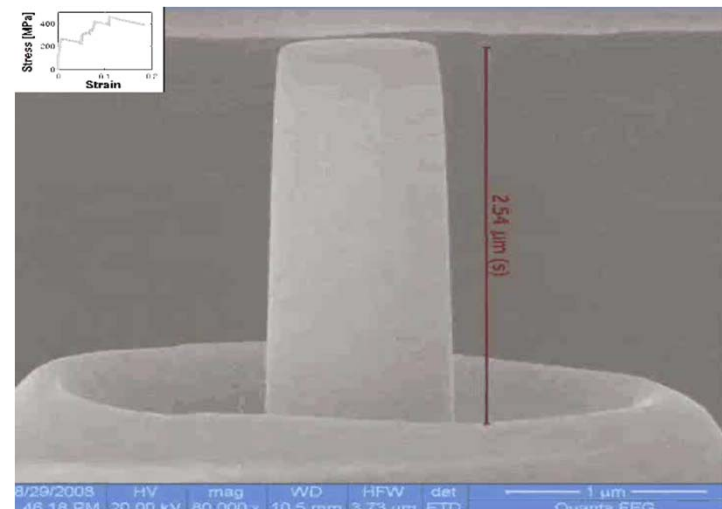
Introduction: Mean-Field Theory of Serrated Flow

Analytics: Jon T. Uhl, Yehuda Ben-Zion,
Michael LeBlanc

DDD Simulations: Georgios Tsekenis,
Phase Field Calculation (PFC): Pak Yuen Chan,
Nigel Goldenfeld

Nanocrystals and Bulk Metallic Glasses:
Liaw, Qiao, Greer, Jennings, Maass,
Wraith, Friedman

High Entropy Alloys:
Liaw, Qiao, Senkov, Miracle, Tang, Tsai,
Laktionova, Tabachnikova, Yeh,
Antonaglia, Xie, Carroll



Funding/Equipment:
NETL, NSF, MCC, SLOAN, UIUC, IBM, MGA



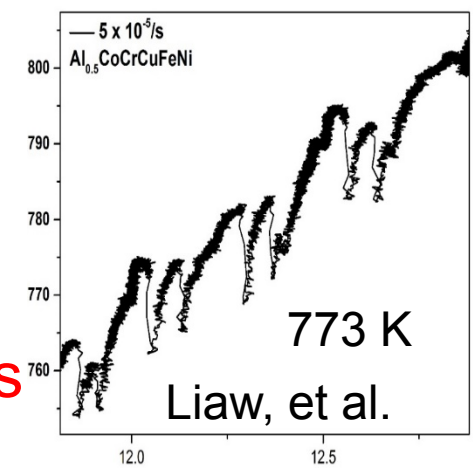
Our Simple Analytic Model of Plasticity

(KD, Ben-Zion, Uhl, PRL 2009, Nature Physics 2011)

One Tuning Parameter:

- Weakening ε
- Applied to Crystals, Bulk Metallic Glasses, HEAs

Stress vs. Strain



Two Experimentally Relevant Loading Conditions:

- Slow strain-rate loading condition:
- Slow stress-rate loading condition

Strain-rate v



Stress F



EXACT Predictions in 2 and 3 Dimensions (no fitting)

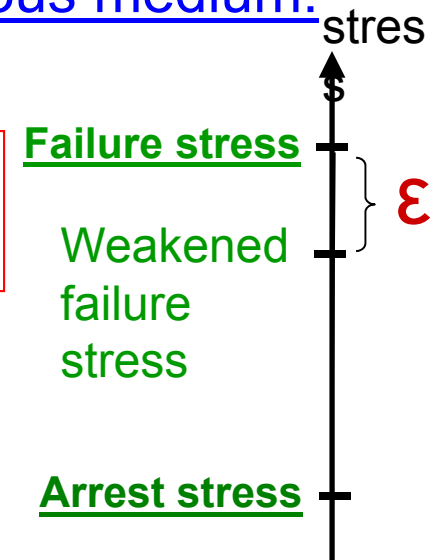
- Histograms of slip-sizes, durations, power spectra, ...
- Brittle ($\varepsilon>0$), ductile ($\varepsilon=0$), & hardening materials ($\varepsilon<0$)

Predictions agree with first experiments,
Many predictions for future experiments...

Coarse grained model for slip evolution in heterogeneous medium:

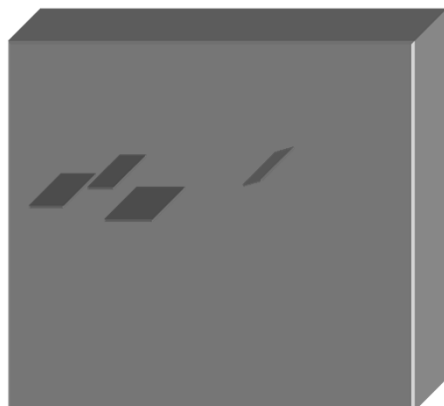
$$\eta \frac{\partial u(r,t)}{\partial t} = F + \sigma_{int}(r,t) - f_R[u, r, \text{history}]$$

Slip velocity ~ stress + interaction + Pinning due to heterogeneities



Interaction:

$$\sigma_{int}(r,t) = \int_{-\infty}^t dt' \int d^d r' J(r-r', t-t') \times [u(r',t') - u(r,t)]$$



Renormalization Group:

Interaction long range $\int dt J(r, t)$

→ MEAN FIELD THEORY:

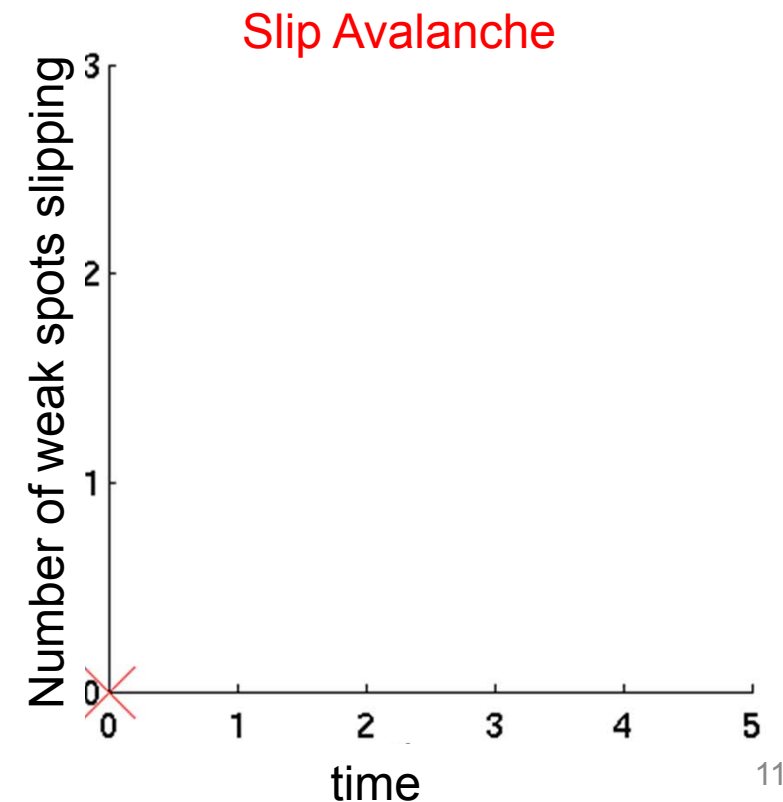
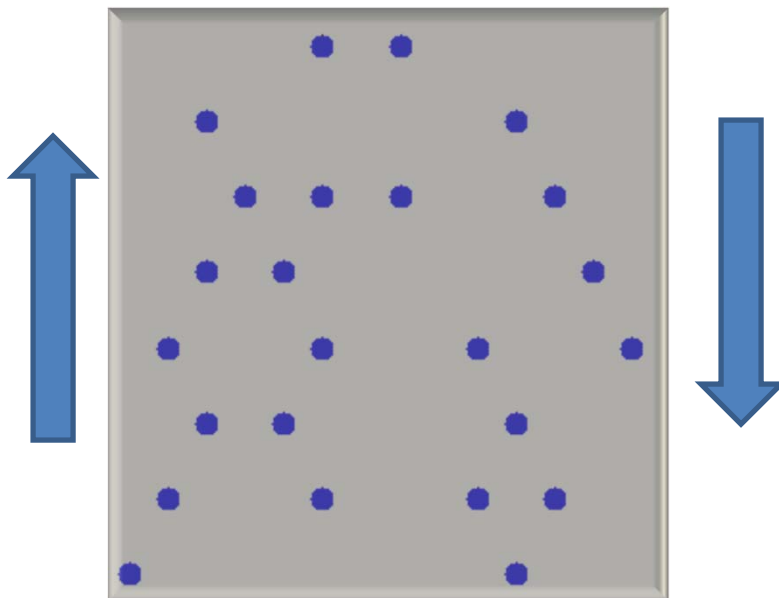
Exact Results !

Related models: Chen, Bak, Obukhov (PRA 1991), Zaiser, Adv. of Phys, 55, 185-245 (2006).

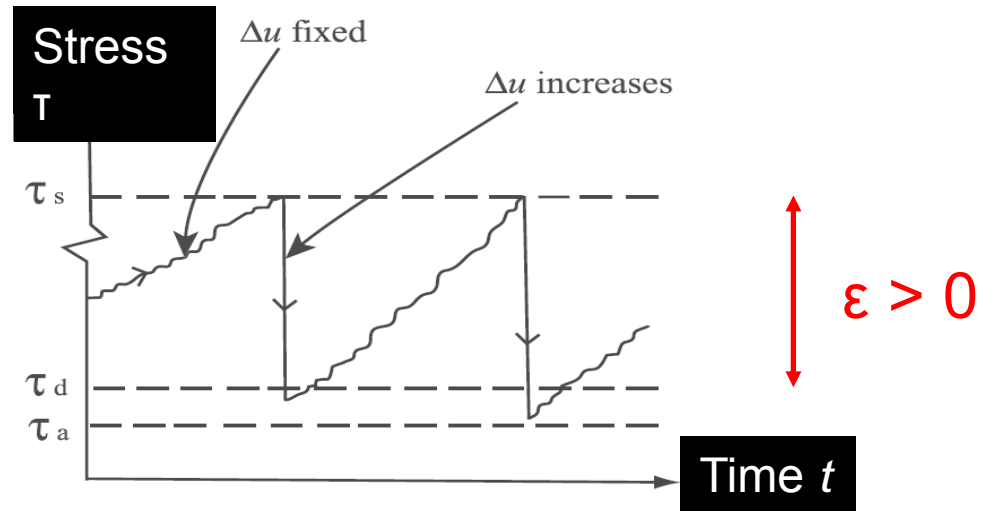
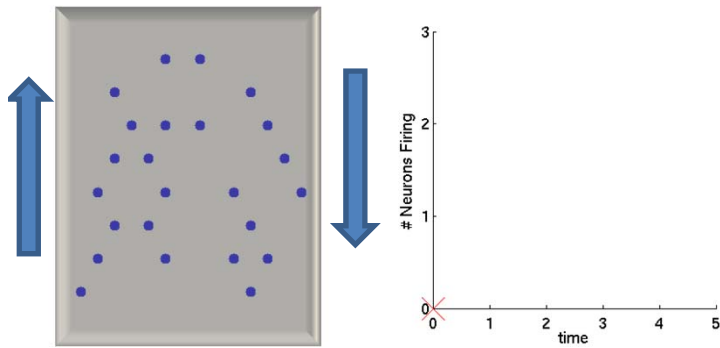
Main Idea of the simple model:

Shear material:

1. Weak spot slips
triggers other weak spots to slip
Slip Avalanche
2. Repeat



COARSE GRAINED Threshold pinning ($f_R[u, r, \text{history}]$)



$$\varepsilon = (\tau_s - \tau_d) / \tau_s = \text{dynamic weakening}$$

weakening ($\varepsilon > 0$)

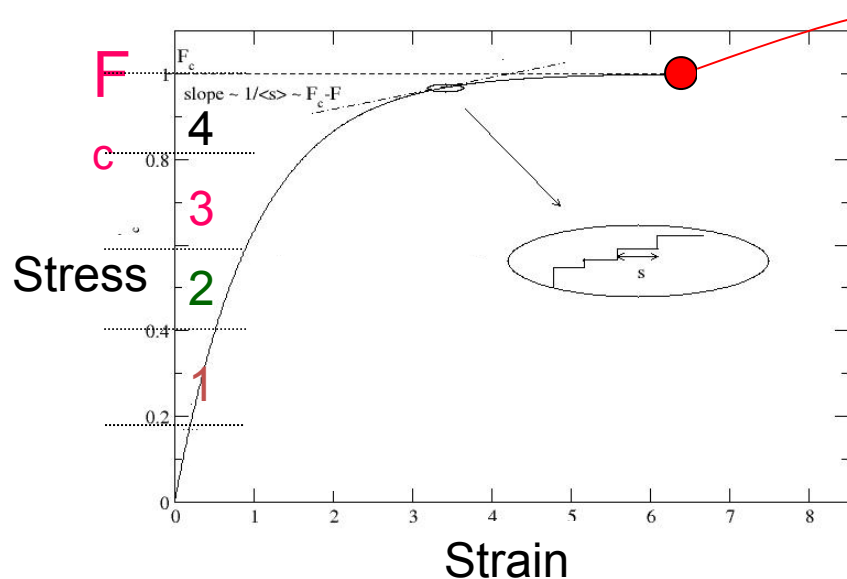
during failure avalanche:
failed regions get weakened by $O(\varepsilon)$
reheal to old strength after avalanche

hardening ($\varepsilon < 0$)

each failure event raises failure threshold
by $\sim |\varepsilon|$,
used to model aftershocks
(Mehta, KD, Ben-Zion, PRE 2006)

Results for $\varepsilon = 0$ for Slowly-Increasing Stress Loading Conditions

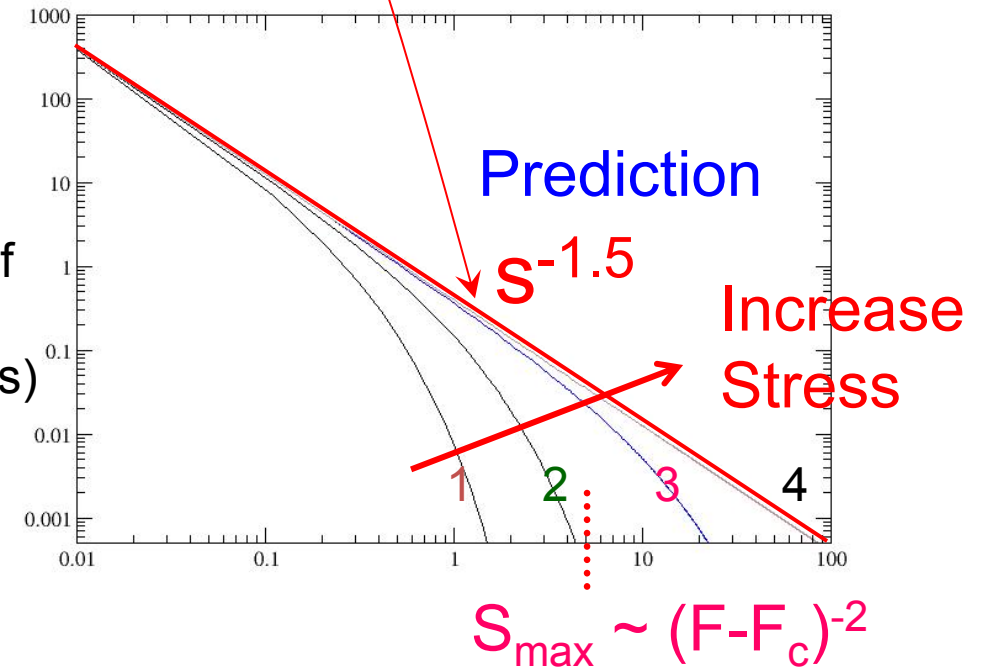
Stress-Strain Curve (Ductile)



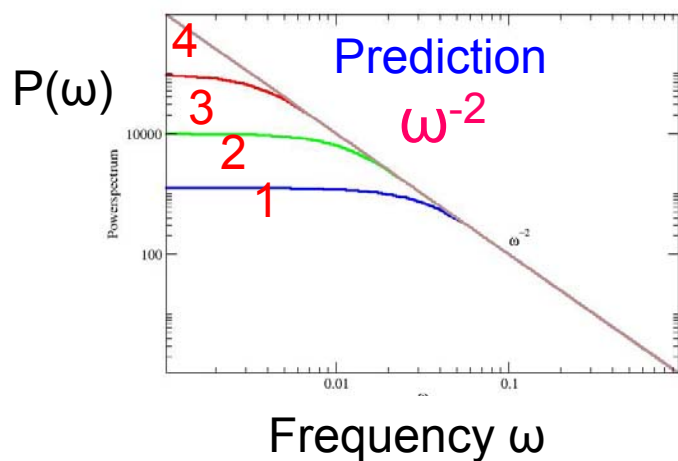
No Fitting Parameters!

Critical Point

Slip Avalanche Size Distribution:



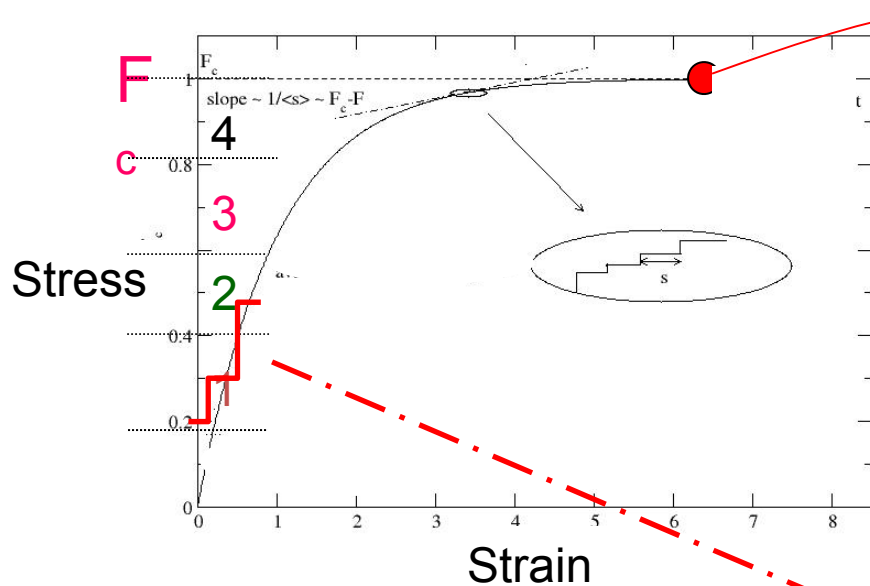
Power-Spectrum



Log(Slip Size S)

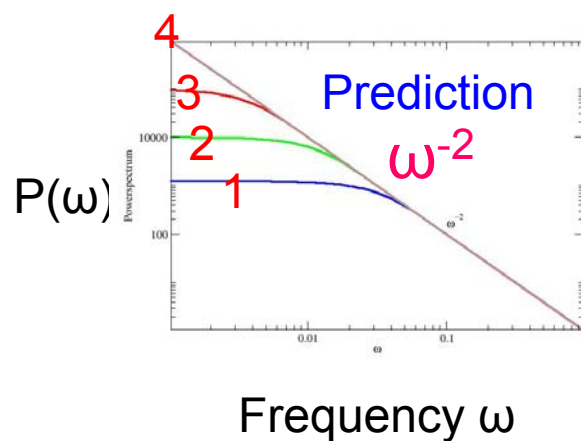
Results for $\varepsilon = 0$ for Fixed Stress Loading Conditions

Stress-Strain Curve (Ductile)

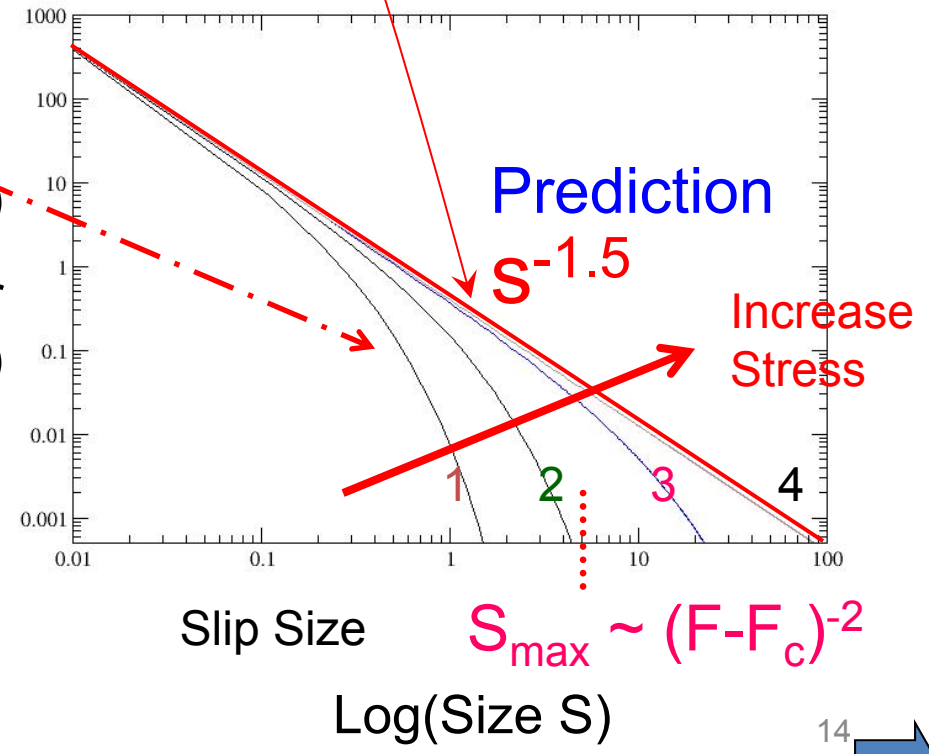


No Fitting Parameters!

Power-Spectrum

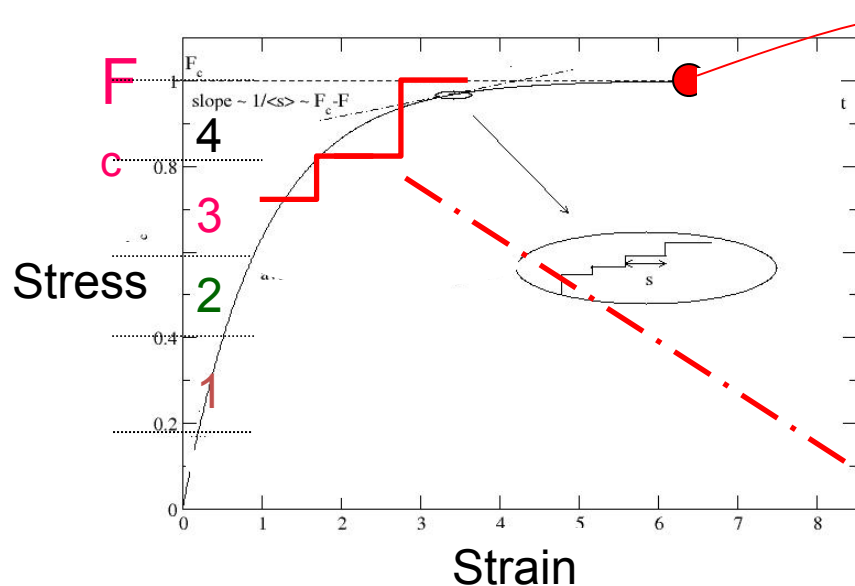


Slip Avalanche Size Distribution:



Results for $\epsilon = 0$ for fixed Stress Loading Conditions

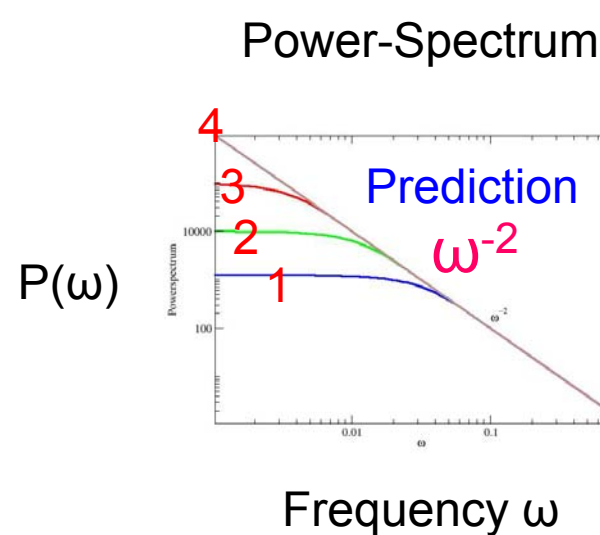
Stress-Strain Curve (ductile)



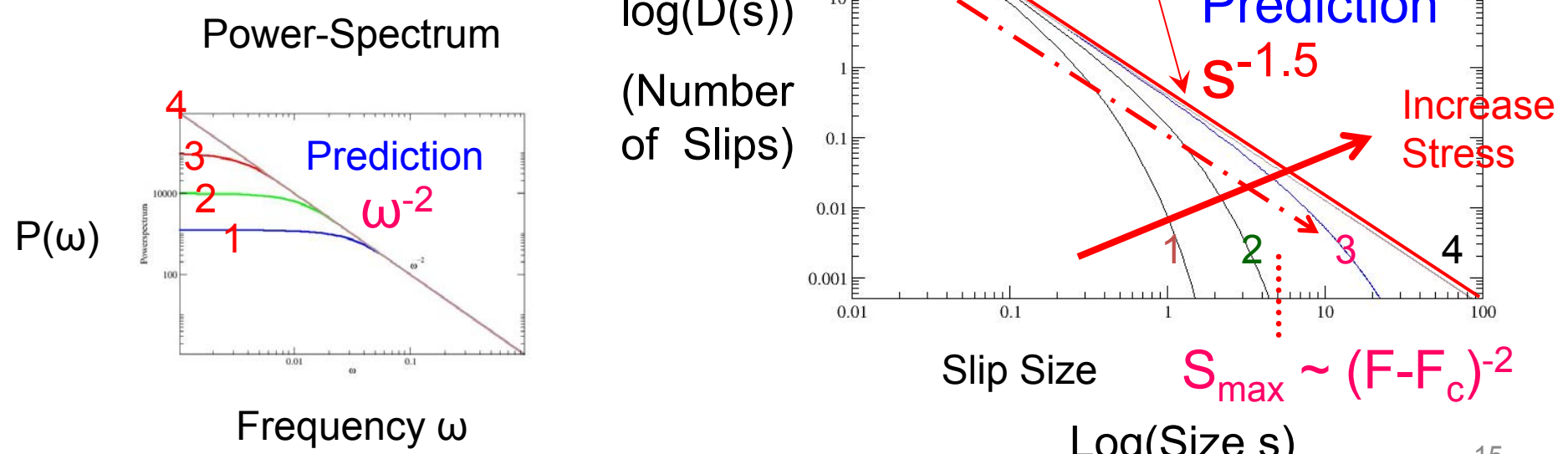
No Fitting Parameters!

Critical Point

Slip Avalanche Size Distribution:



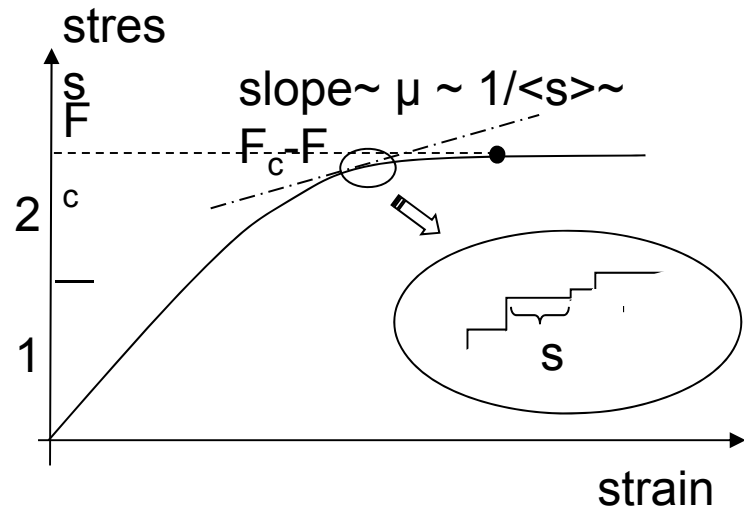
$\log(D(s))$
(Number
of Slips)



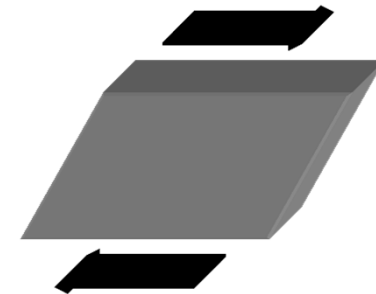
15



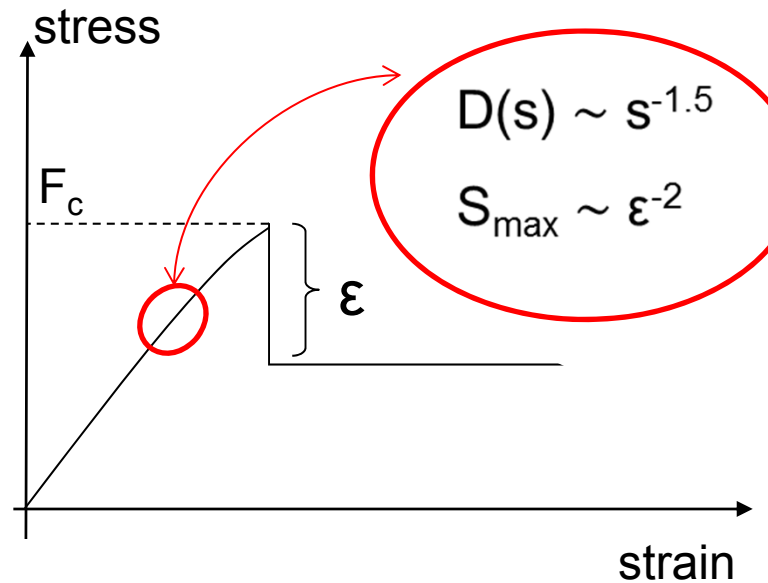
Predictions without weakening (“ductile”) ($\varepsilon = 0$):



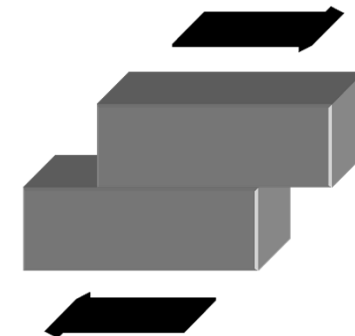
cont. depinning transition
and distributed slip



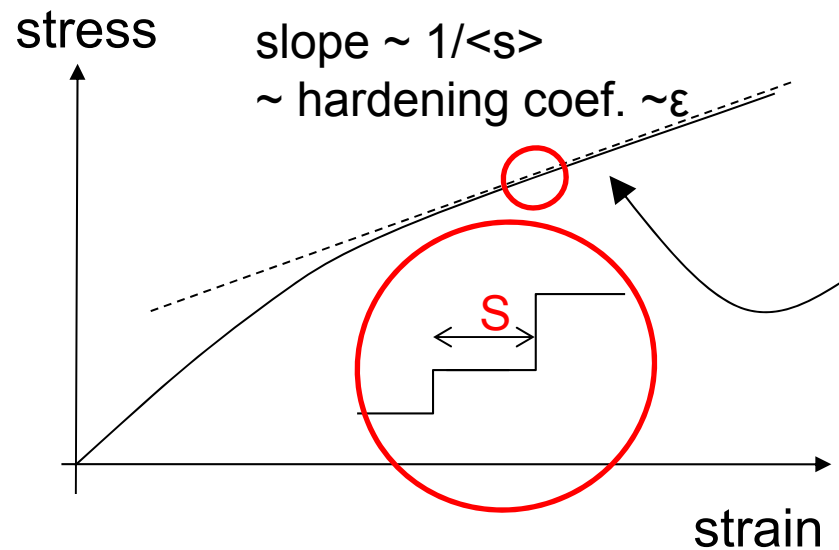
Predictions with weakening (“brittle”) ($\varepsilon > 0$):



first order depinning transition
and slip localization



Stress strain curve in the presence of hardening (“ductile”): ($\varepsilon < 0$)



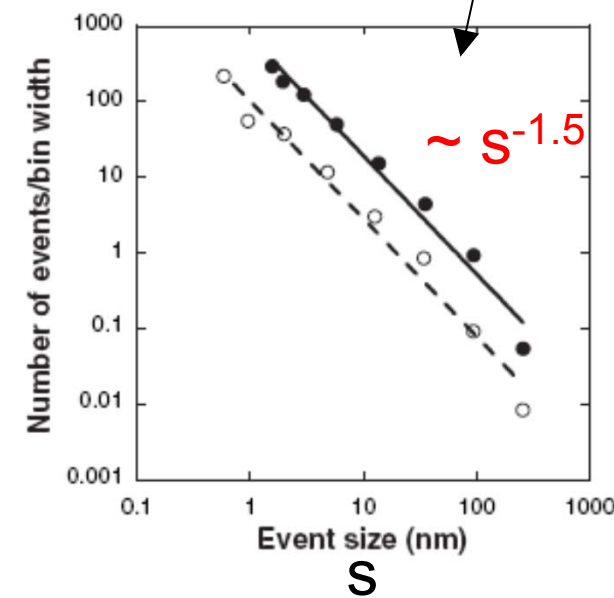
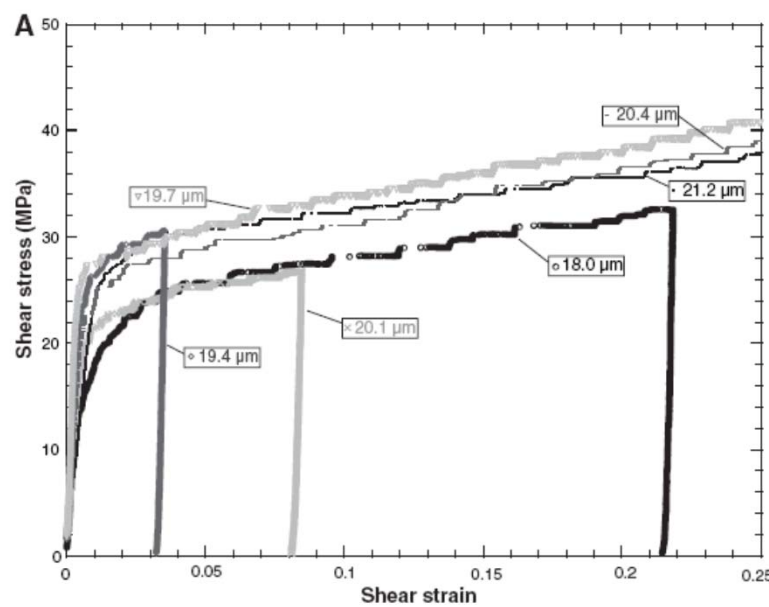
$$D(s) \sim s^{-1.5}$$

$$P(\omega) \sim \omega^{-2}$$

$$D(T) \sim T^{-2}$$

etc.

distributed
deformation



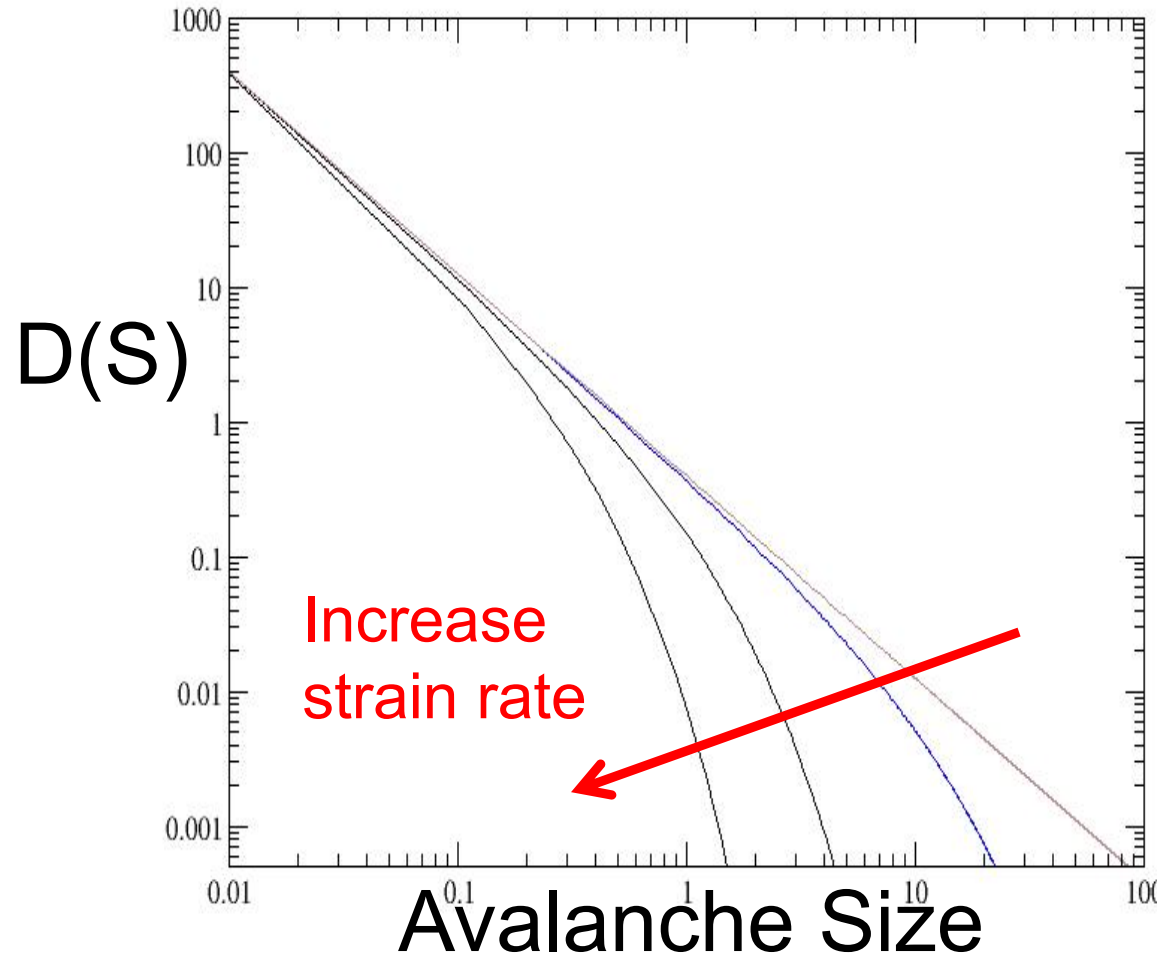
No fitting parameters
Agrees with experiment

(Dennis M. Dimiduk, Chris Woodward, Richard LeSar, Michael D. Uchic. Science 2006)

Can we check the
analytic mean field
theory predictions with
experiments ?

Avalanche (Serration) Size Distributions at Different Strain Rates (Model Prediction)

$$D(S) \sim S^{-\tau} F(S \Omega^\lambda), \quad \tau = 1.5$$

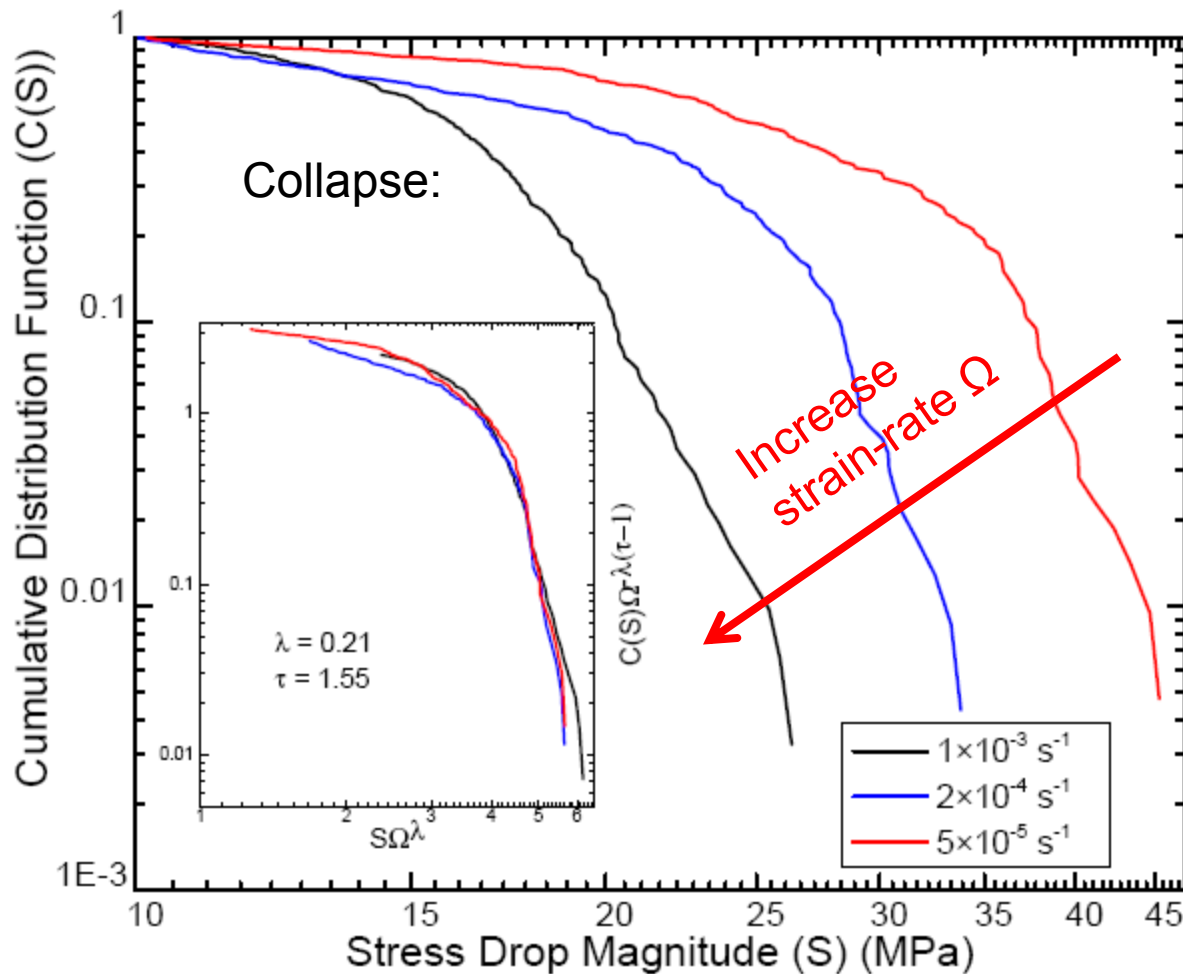


BULK METALLIC GLASSES:

Junwei Qiao, Peter Liaw, Xie Xie: $\text{Zr}_{64.13}\text{Cu}_{15.75}\text{Ni}_{10.12}\text{Al}_{10}$ ingots (2mm x 4mm)

James Antonaglia, KD: Comparison to model prediction for cumulative

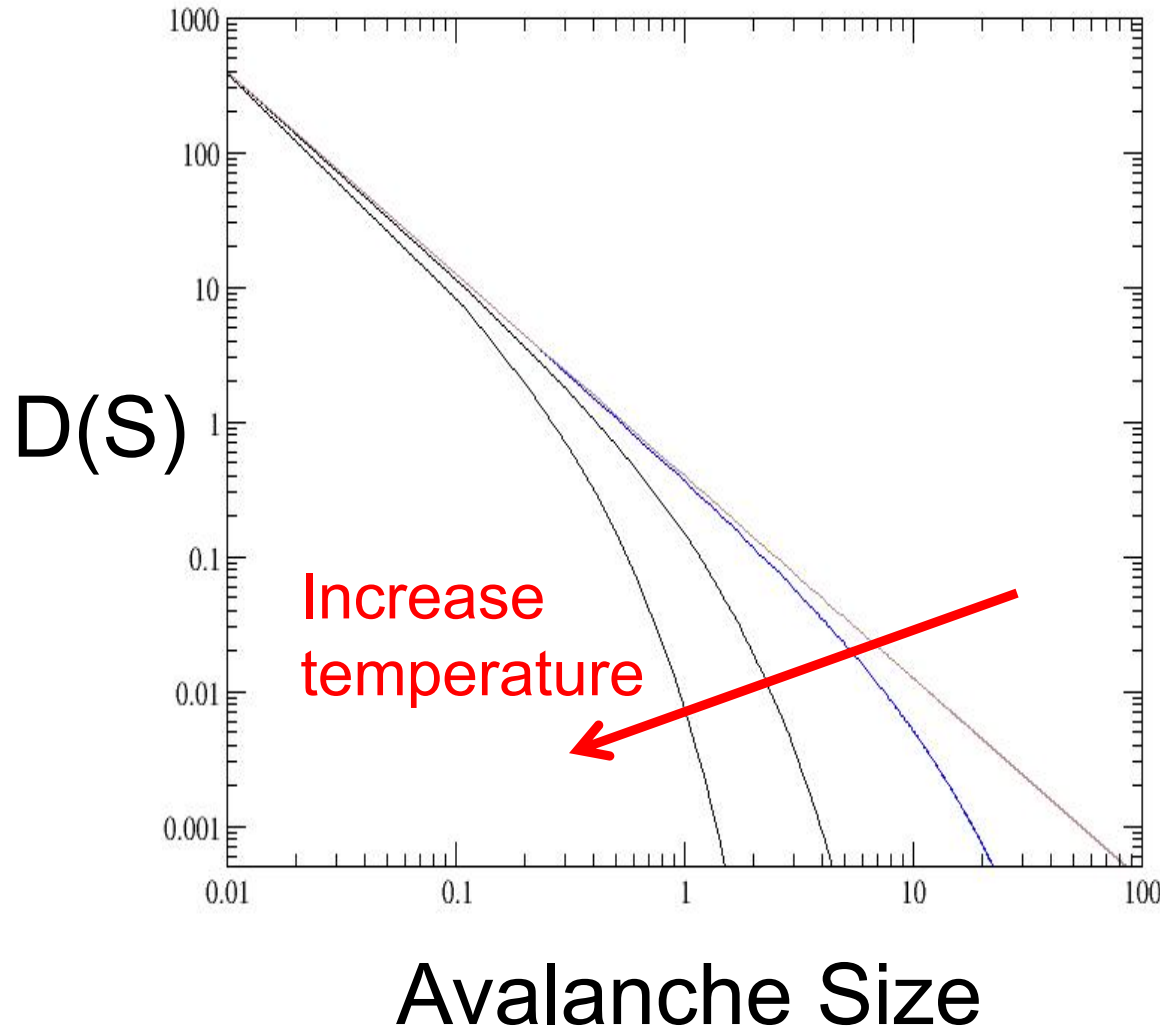
avalanche size distribution: $C(S) \sim S^{-(\tau-1)} F(S \Omega^\lambda)$, $\tau = 1.5$



[Antonaglia, Xie, Wraith,
Qiao, Zhang, Liaw, Uhl,
Dahmen,](#)

[Nature Scientific Reports
4, 4382 \(2014\).](#)

Avalanche (Serration) Size Distributions at Different Temperatures (Model Prediction)



Comparison to High-Entropy Alloys:

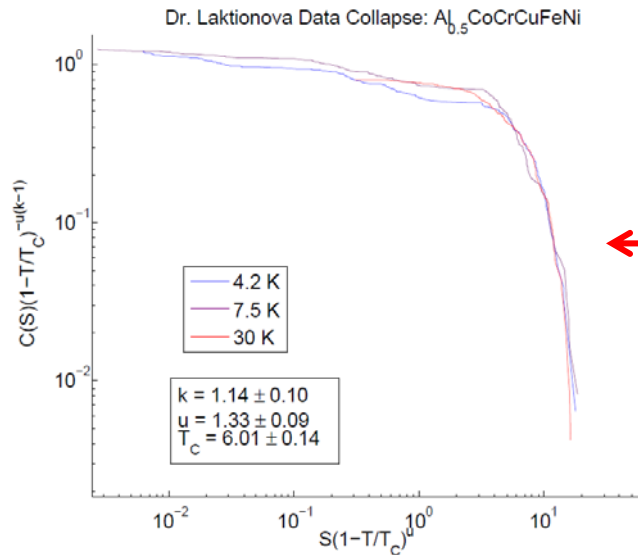
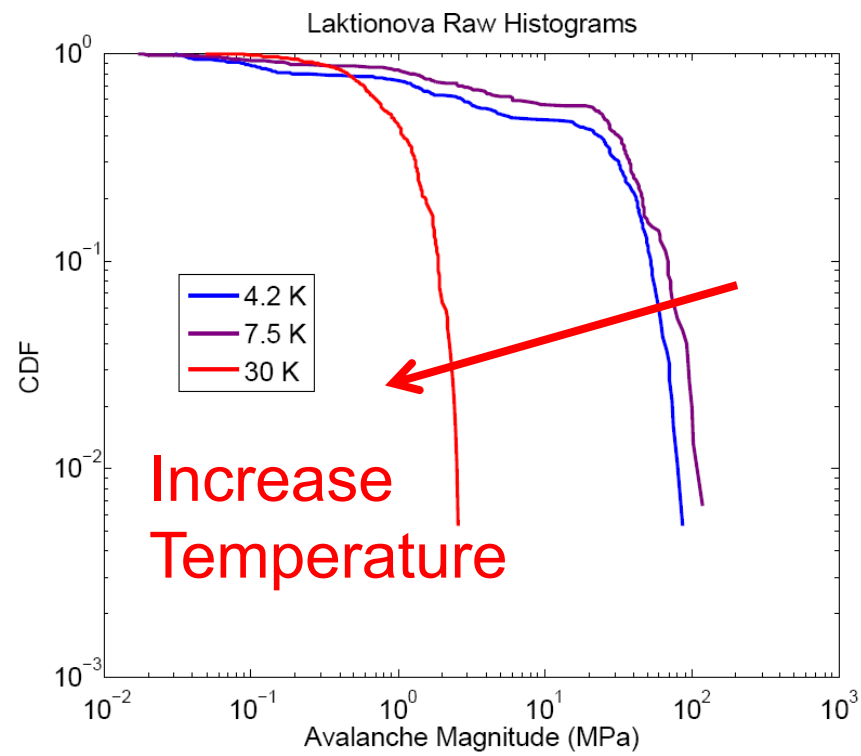
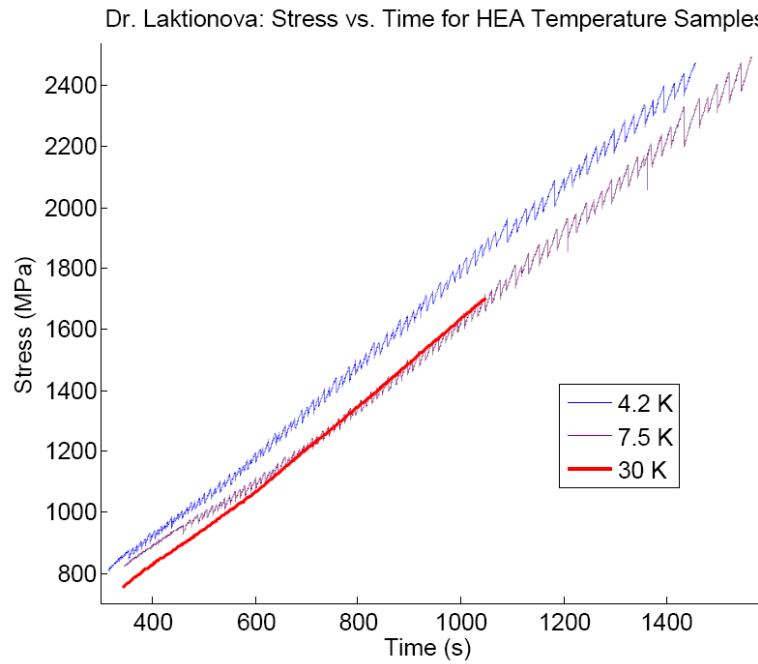
Microstructure Properties of High-Entropy Alloys

(Zhang, Zuo, Tang, Gao, KD, Liaw, Lu)

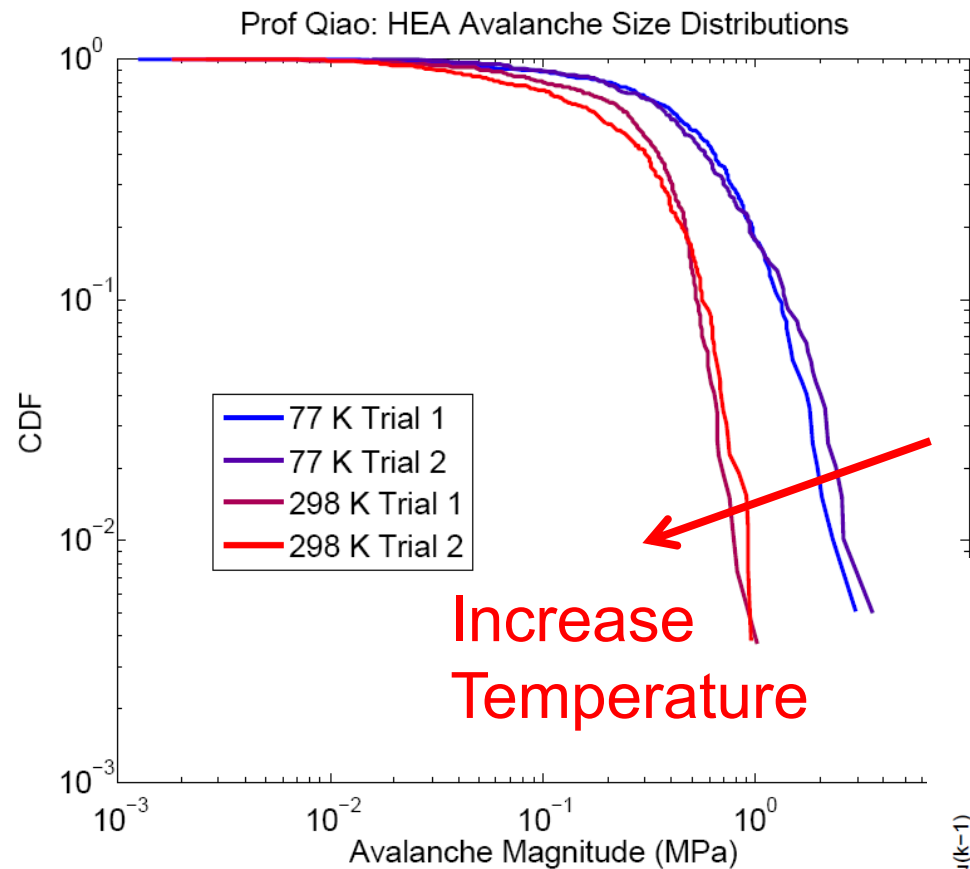
Progress in Materials Science 61,

1-93 2014

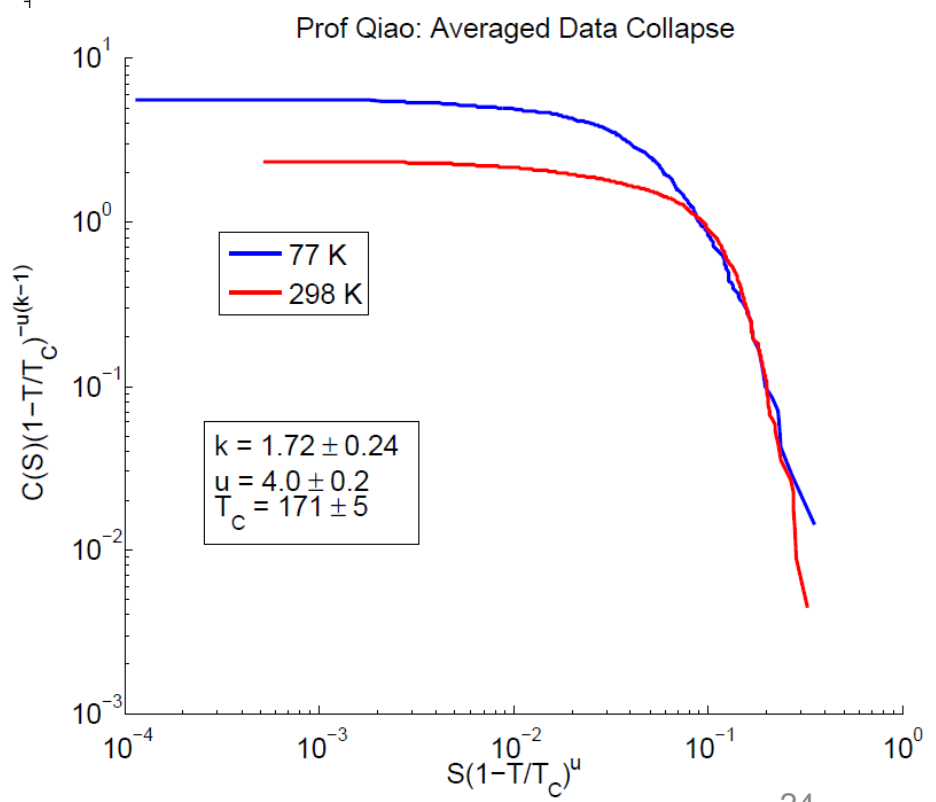
High Entropy Alloys: $\text{Al}_{0.5}\text{CoCrCuFeNi}$ (Laktionova)

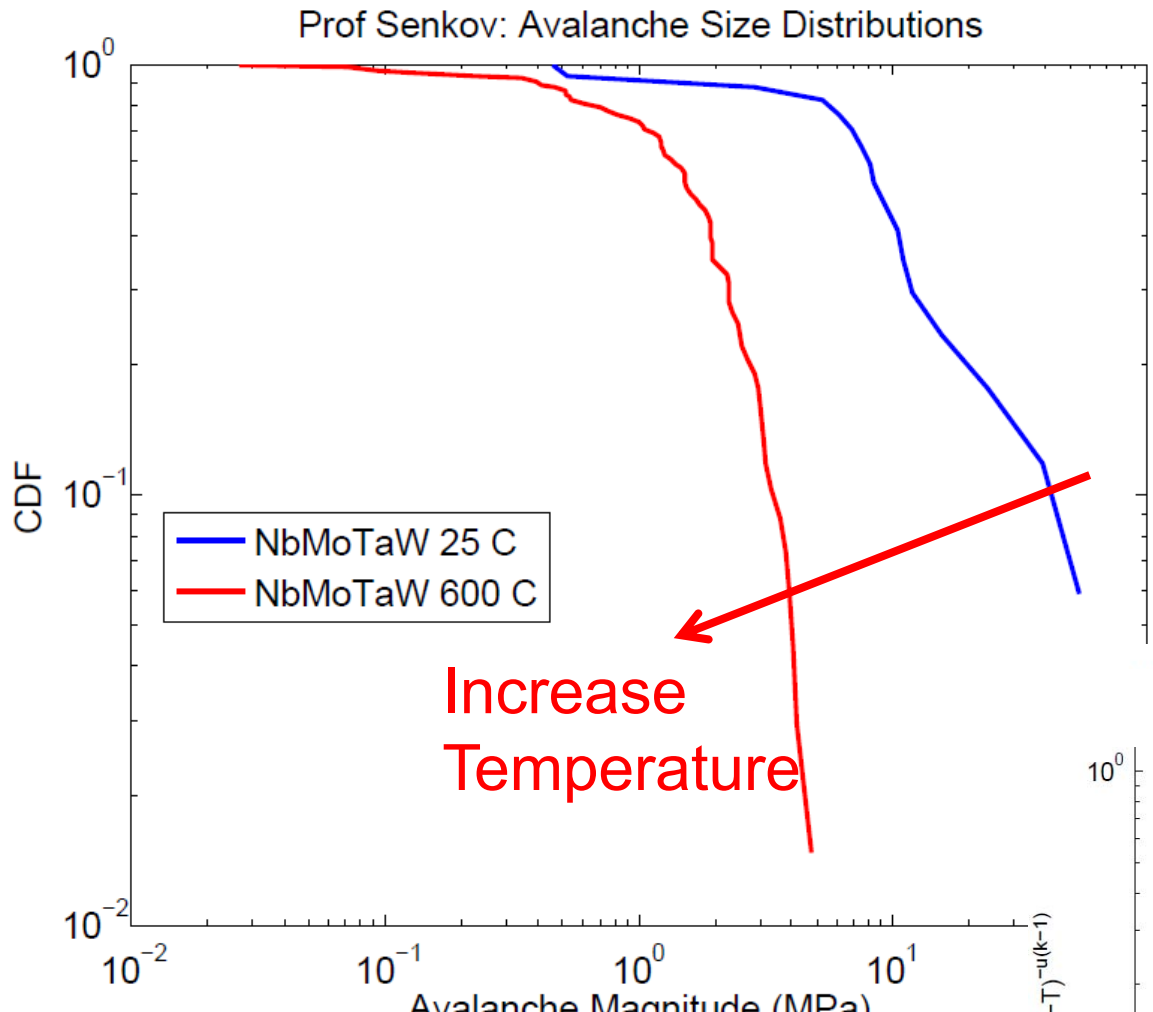


Curves Collapse,
but need more
data, especially
at more
temperatures



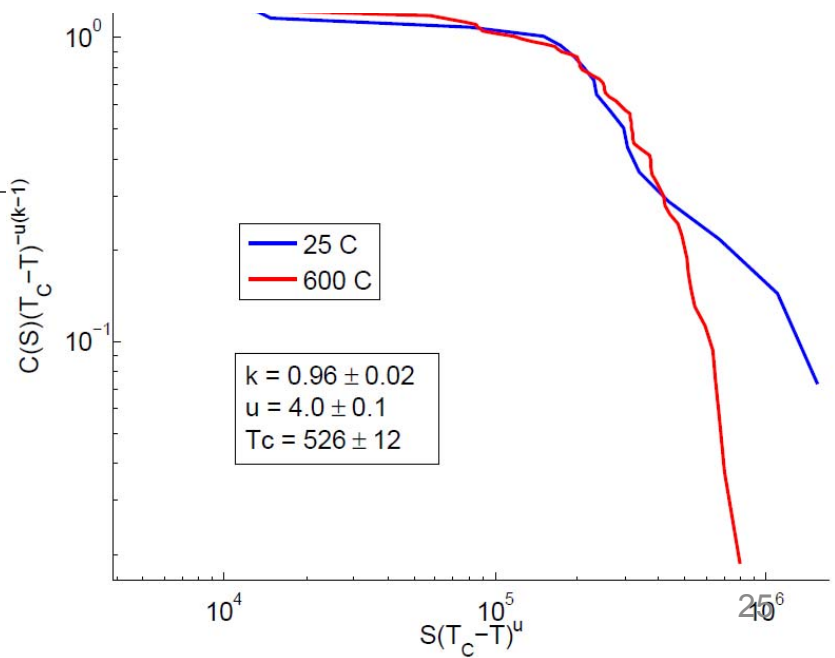
**Liaw, Qiao, Xie,
Antonaglia, KD
AlCoCrFeNi**



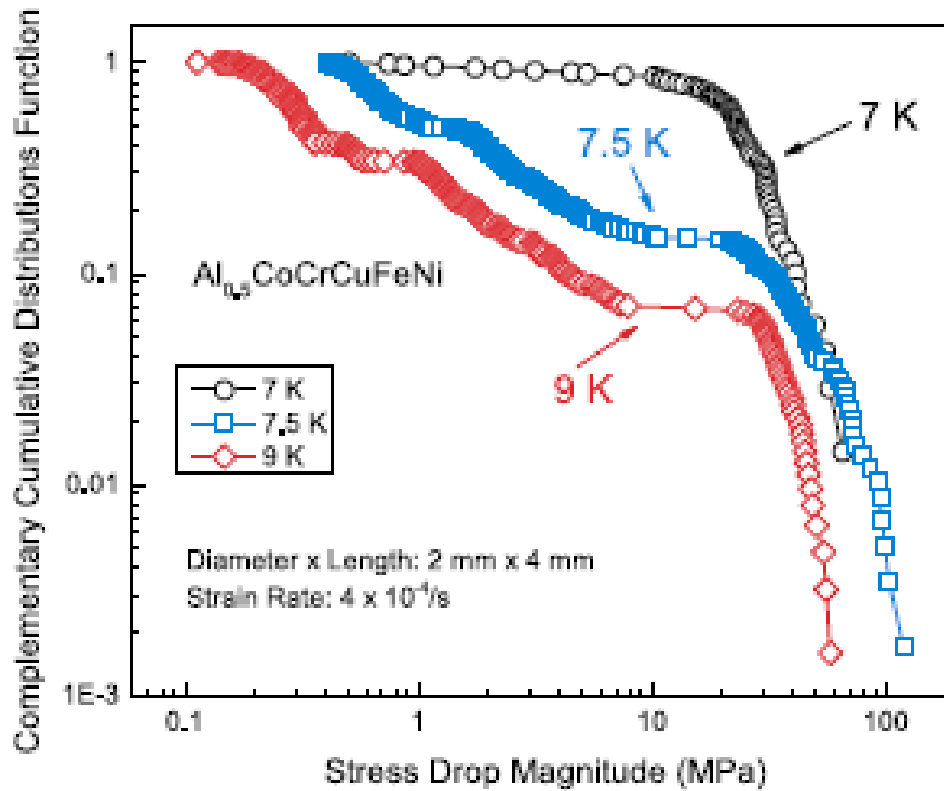


Senkov: NbMoTaW

Collapse (?)
More data at more
temperatures will
tell.



Tool to Discover Transitions in Materials ?



Antonaglia, Xie, Tang, Tsai, Qiao, Zhang,
Laktionova, Tabachnikova, Carroll, Yeh, Senkov,
Gao, Uhl, Liaw, Dahmen, **JOM 66 (10), 2002 (2014).**

Experimental Results

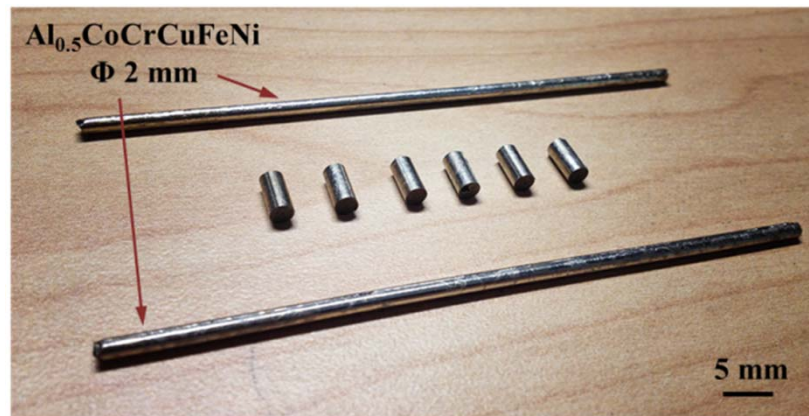
Preparation of $\text{Al}_{0.5}\text{CoCrCuFeNi}$ Alloy

Al, Co, Cr, Cu, Fe, and Ni with purity higher than 99.9%

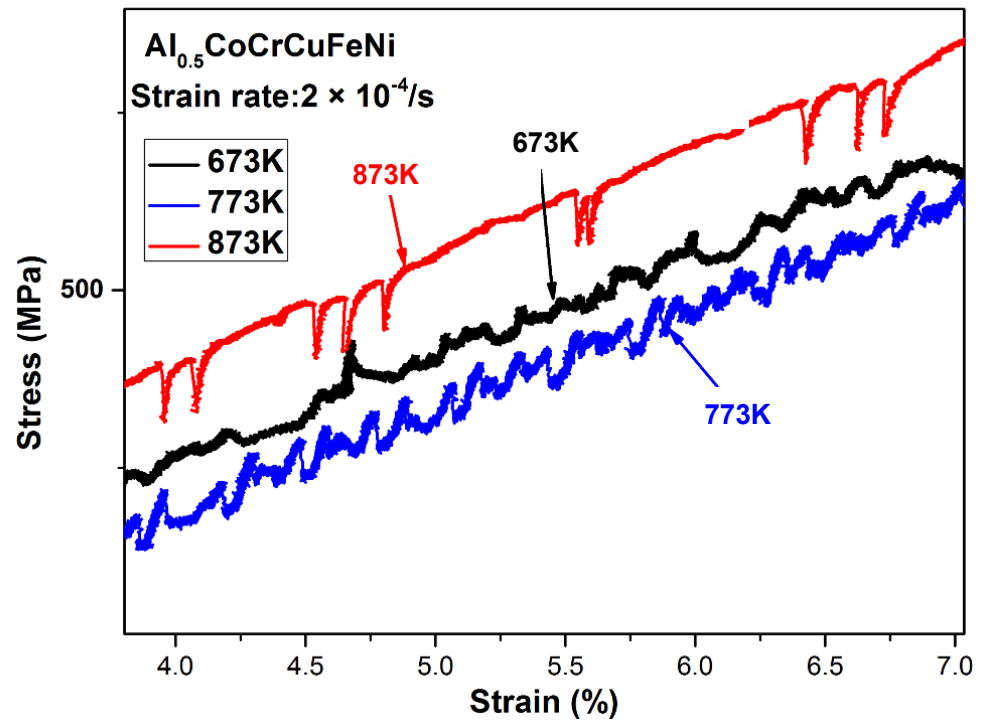
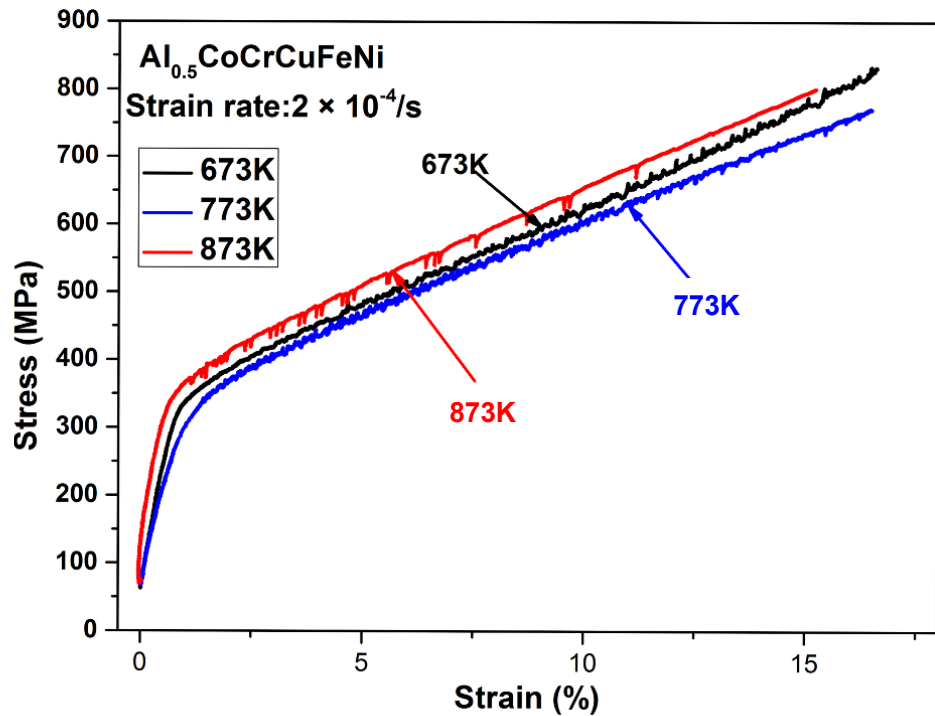
Arc-melting the mixtures and then drop-cast into a water-cooled copper mold with 2 mm in diameter.

Rods machined into specimens with 2 mm in diameter and 4 mm in length.

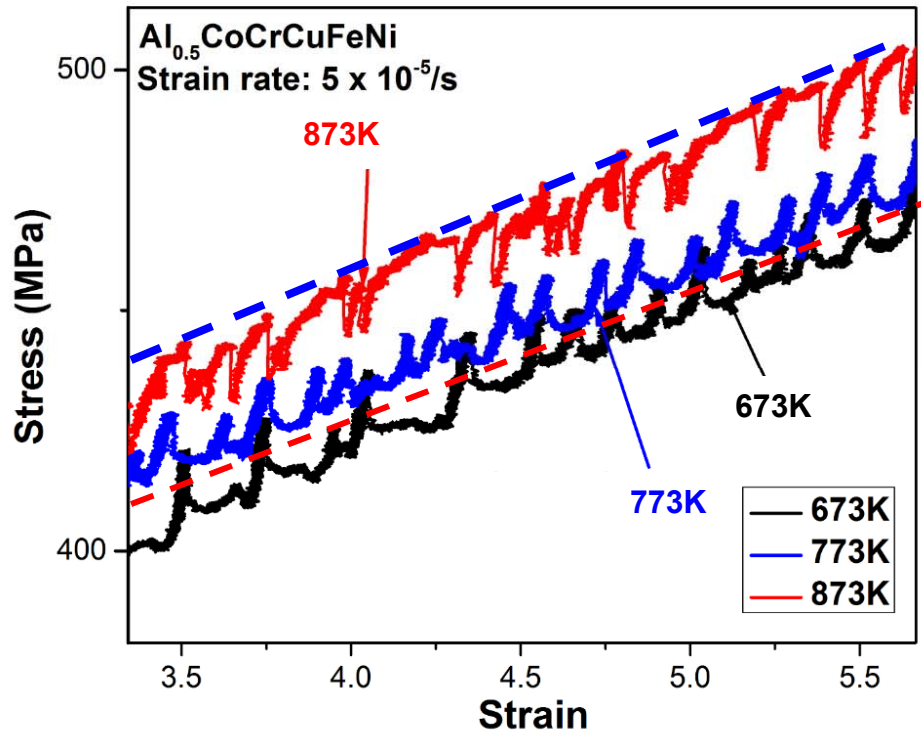
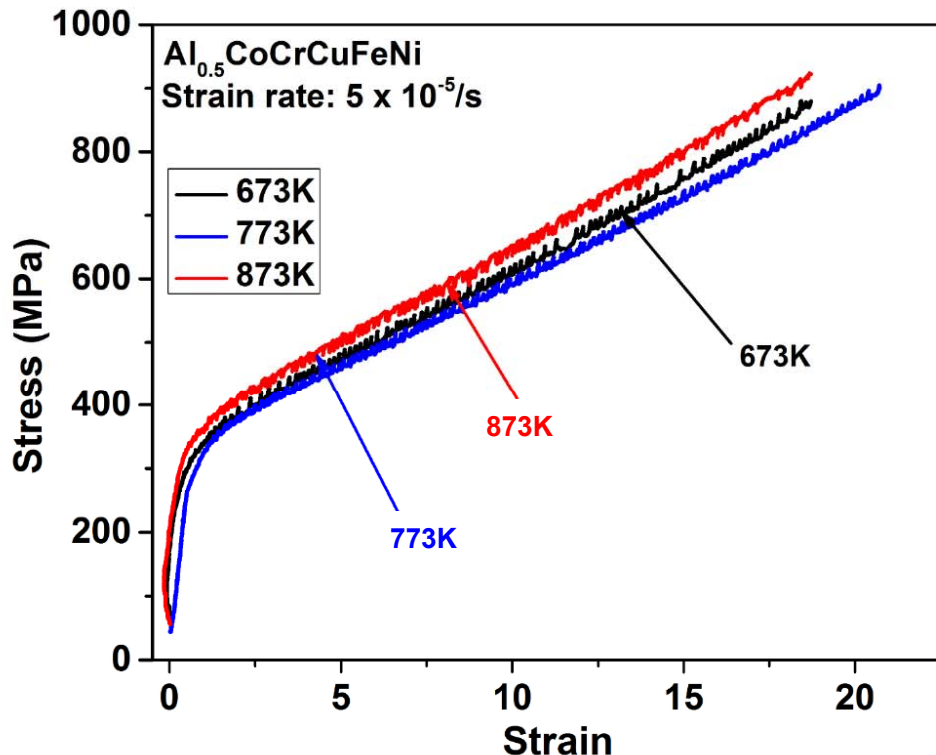
Compression tests conducted using the Materials Test System (MTS) servohydraulic-testing machine with displacement control



Strain Rate of $2 \times 10^{-4}/\text{s}$ at Temperatures of 673K, 773K, and 873K



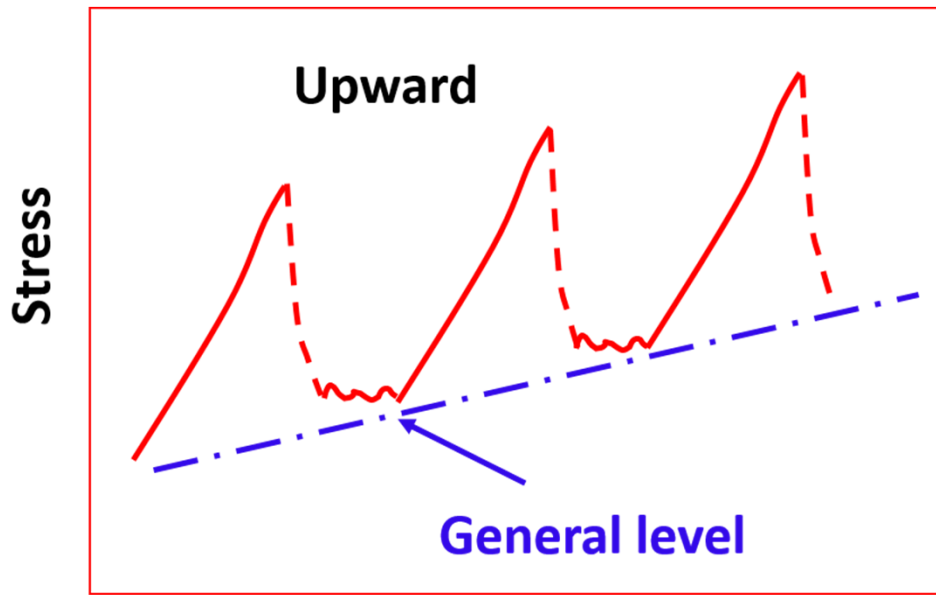
Strain Rate of $5 \times 10^{-5}/\text{s}$ at Temperatures of 673K, 773K, and 873K



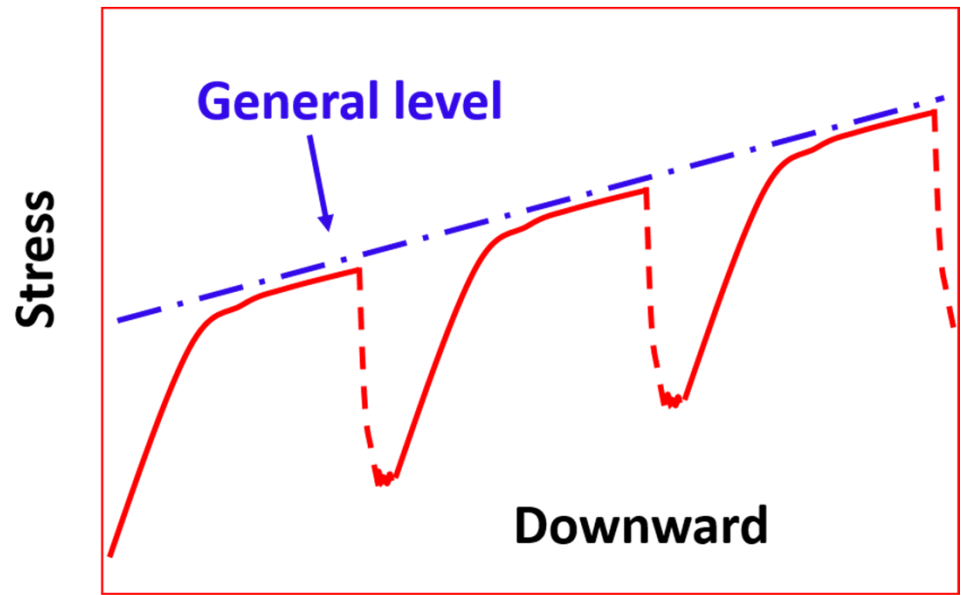
Serrations change from upward to downward direction when temperature increase, which are also observed in 5456 aluminum alloy tested at strain rate of $5.4 \times 10^{-4}/\text{s}$ from 173K to 333K.

1. S. Fu, T. Cheng, Q. Zhang, Q. Hu, and P. Cao, Two mechanisms for the normal and inverse behaviors of the critical strain for the Portevin–Le Chatelier effect, 60, *Acta Materialia*, 2012. pp. 6650-6656.

Illustration of Upward and Downward Directions of Serrations

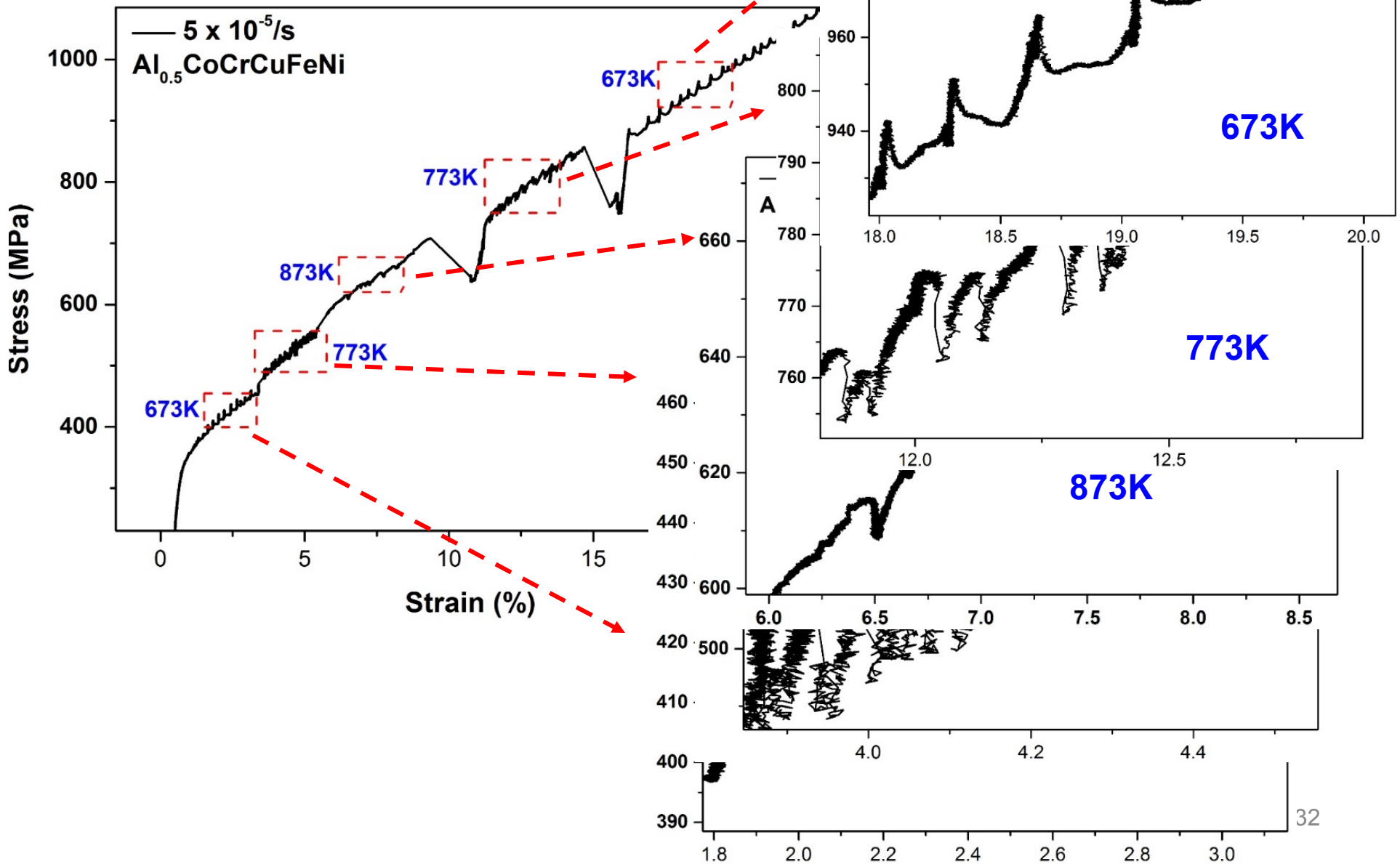


Low temperature



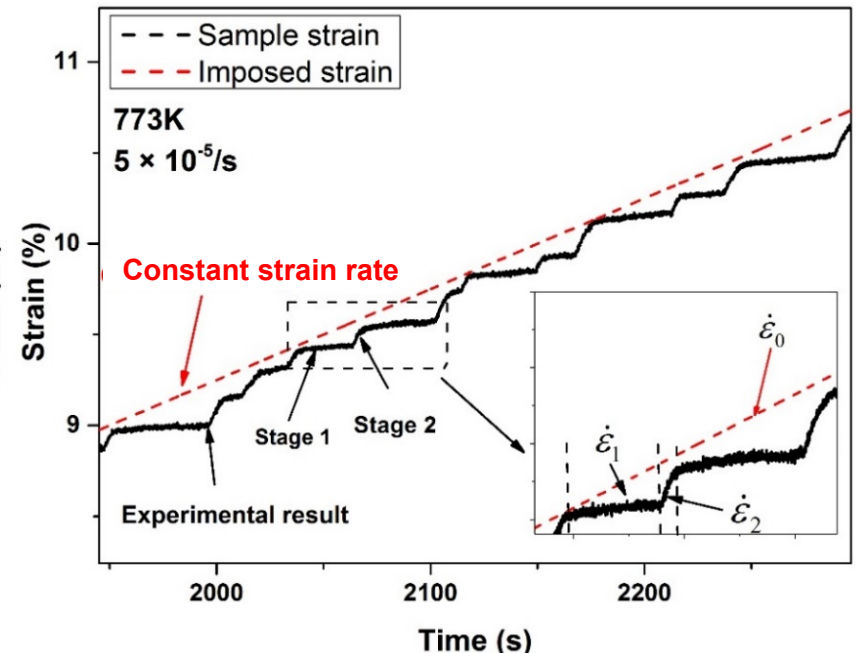
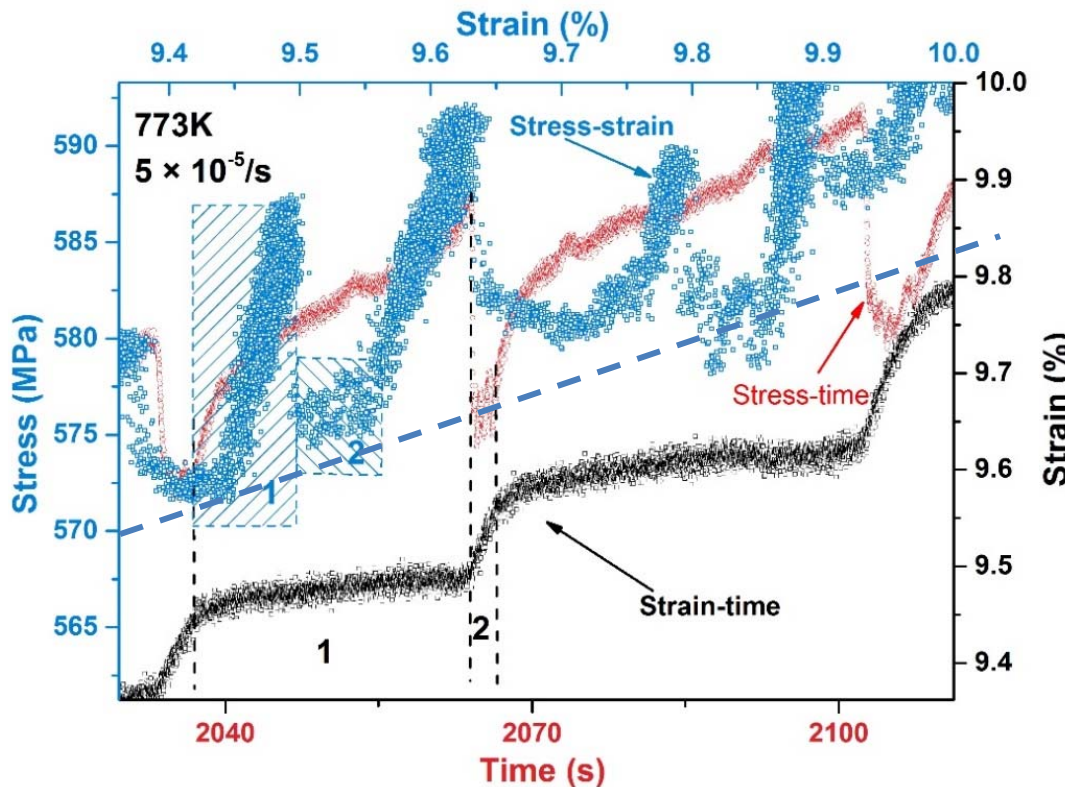
High temperature

Changing Temperatures During Compression Tests



Explanation of Upward and Downward Serrations

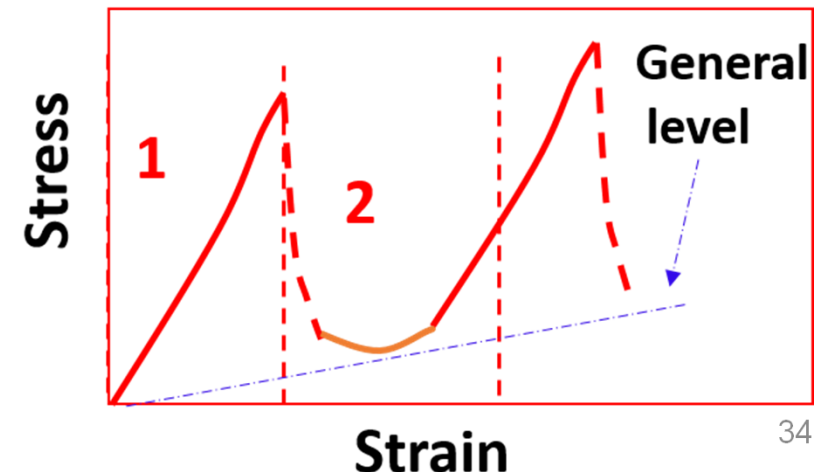
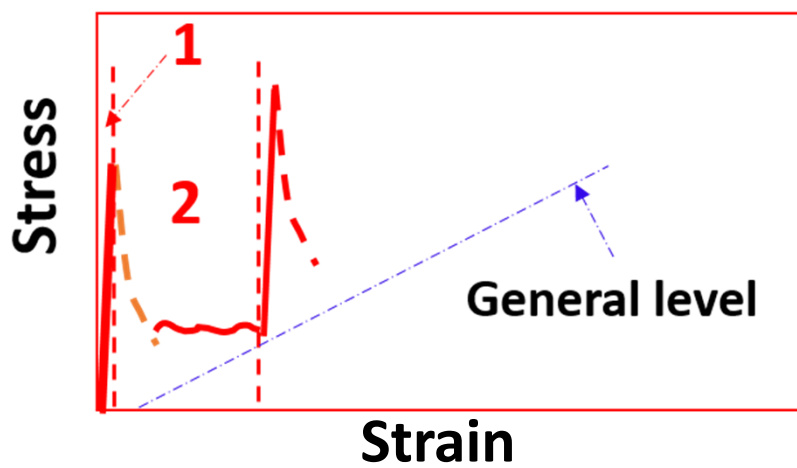
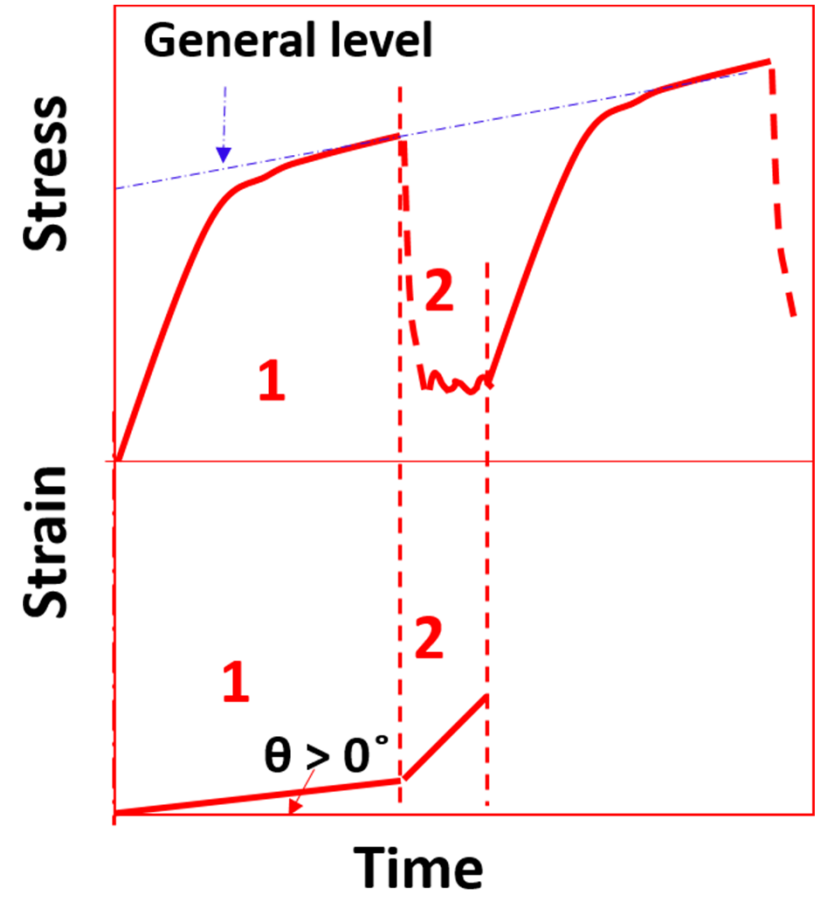
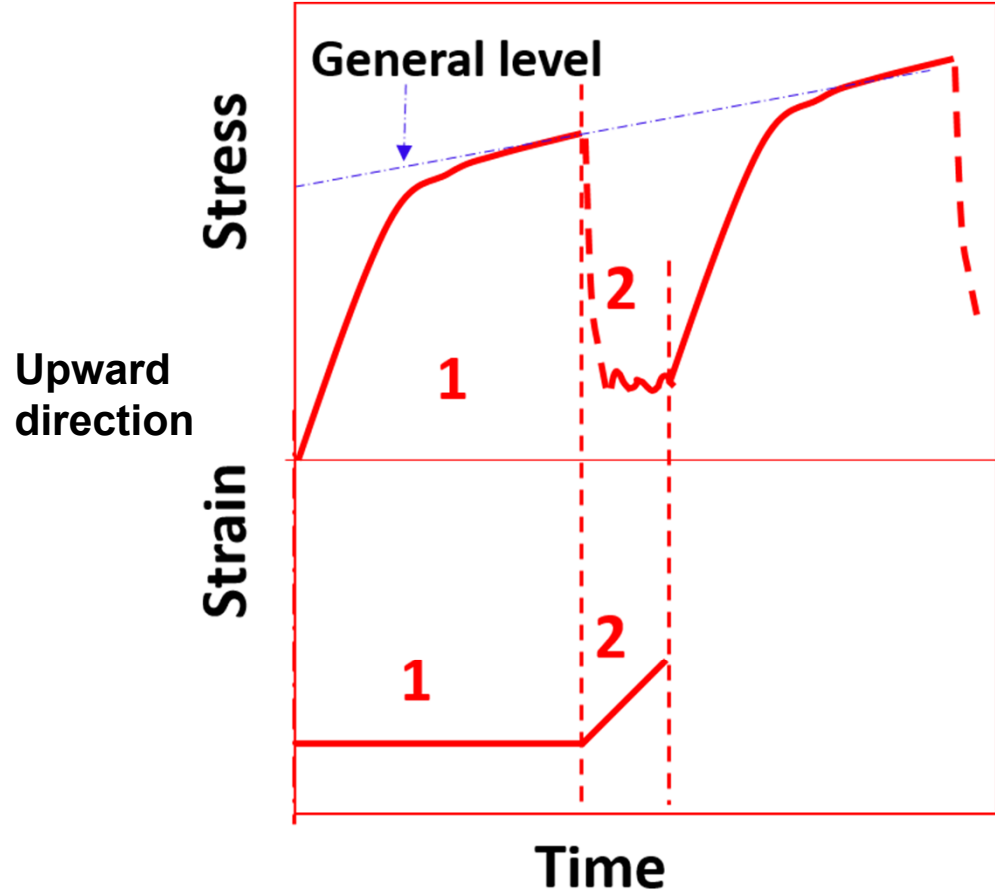
At strain rate $5 \times 10^{-5}/\text{s}$ with temperature of 773K



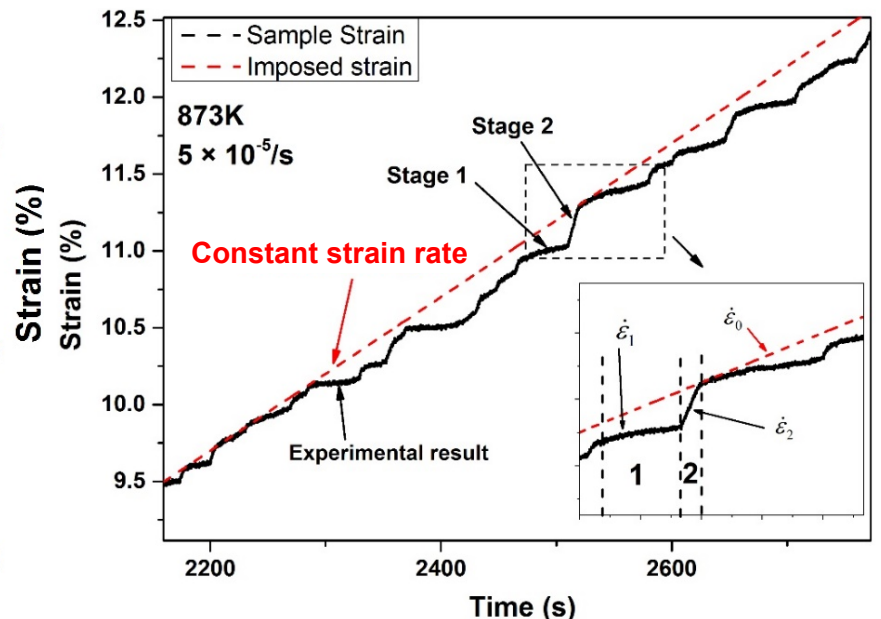
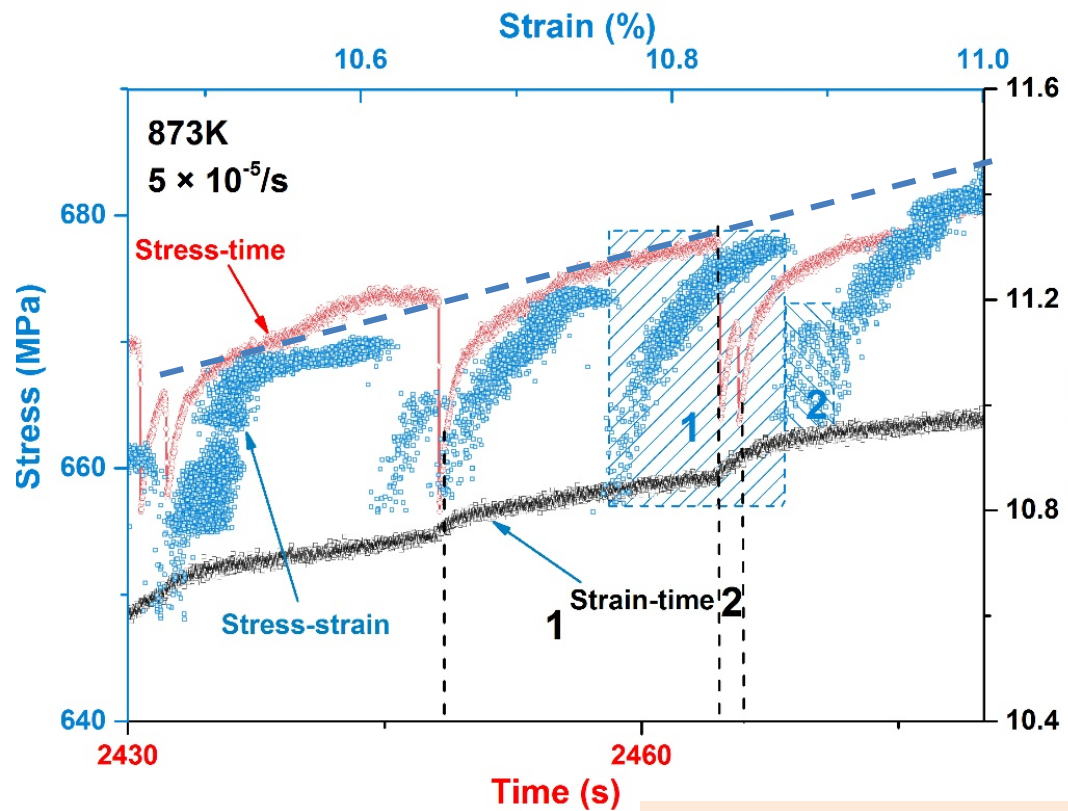
Interaction between the machine
and samples

$$\begin{aligned}\dot{\varepsilon}_0 &= 5 \times 10^{-5}/\text{s} \\ \dot{\varepsilon}_1 &= 1.15 \times 10^{-5}/\text{s} \\ \dot{\varepsilon}_2 &= 2.22 \times 10^{-4}/\text{s}\end{aligned}$$

Illustration of upward direction



At Strain Rate $5 \times 10^{-5}/\text{s}$ with Temperature of 873K



$$\dot{\varepsilon}_0 = 5 \times 10^{-5}/\text{s}$$

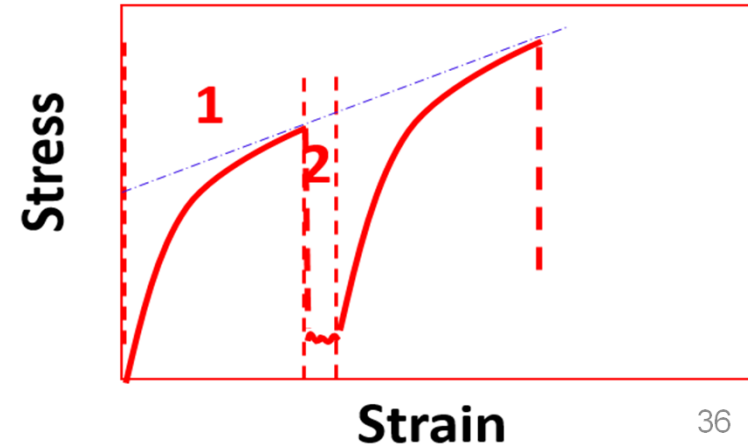
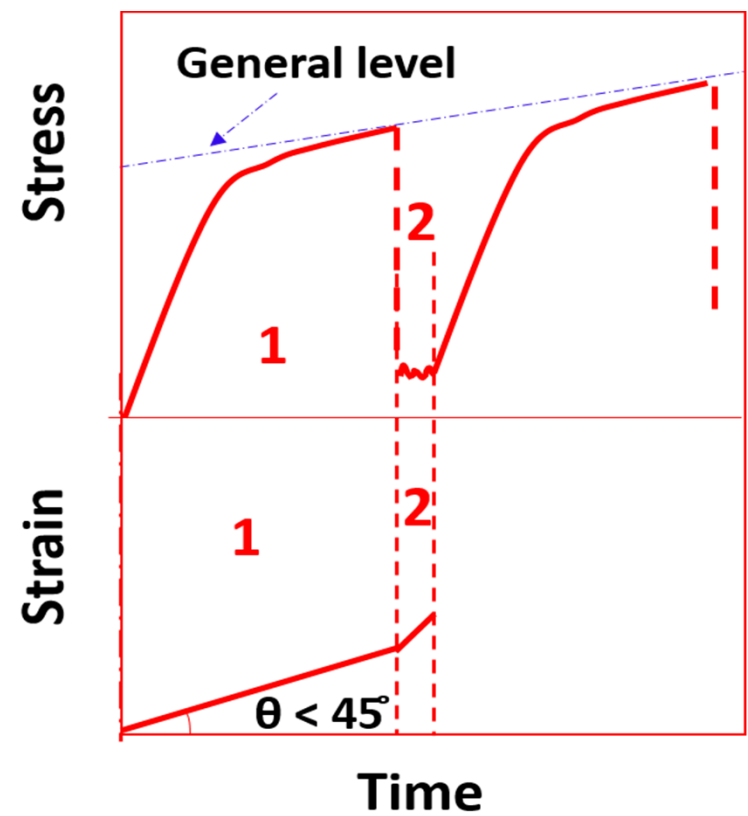
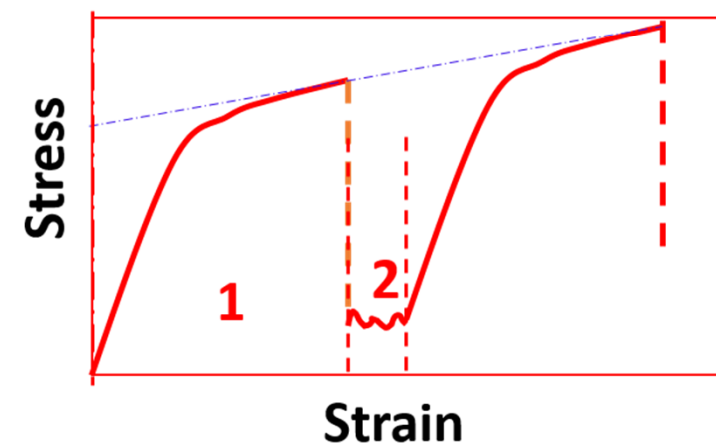
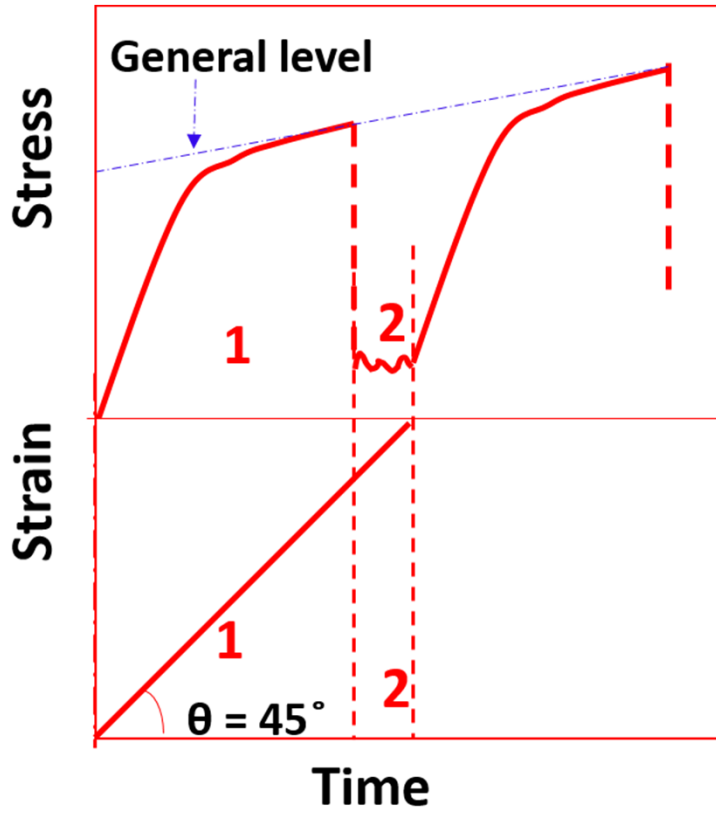
$$\dot{\varepsilon}_1 = 1.93 \times 10^{-5}/\text{s}$$

$$\dot{\varepsilon}_2 = 2.54 \times 10^{-4}/\text{s}$$

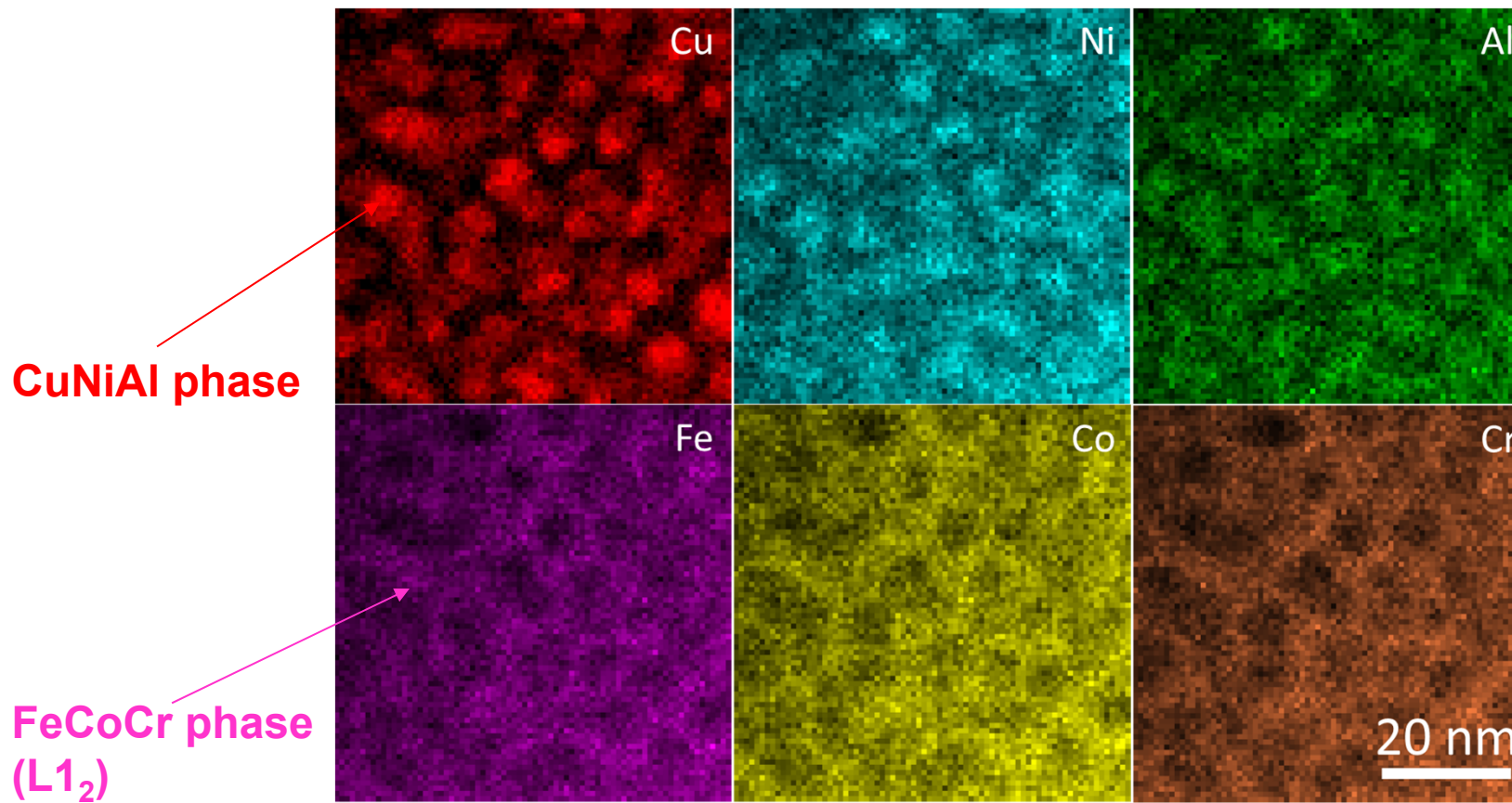
Assuming that at a strain rate of 1 s^{-1} , the angle θ between horizontal line and strain-time curve should be 45°

Illustration of downward direction

Downward direction

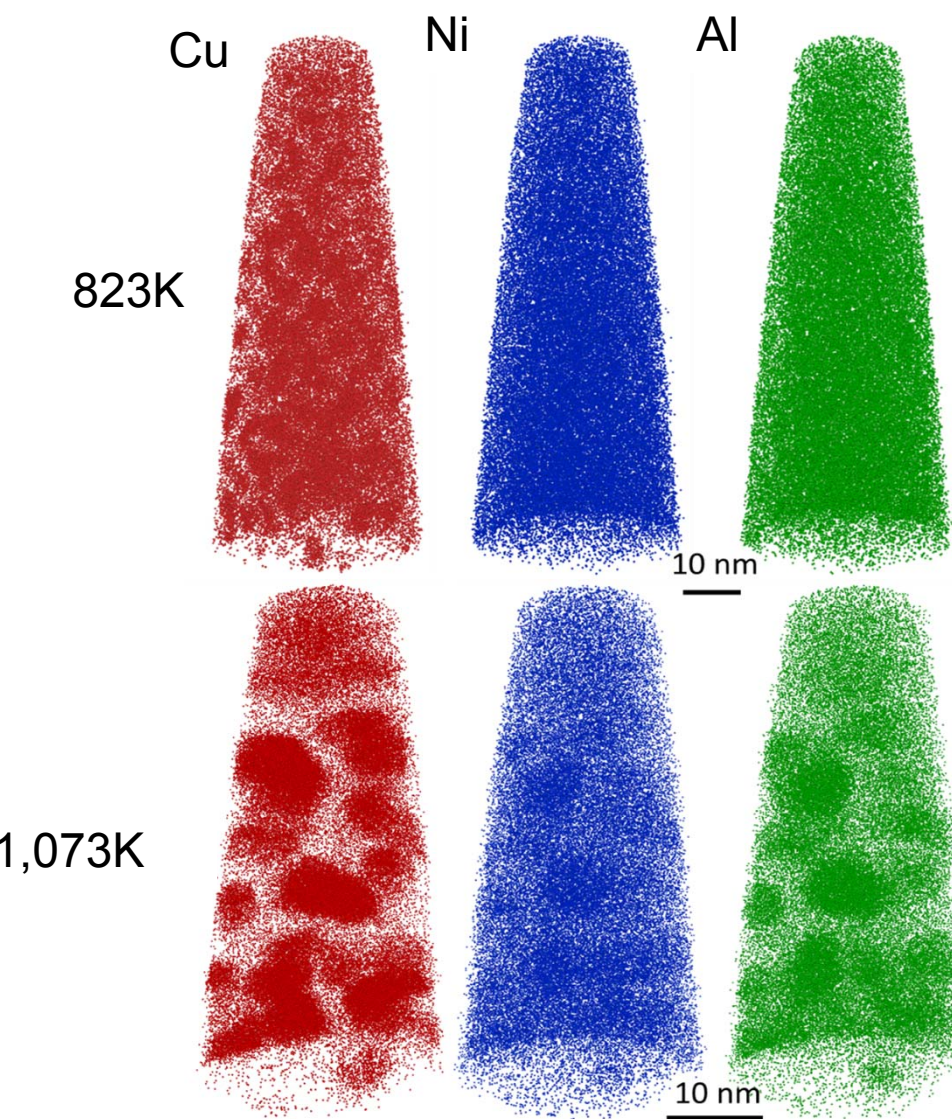


Energy Dispersive-Spectroscopy (EDS) Mapping of Each Elements



Scanning transmission electron microscopy energy-dispersive X-ray spectroscopy (STEM-EDS) mapping of the matrix phase in the sample compressed at 1,073K with strain rate of $5 \times 10^{-5}/\text{s}$

Reconstructed three-dimensional (3D) atom probe tomography (APT) after compression tests at the strain rate of $5 \times 10^{-5}/\text{s}$ with temperatures of 823K, and 1,073K



3D APT chemical mappings of the tested sample at 823K and 1,073K. The decomposition of the solid-solution phase into a NiAl phase can be seen with increasing annealing temperature.

Publications

1. M.-R. Chen, S.-J. Lin, J.-W. Yeh, S.-K. Chen, Y.-S. Huang, and C.-P. Tu, "Microstructure and Properties of Al_{0.5}CoCrCuFeNiTi_x (x=0–2.0) High-Entropy Alloys", *Materials Transactions*, 2006, 47(5), pp. 1395-1401.
2. J. Antonaglia, X. Xie, G. Schwarz, M. Wraith, J. Qiao, Y. Zhang, P. K. Liaw, J. T. Uhl, and **K. A. Dahmen**, "Tuned critical avalanche scaling in bulk metallic glasses", *Sci. Rep.*, 2014, 4, pp. 4382.
3. S. Y. Chen, X. Yang, **K. Dahmen**, P. Liaw, and Y. Zhang, "Microstructures and Crackling Noise of Al_xNbTiMoV High Entropy Alloys", *Entropy*, 2014, 16(2), pp. 870-884.
4. H. L. Hong, Q. Wang, C. Dong, and P. K. Liaw, "Understanding the Cu-Zn brass alloys using a short-range-order cluster model: significance of specific compositions of industrial alloys", *Sci. Rep.*, 2014, 4, pp. 7065.
5. E. W. Huang, J. Qiao, B. Winiarski, W. J. Lee, M. Scheel, C. P. Chuang, P. K. Liaw, Y. C. Lo, Y. Zhang, and M. Di Michiel, "Microyielding of core-shell crystal dendrites in a bulk-metallic-glass matrix composite", *Sci. Rep.*, 2014, 4, pp. 4394.
6. L. Huang, E. M. Fozo, T. Zhang, P. K. Liaw, and W. He, "Antimicrobial behavior of Cu-bearing Zr-based bulk metallic glasses", *Mater. Sci. Eng. C. Mater. Biol. Appl.*, 2014, 39, pp. 325-9.
7. H. Jia, F. Liu, Z. An, W. Li, G. Wang, J. P. Chu, J. S. C. Jang, Y. Gao, and P. K. Liaw, "Thin-film metallic glasses for substrate fatigue-property improvements", *Thin Solid Films*, 2014, 561, pp. 2-27.

Publications (cont'd)

8. Z. Tang, L. Huang, W. He, and P. Liaw, "Alloying and Processing Effects on the Aqueous Corrosion Behavior of High-Entropy Alloys", *Entropy*, 2014, 16(2), pp. 895-911.
9. T. T. Z. Yong Zhang, Zhi Tang, Michael C. Gao, **Karin A. Dahmen**, and Z. P. L. Peter K. Liaw, "Microstructures and properties of high-entropy", *Progress in Materials Science*, 2014, 61, pp. 93, p. 1.
10. P. F. Yu, S. D. Feng, G. S. Xu, X. L. Guo, Y. Y. Wang, W. Zhao, L. Qi, G. Li, P. K. Liaw, and R. P. Liu, "Room-temperature creep resistance of Co-based metallic glasses", *Scripta Materialia*, 2014, 90-91, pp. 45-48.
11. Y. Zhang, M. Li, Y. D. Wang, J. P. Lin, **K. A. Dahmen**, Z. L. Wang, and P. K. Liaw, "Superelasticity and Serration Behavior in Small-Sized NiMnGa Alloys", *Advanced Engineering Materials*, 2014, 16(8), pp. 955-960.
12. Y. Zhang, Z. P. Lu, S. G. Ma, P. K. Liaw, Z. Tang, Y. Q. Cheng, and M. C. Gao, "Guidelines in predicting phase formation of high-entropy alloys", *MRS Communications*, 2014, 4(2), pp. 57-62.
13. L. J. Santodonato, Y. Zhang, M. Feygenson, C. M. Parish, M. C. Gao, R. J. Weber, J. C. Neuefeind, Z. Tang, and P. K. Liaw, "Deviation from high-entropy configurations in the atomic distributions of a multi-principal-element alloy", *Nature Communications*, 2015, 6, pp. 5964.

2014 TMS meetings San Diego, CA, USA, February 16-20, 2014
Presentations

1. Micro-segregation and Metastable Phase Stability of Cast Ti-Zr-Hf-Ni-Pd-Pt High Entropy Alloys, Y. Yokoyama, S. Itoh, Y. Murakami, I. Narita, G. Wang, and P. K. Liaw.
2. Modeling Plastic Deformation and the Statistics of Serrations in the Stress Versus Strain Curves of Bulk Metallic Glasses, **K. Dahmen**, J. Antonaglia, X. Xie, J. W. Qiao, Y Zhang, J. Uh, and P. K. Liaw.
3. Aluminum Alloying Effects on Lattice Types, Microstructures, and Mechanical Behavior of High-entropy Alloys Systems, Z. Tang, M. Gao, H. Y. Diao, T. F. Yang, J. P. Liu, T. T. Zuo, Y. Zhang, Z. P. Lu, Y. Q. Cheng, Y. W. Zhang, **K. Dahmen**, P. K. Liaw, and T. Egami.
4. Characterization of Inhomogeneous Deformation and Serrated Flows in Bulk Metallic Glasses, X. Xie, J. Antonaglia, J. W. Qiao, G. Y. Wang, Y. Zhang, Y. Yokoyama, **K. Dahmen**, and P. K. Liaw.
5. The Influence of Cu and Al on the Microstructure, Mechanical Properties and Deformation Mechanisms in the High Entropy Alloys CrCoNiFeCu, CrCoNiFeAl1.5 and CrCoNiFeCuAl1.5, B. Welk, B. B. Viswanathan, M. Gibson, P. K. Liaw, and H. Fraser.
6. Ultra Grain Refinement in High Entropy Alloys: N. Tsuji, I. Watanabe, N. Park, D. Terada, A. Shibata, Y. Yokoyama, P. K. Liaw.

2014 TMS meetings San Diego, CA, USA, February 16-20, 2014
Presentations (cont'd)

7. Nanostructure Evolution through High-pressure Torsion and Recrystallization in a High-entropy CrMnFeCoNi Alloy, N. Park, A. Shibata, D. Terada, Y. Yokoyama, P. K. Liaw, and N. Tsuji.
8. Environmental-temperature Effect on a Ductile High-entropy Alloy Investigated by In Situ Neutron-diffraction Measurements, E. W. Huang, C. Lee, D. J. Yu, K. An, P. K. Liaw, and J. W. Yeh.
9. Mechanical Behavior of an Al0.1CoCrFeNi High Entropy Alloy, M. Komarasamy, N. Kumar, Z. Tang, R. Mishra, and P. K. Liaw.
10. Using the Statistics of Serrations in the Stress Strain Curves to Extract Materials Properties of Slowly-sheared High Entropy Alloys, Karin Dahmen, X. Xie, J. Antonaglia, M. Laktionova, E. Tabachnikova, J. W. Qiao, J. W. Yeh, C. W. Tsai, J. Uh, and P. K. Liaw.
11. Characterizing Multi-component Solid Solutions Using Order Parameters and the Bragg-Williams Approximation, L. Santodonato, and P. K. Liaw.
12. The Influence of Alloy Composition on the Interrelationship between Microstructure Mechanical Properties of High Entropy Alloys with BCC/B2 Phase Mixtures, B. Welk, D. Huber, J. Jensen, G. Viswanathan, R. Williams, P. K. Liaw, M. Gibson, D. Evans, and H. Fraser.

2014 TMS Meeting, San Diego, CA, USA, February 16-20, 2014
Presentations (cont'd)

13. The Oxidation Behavior of AlCoCrFeNi High-entropy Alloy at 1023-1323K (750-1050°C),
Wu Kai, W.S. Chen, C.C. Sung, Z. Tang, and P. K. Liaw.
14. 2014 TMS Meeting, San Diego, CA, USA, February 16-20, 2014 Strain-rate Effects on the
Structure Evolution of High Entropy Alloys, X. Xie, J. Antonaglia, J. P. Liu, Z. Tang, J. W.
Qiao, G. Y. Wang, Y. Zhang, **K. Dahmen**, and P. K. Liaw.
15. 2014 TMS Meeting, San Diego, CA, USA, February 16-20, 2014 Neutron diffraction studies
on creep deformation behavior in a high-entropy alloy CoCrFeMnNi under high
temperature and low strain rate, W. C. Woo, E. W. Huang, J. W. Yeh, P. K. Liaw, and H.
Choo.
16. 2014 TMS Meeting, San Diego, CA, USA, February 16-20, 2014 The Hot Corrosion
Resistance Properties of Al_xFeCoCrNi, S. Y. Yang, M. Habibi, L. Wang, S. M. Guo, Z. Tang,
P. K. Liaw, L. X. Tan, C. Guo, and M. Jackson.

2014

Presentations (cont'd)

17. University of Science and Technology, Beijing, China, June 9, 2014 (Invited) Characterization of Serrated Flows in High-Entropy Alloys and Bulk-Metallic Glasses, P. K. Liaw.
18. Beihang University, Beijing, China, June 10, 2014 (Invited) Characterization of Serrated Flows in High-Entropy Alloys and Bulk-Metallic Glasses, P. K. Liaw.
19. Workshop on Deformation, Damage and Life Prediction of Structural Materials, National Institute of Materials Science, Japan, June 23-24, 2014 (Keynote) Fatigue Behavior of Bulk Metallic Glasses and High Entropy Alloys, Peter K. Liaw.
20. 2014 Gordon Research Conferences, Hong Kong, China, July 20-25, 2014 (poster) Loading Condition Effects on the Serrated Flows in Bulk Metallic Glasses (BMGs), X. Xie, J. Antonaglia, J. W. Qiao, Y. Zhang, G. Y. Wang, **K. A. Dahmen**, and P. K. Liaw.
21. 2014 Gordon Research Conferences, Hong Kong, China, July 20-25, 2014 (poster) Loading Condition Effects on the Serrated Flows in Bulk Metallic Glasses (BMGs), X. Xie, J. Antonaglia, J. W. Qiao, Y. Zhang, G. Y. Wang, **K. A. Dahmen**, and P. K. Liaw.
22. Central South University, Changsha, Hunan, China, July 26th, 2014 (Invited) Serration Behaviors of High Entropy Alloys and Bulk Metallic Glasses, X. Xie, J. Antonaglia, J. W. Qiao, Y. Zhang, G. Y. Wang, Y. Yokoyama, **K. A. Dahmen**, and P. K. Liaw.

2014

Presentations (cont'd)

23. Dalian University of Technology, Dalian, Liaoning, China, July 28th, 2014 (Invited)
Serration Behaviors of High Entropy Alloys and Bulk Metallic Glasses, X. Xie, J. Antonaglia, J. W. Qiao, Y. Zhang, G. Y. Wang, Y. Yokoyama, **K. A. Dahmen**, and P. K. Liaw.
24. University of California, Los Angeles, California, US, October 17th, 2014 (Invited)
Serration Behaviors of High Entropy Alloys and Bulk Metallic Glasses, X. Xie, J. Antonaglia, J. W. Qiao, Y. Zhang, G. Y. Wang, Y. Yokoyama, **K. A. Dahmen**, and P. K. Liaw.
25. Yale University, New Haven, Connecticut, US, October 10th, 2014 (Invited) Serration Behaviors of High Entropy Alloys and Bulk Metallic Glasses, X. Xie, J. Antonaglia, J. W. Qiao, Y. Zhang, G. Y. Wang, Y. Yokoyama, **K. A. Dahmen**, and P. K. Liaw.
26. University of Cambridge, Cambridge, United Kingdom, December 8th, 2014 (Invited)
Serration Behaviors of High Entropy Alloys and Bulk Metallic Glasses, X. Xie, J. Antonaglia, J. W. Qiao, Y. Zhang, G. Y. Wang, Y. Yokoyama, **K. A. Dahmen**, and P. K. Liaw.

2015 TMS Meeting, Orlando, FL, USA, March 15-19, 2015

Presentations

- 27. (Invited) On the Friction Stress and Hall-Petch Coefficient of a Single Phase Face-Centered-Cubic High Entropy Alloy, Al0.1FeCoNiCr, Nilesh Kumar, Mageshwari Komarasamy, Zhi Tang, Rajiv Mishra, and Peter Liaw.**
- 28. (Invited) Strength and Deformation of Individual Phases in High-Entropy Alloys, A. Giwa, Haoyan Diao, Xie Xie, S, Y, Chen, Zhi Tang, Karin Dahmen, and Peter Liaw.**
- 29. Al-Co-Cr-Fe-Ni Phase Equilibria and Properties, Zhi Tang, Oleg Senkov, Chuan Zhang, Fan Zhang, Carl Lundin, and Peter Liaw.**
- 30. Fatigue Behavior of an Al0.1CoCrNiFe High Entropy Alloy, Bilin Chen, Xie Xie, Shuying Chen, Ke An, and Peter Liaw.**
- 31. (Invited) Flow and Fracture Behavior of a High Entropy Alloy, Yong Zhang, Peter Liaw, and John Lewandowski.**
- 32. (Invited) Modeling Plastic Deformation and the Statistics of Serrations in the Stress versus Strain Curves of Bulk Metallic Glasses and Other Materials, Karin Dahmen, James Antonaglia, Wendelin Wright, Xiaojun Gu, Xie Xie, Michael LeBlanc, Junwei Qiao, Yong Zhang, Todd Hufnagel, Jonathan Uhl, and Peter Liaw.**

2015 2015 TMS Meeting, Orlando, FL, USA, March 15-19, 2015
Presentations (cont'd)

33. (Invited) Deformation Twinning in the High-Entropy Alloy Induced by High Pressure Torsion at Room Temperature, Gong Li1, P.F. Yu, P.K. Liaw, and R.P. Liu.
34. Microstructures and Mechanical Behavior of Multi-Component AlxCrCuFeMnNi High-Entropy Alloys, Haoyan Diao, Zhinan An1; Xie Xie, Gongyang Wang, Chuan Zhang, Fan Zhang, Guangfeng Zhao, Fuqian Yang, **Karin Dahmen**, and Peter Liaw.
35. The Characterization of Serrated Plastic Flow in High Entropy Alloys, Shuying Chen, Xie Xie, James Antonaglia, Junwei Qiao, Yong Zhang, **Karin Dahmen** and Peter Liaw.
36. (Invited) A Model for the Deformation Mechanisms and the Serration Statistics of High Entropy Alloys, **Karin Dahmen**, Bobby Carroll, Xie Xie, Shuying Chen, James Antonaglia, Braden Brinkman, Michael LeBlanc, Marina Laktionova, Elena Tabachnikova, Zhi Tang, Junwei Qiao, Jien Wei Yeh, Chi Lee, Che Wei Tsai, Jonathan Uhl, and Peter Liaw.
37. (Invited) Segregation and Ti-Zr-Hf-Ni-Pd-Pt High Entropy Alloy under Liquid State, Y. Yokoyama, Norbert Mattern, Akitoshi Mizuno, Gongyang Wang, and Peter Liaw.
38. (Invited) Computational-Thermodynamics-Aided Development of Multiple-Principal-Component Alloys, Chuan Zhang, Fan Zhang, Shuanglin Chen, Weisheng Cao, Jun Zhu, Zhi Tan, Haoyan Diao, and Peter Liaw.
39. (Invited) Sputter Deposition Simulation of High Entropy Alloy via Molecular Dynamics Methodology, Yunche Wang, Chun-Yi Wu, Nai-Hua Yeh, and Pete Liaw. 140

Conclusions

- The prediction of the simple avalanche model could be used to describe the serration behavior
- The serrated flow with different types could be observed in $\text{Al}_{0.5}\text{CoCrCuFeNi}$ alloys in a certain temperature and strain rate range.
- The serration changes from the upward to downward directions with the temperature increasing from 673K to 873K.
- The possible explanations for the upward and downward serrations are suggested.
- Nanophases of Cu-rich and FeCoCr-rich L1_2 phases were found after high-temperature deformation.

Backup Slides

rocedure (Chi Lee, Che-Wei Tsai, Jien Wie Yeh, Peter Li)



I. Experimental Procedure

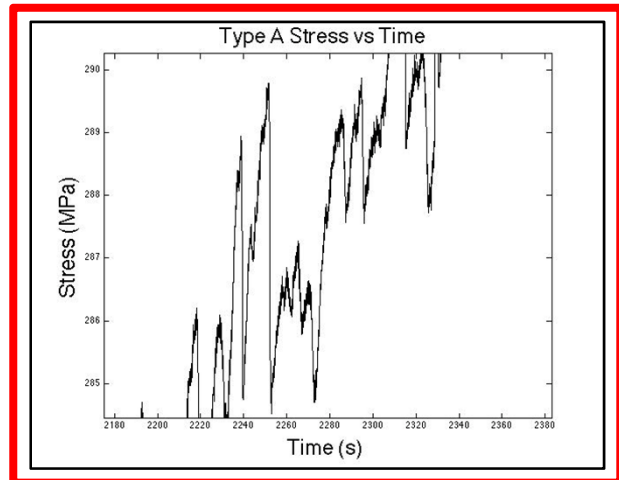
1. CoCrFeMnNi cut into strips
2. Strips tensile-stretched at different temperatures
3. Stress data recorded

II. Data Analysis

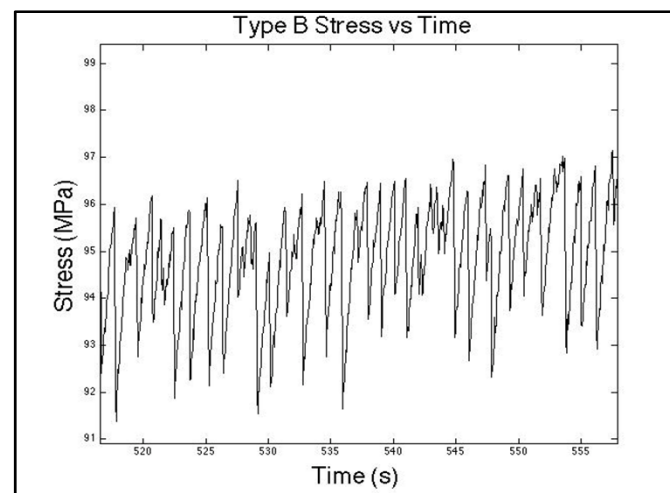
Size distributions compiled and compared with theory



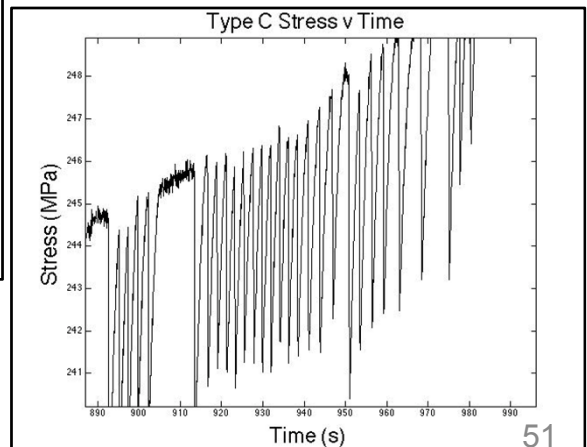
Chi Lee, Che-Wei Tsai, Jien Wie Yeh, Peter Liaw, Bobby Carroll, Michael LeBlanc, Braden Brinkman, Jonathan T. Uhl, KD



TYPE A: CoCrFeMnNi at 375°C at 10^{-4} /s strain rate
– Exhibits power law slip size distributions [with the mean field exponent \$\kappa=1.5\$!](#)



Type B example from CoCrFeNi 700°C at 10^{-4} /s strain rate.

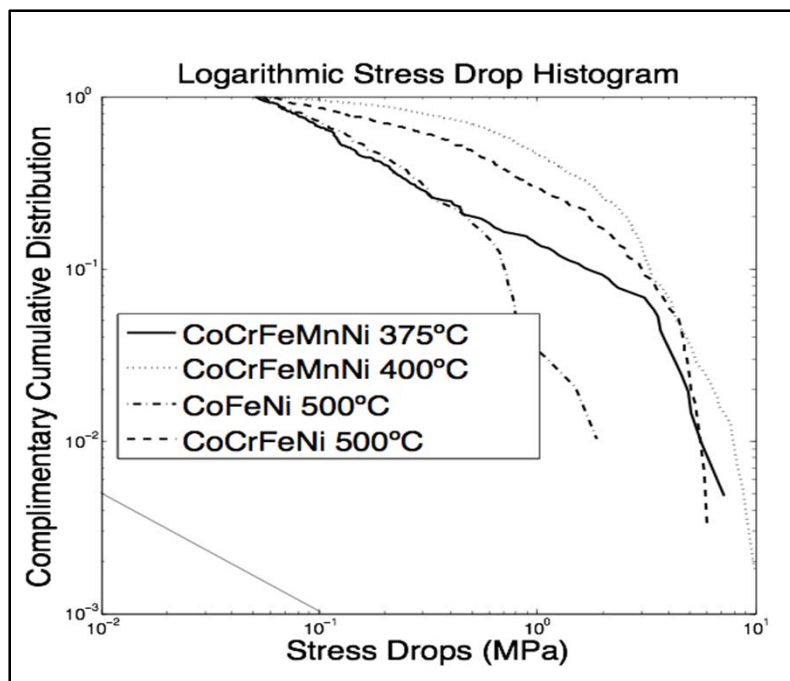


Type C example from CoCrFeNi 600°C at 10^{-4} strain rate.

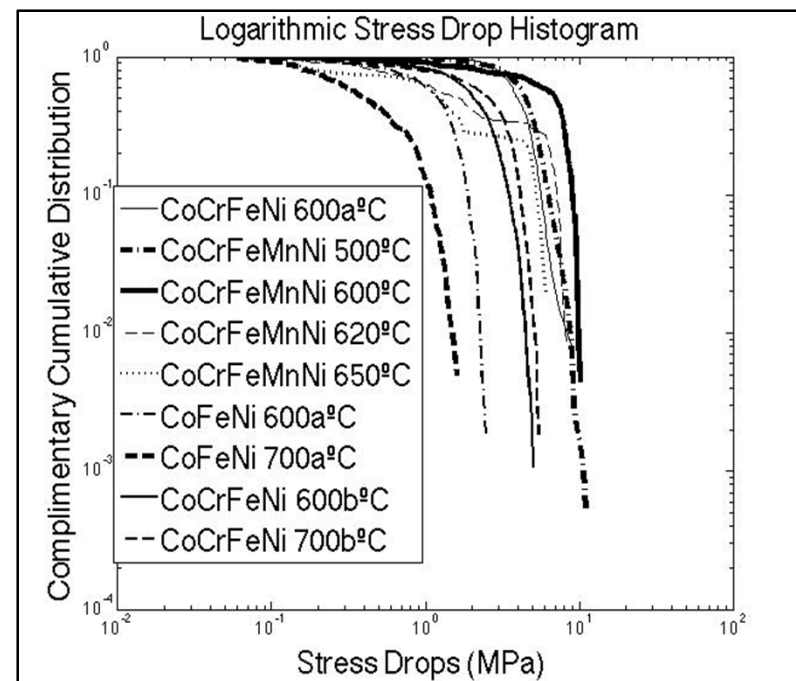
Slip Size Distributions for different materials and temperatures

Chi Lee, Che-Wei Tsai, Jien Wie Yeh, Peter Liaw,
Bobby Carroll, Michael LeBlanc, Braden Brinkman, Jonathan T. Uhl, KD

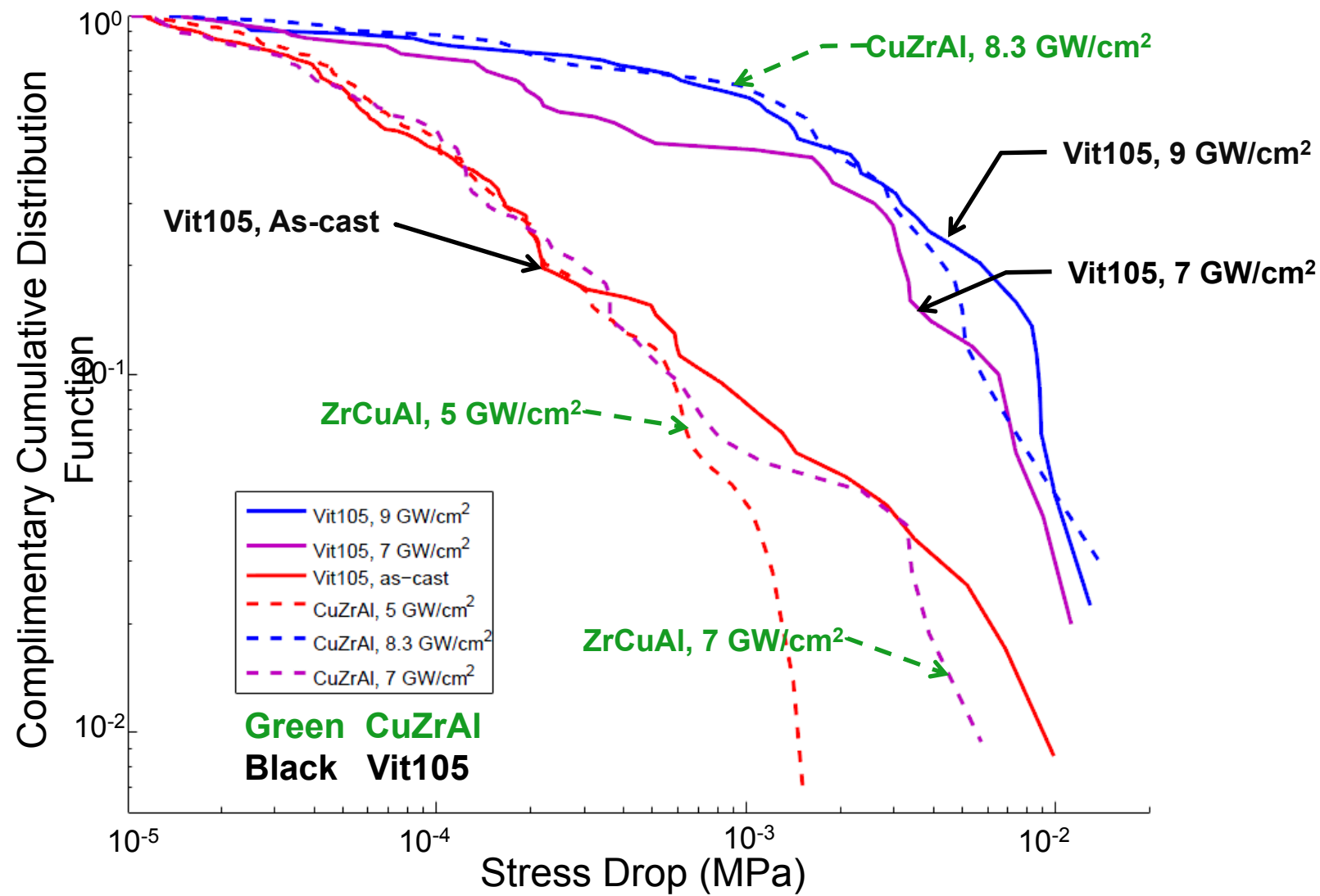
Type A or close to Type A



Type B and C

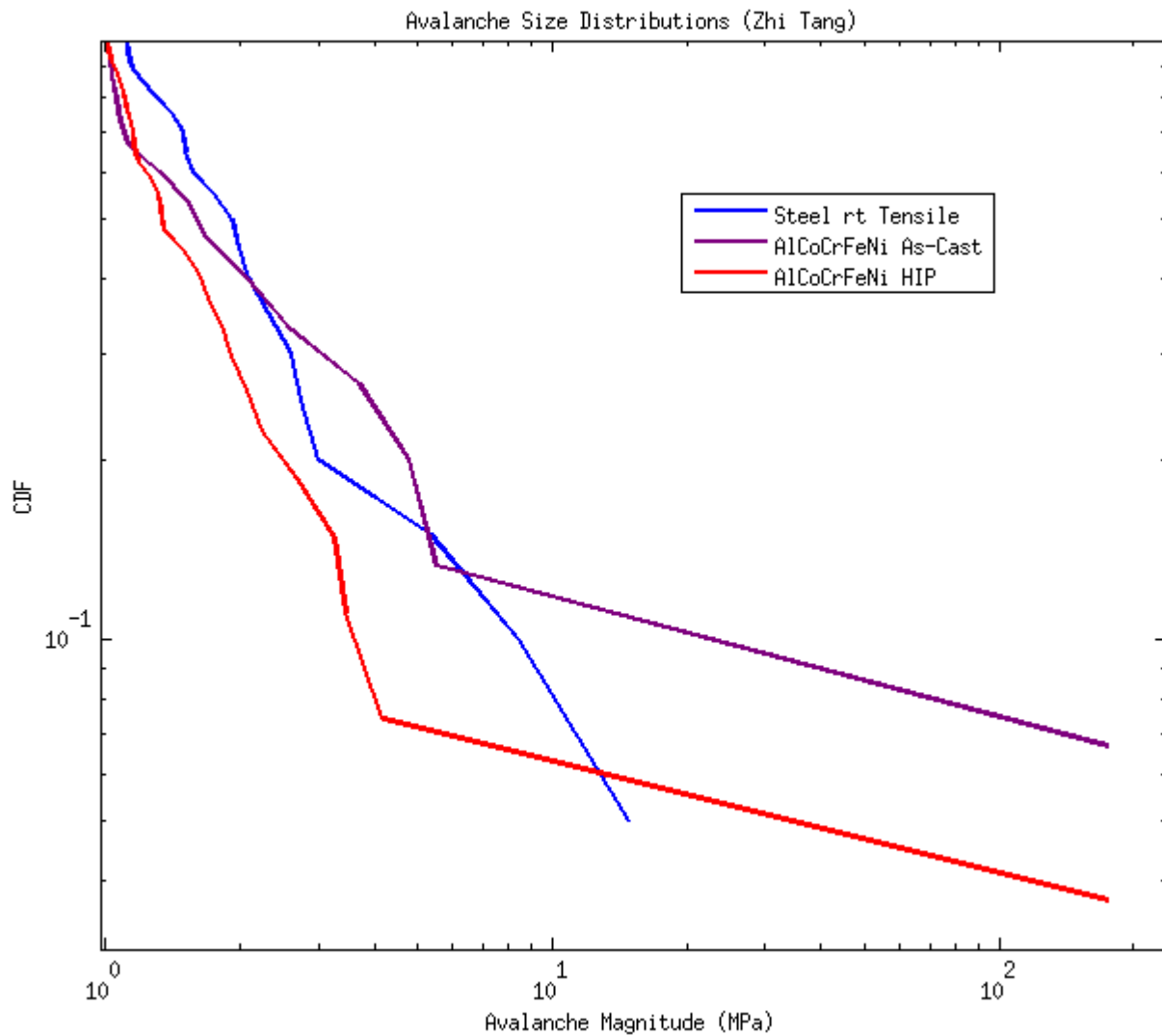


BMG: Avalanche size distributions after Laser Treatment (X. Xie, P. Liaw, Tue. 12:05pm, Bowie A)

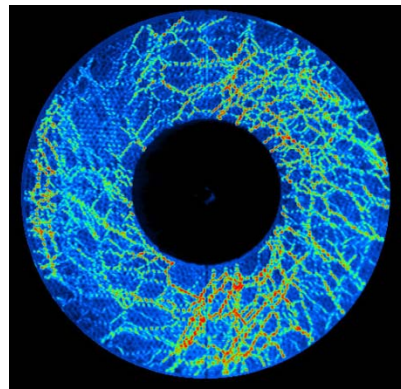
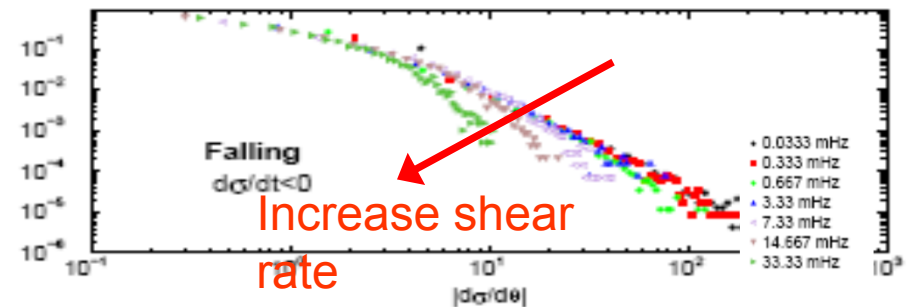
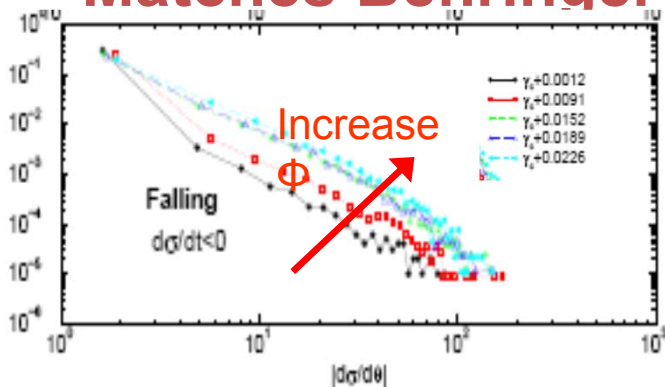


$\text{Vit105} = \text{Zr}_{52.5}\text{Cu}_{17.9}\text{Ni}_{14.6}\text{Al}_{10}\text{Ti}_5$, $\text{ZrCuAl} = \text{Zr}_{50}\text{Cu}_{40}\text{Al}_{10}$

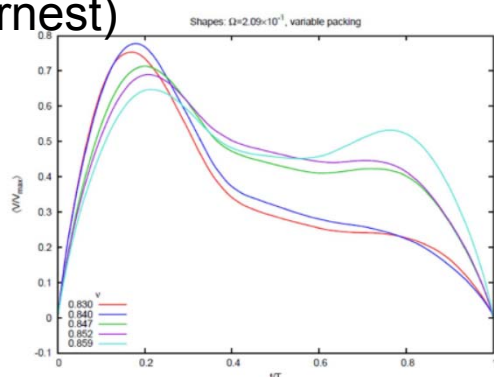
Zhi Tang, Peter Liaw AlCoCrFeNi (tensile tests): future theory



Matches Behringer and Hartley's experiments (Tyler)



Avalanche Shapes (Tyler Earnest)

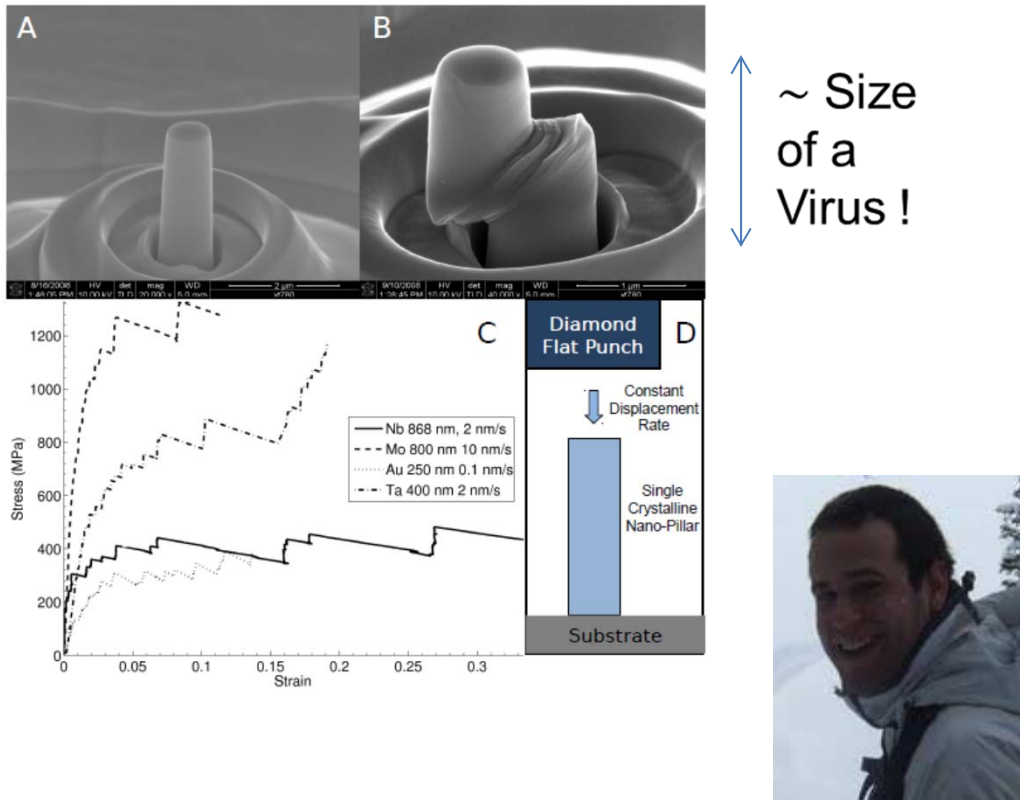


| Power law exponent or other universal quantity | Mean Field Theory (MFT) | granular experiment [6,8-10,20-21,29] | granular simulation [2-4] |
|--|--|---------------------------------------|--|
| avalanche size distribution $D(s) \sim s^{-\kappa}$ | $\kappa=1.5$ | $\kappa=1.5$ | |
| avalanche duration distribution $D(T) \sim T^{-\alpha}$ | $\alpha=2$ | $\alpha=2$ or exponential? | |
| stress drop rate distribution $\sim D(V) \sim V^{-\psi}$ | $\psi=2$ | $\psi=2$ [29] | |
| power spectrum $P(\omega) \sim \omega^\phi$ | $\phi=2$ if $v \approx 1$; $\phi=0$ if $v \ll 1$ | $\phi=1.8-2.5, 2$ | $\phi=2$ if solid $\phi=0$ if fluid |
| Source time function averaged over avalanches of duration T. | Symmetric (parabola) | Symmetric (parabola ? Gaussian ?) | Symmetries in fctn ? |
| Stick slip statistics | Yes, if $\varepsilon > 0$ and $v > v^*$ | Yes, sometimes | Yes (mode switching) |
| Mode switching (between powerlaw and stick slip) | Yes, if $\varepsilon > 0$ and $v > v^*$ | Yes, sometimes | Yes in solid regime |

Checking the Predictions of Simple Analytic Model with Experiments on μm -size and nano-crystal

(Nir Friedman, Jennings, Tsekenis, Kim, Tao, Uhl, Greer, KD, PRL 2012)

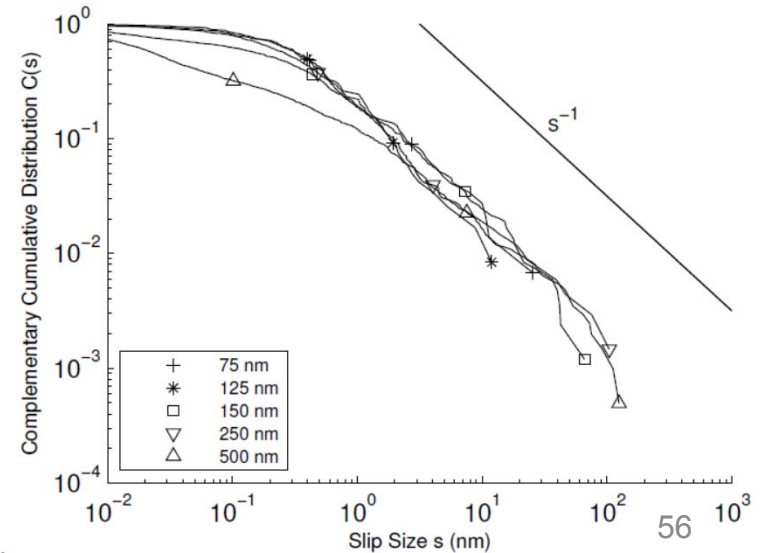
Greer group (Caltech) Experiments: Compressing Nanopillars, the Size of a Virus:



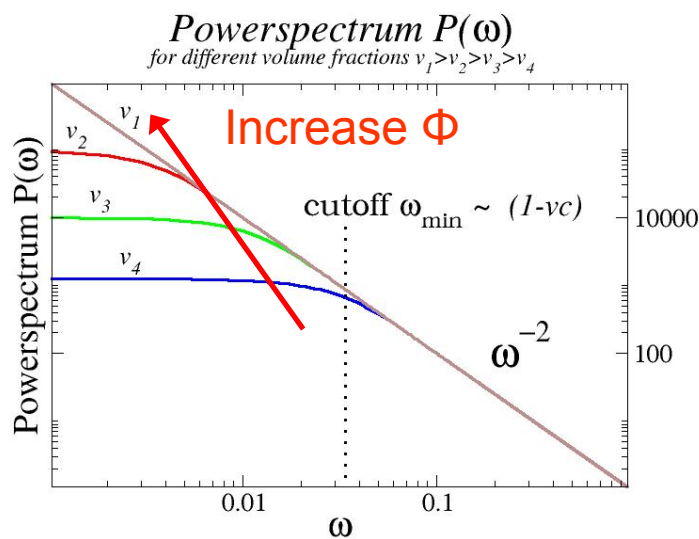
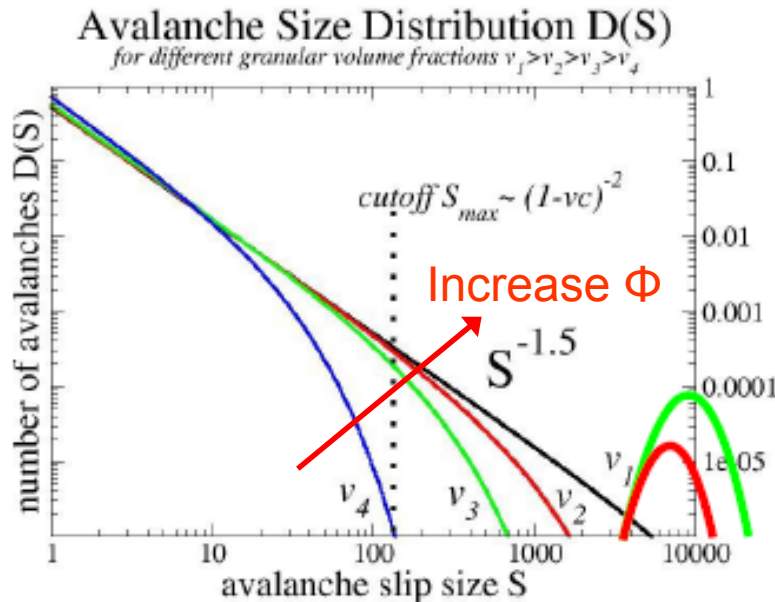
Nir
Friedman

**Experiments agree
with simple mean field
model predictions**

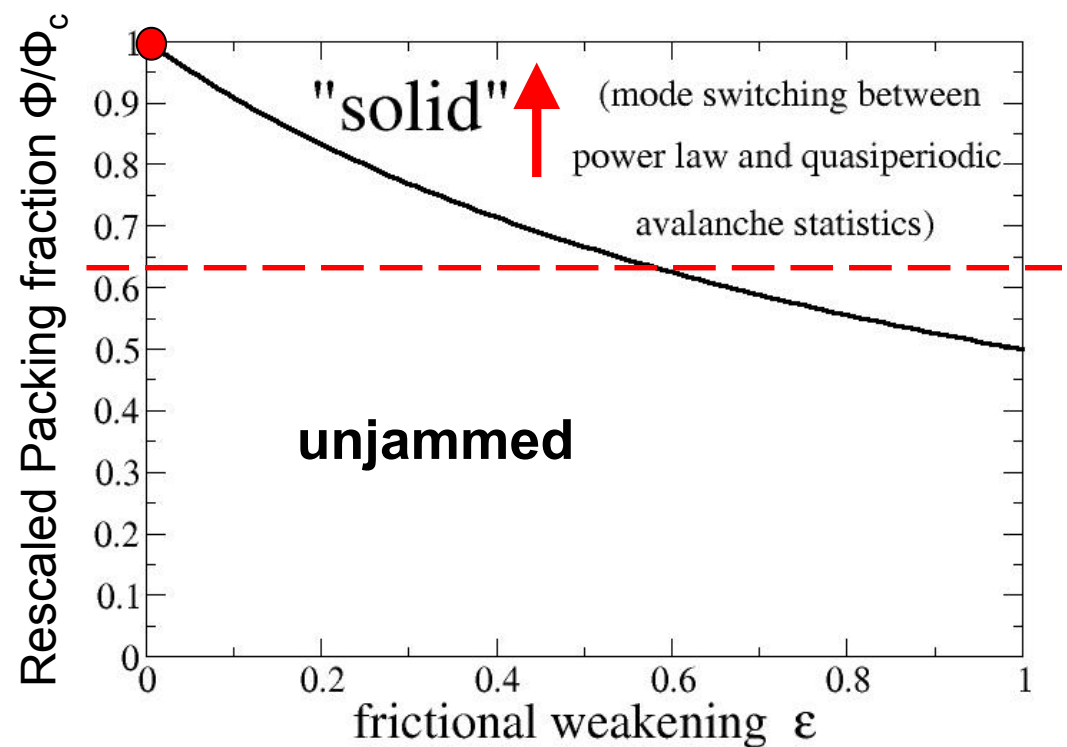
(FCC, BCC and 7 different materials)



Model results for avalanches in sheared granular



Braden Brinkman Th 4:54pm
Dynamical Phase Diagram



KD, D. Ertas, Y. Ben-Zion, PRE 1998

KD, Ben-Zion, Uhl, Nature Physics 2011

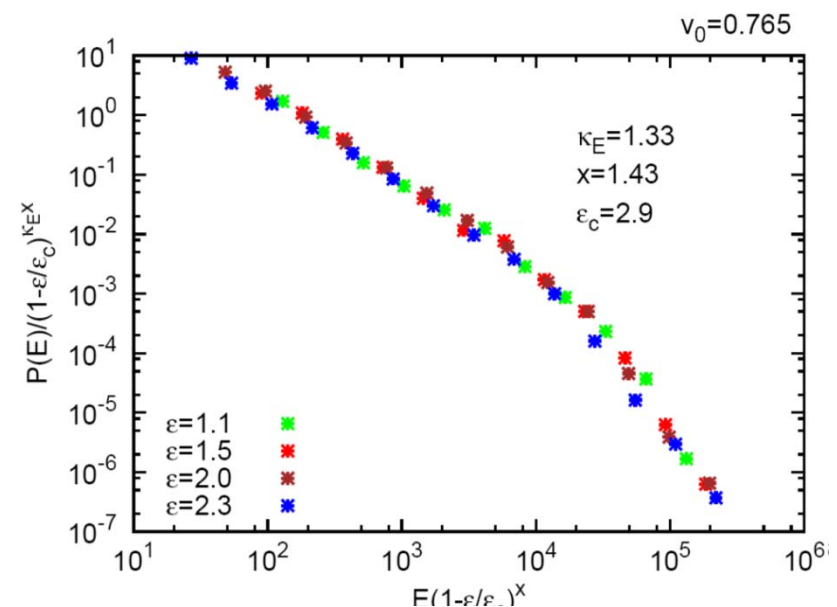
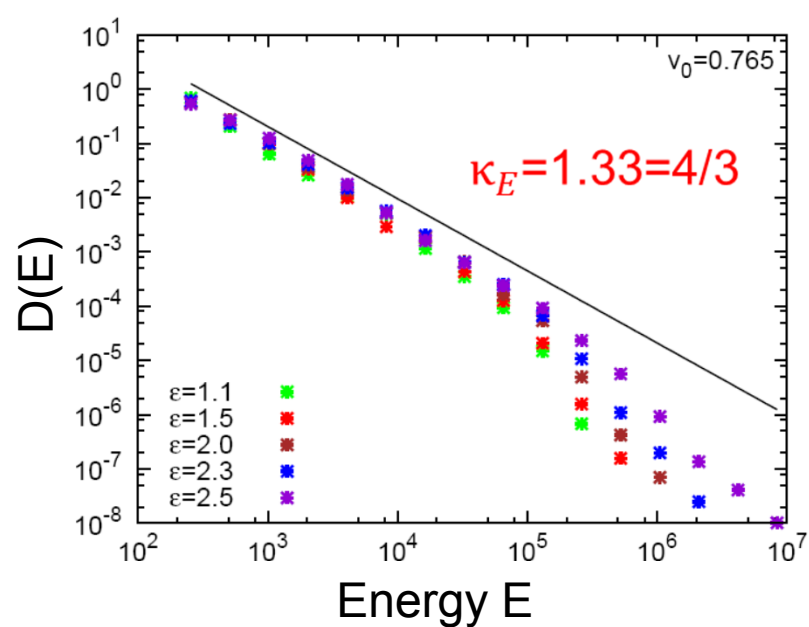
Simulations and Simple Model agree! (PRL12, PRE 2013, EPL 2013)

DDD and PFC: Tsekenis, Chan, Fehm, Goldenfeld, Dantzig, Uhl, KD MFT: LeBlanc, Angheluta, Goldenfeld, KD;
 Discrete Dislocation Dynamics Simulations, Phase Field Crystal Simulations (PFC code from the Goldenfeld Group)

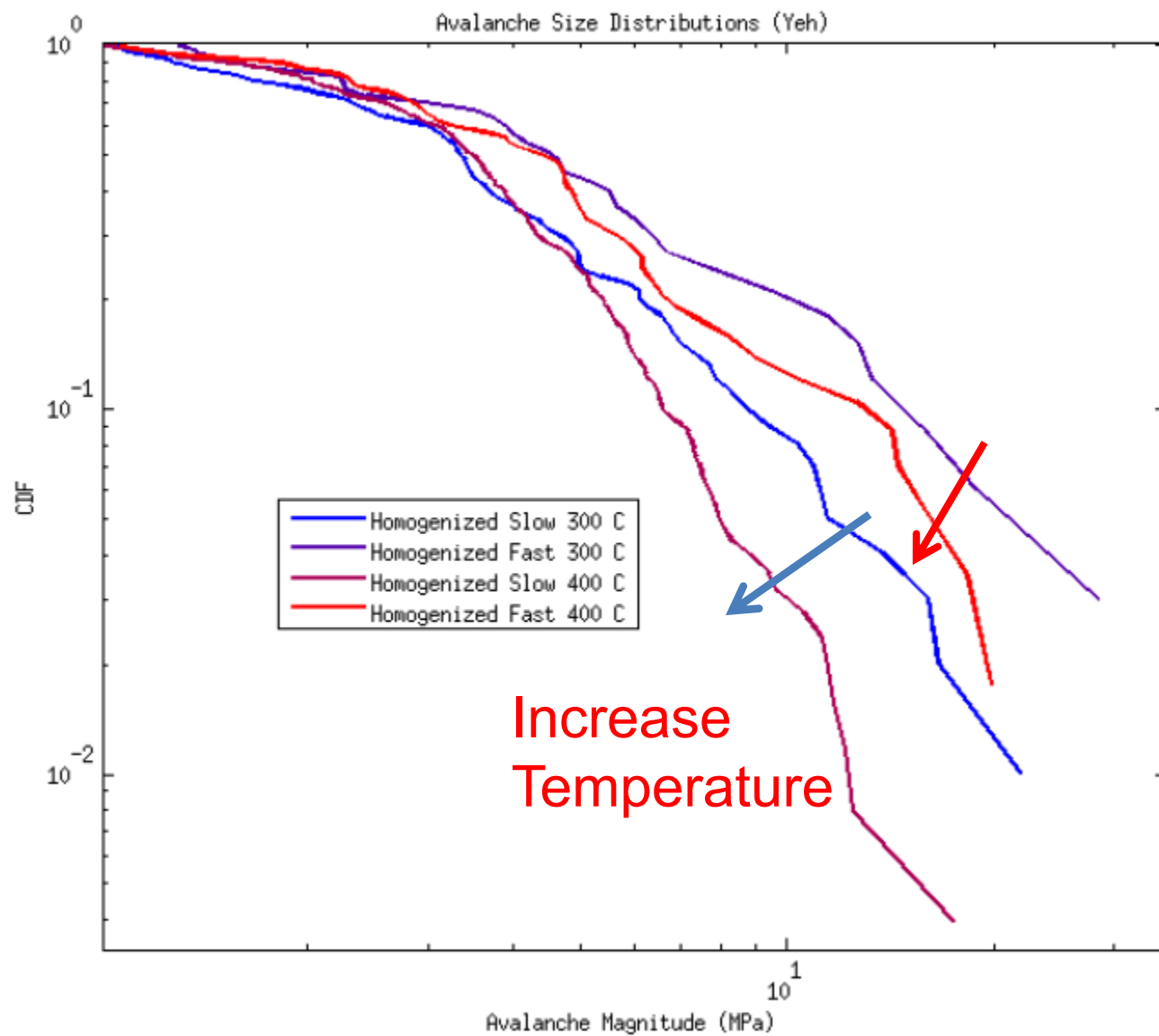
| quantity | exponent | our simulations | MFT simulations | experiments |
|--|--------------------------------------|-----------------|-----------------|--|
| $D_S(S, \tau)$ | κ | ~ 1.5 | $\frac{3}{2}$ | 1.4[1, 2] 1.5[3] |
| $D(V_{\max})$ | — | — | 2 | — 2.0 ± 0.1 [4], 1.5-2[5], 1.2-2.2[6] |
| $D_S(S, \tau)$ | $\frac{1}{\sigma}$ | 2 | 2 | 2[1] |
| $D_T(T, \tau)$ | $1 + \frac{\kappa-1}{\sigma\nu z}$ | 2.0 | 2 | |
| $D_T(T, \tau)$ | νz | 1 | 1 | |
| $D_E(E, \tau)$ | $1 + \frac{\kappa-1}{2-\sigma\nu z}$ | 1.3 | $\frac{4}{3}$ | |
| $D(V_{\max}^2)$ | — | — | 3/2 | 1.8 ± 0.2 [7] 1.6[7], 1.5 ± 0.1 [4] |
| $D_E(E, \tau)$ | $\frac{2-\sigma\nu z}{\sigma}$ | 3 | 3 | |
| $\langle S \rangle \sim T^{1/\sigma\nu z}$ | $1/\sigma\nu z$ | ~ 2.0 | 2 | |
| $\langle T \rangle \sim S^{\sigma\nu z}$ | $\sigma\nu z$ | ~ 0.5 | $\frac{1}{2}$ | |
| $\langle E \rangle \sim S^{2-\sigma\nu z}$ | $2 - \sigma\nu z$ | ~ 1.5 | $\frac{3}{2}$ | |
| $V(t)_{\text{shapes}} \sim T^{\frac{1}{\sigma\nu z}-1}$ | $\frac{1}{\sigma\nu z}$ | ~ 2 | 2 | |
| $PS_{\text{int}}(\omega)$ | $\frac{1}{\sigma\nu z}$ | ~ 2 | 2 | |
| $\langle v \rangle \sim (1 - \frac{\tau}{\tau_c})^\beta$ | β | ~ 1.1 | 1 | 1.8[8] |

Simple Analytic Mean Field Theory Predictions agree also with Phase Field Crystal Simulations at Finite Temperature

(Chan, Tsekenis, Dantzig, Dahmen, Goldenfeld PRL 2010 and ongoing)



Yeh: Al₅Cr₁₂Fe₃₅Mn₂₈Ni₂₀

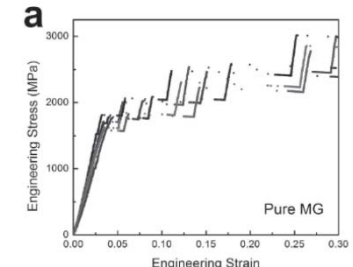


One Tuning Parameter:

- Weakening ϵ

Two Experimentally Relevant Boundary Conditions:

- Slow strain-rate loading condition ($<10^{-4}/\text{s}$)
- Slow stress-rate loading condition

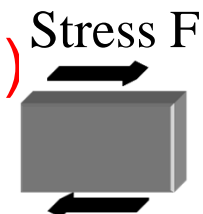


Strain-rate v



EXACT Predictions in 3 Dimensions (no fitting)

- Histograms of slip-sizes, durations, power spectra, ...
- Brittle ($\epsilon>0$), ductile ($\epsilon=0$), & hardening materials ($\epsilon<0$)



Applied to: Crystals, BMGs, High Entropy Alloys,...

Predictions agree with first experiments,

Many predictions for future experiments...

Useful for: materials tests, parameters, lifetime,...

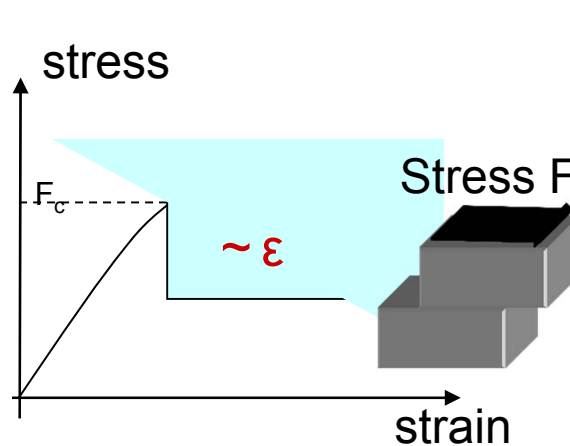
Our Simple Analytic Model of Plasticity (PRL '09, '12, Nature Physics '11, Adv. Fctl. Materials '12)

Microstructure properties of high-entropy Alloys (Zhang, Zuo, Tang, Gao, KD, Liaw, Lu) Prog. Mat. Sc. 2014

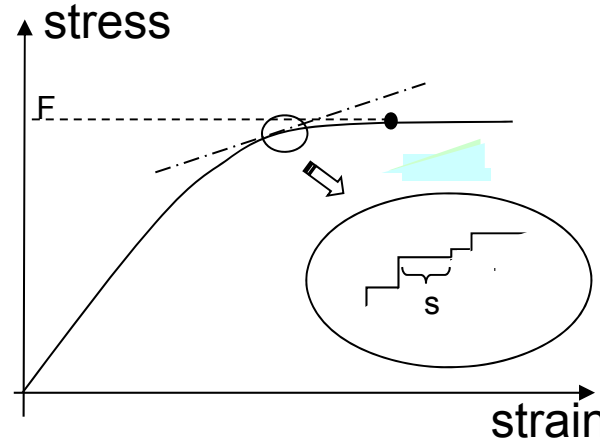
Simple Analytic Model for deformation under shear:

Main Results:

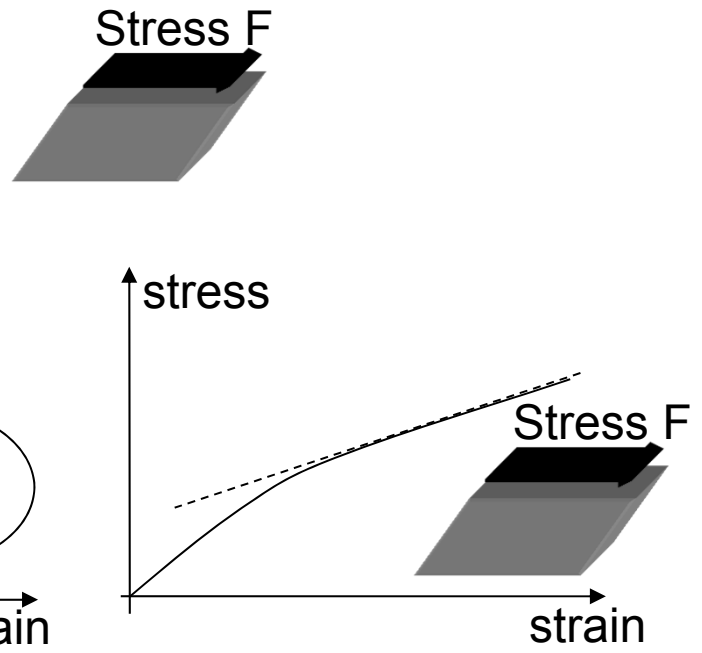
- For slowly increasing stress boundary condition:



Brittle ($\varepsilon > 0$)



Plastic ($\varepsilon = 0$)



Hardening ($\varepsilon < 0$)

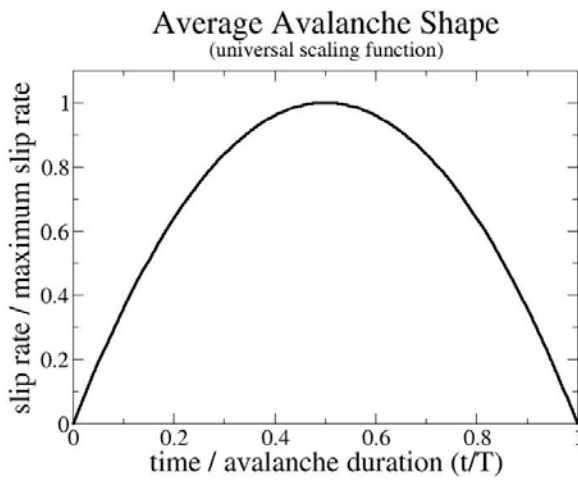
- Avalanche-size distributions (power laws with stress dependent cutoff)
- Power spectra, Scaling functions!
- Scaling behavior agrees with experiments!

- For slow strain-rate boundary condition:

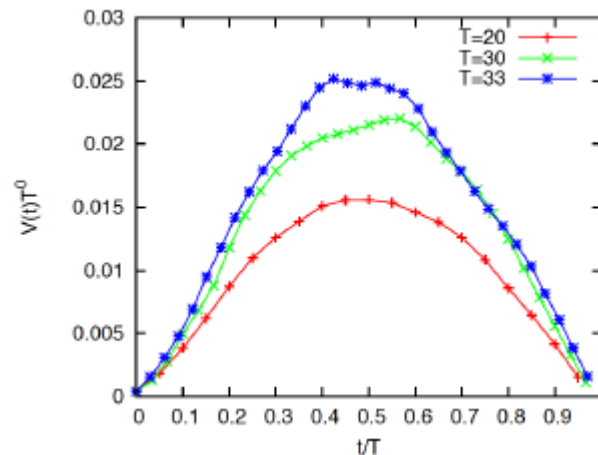
Same scaling behavior and phase diagram as single earthquake fault zone model

Predictions of Simple Analytic Model Agree with Discrete Dislocation-Dynamics Simulations

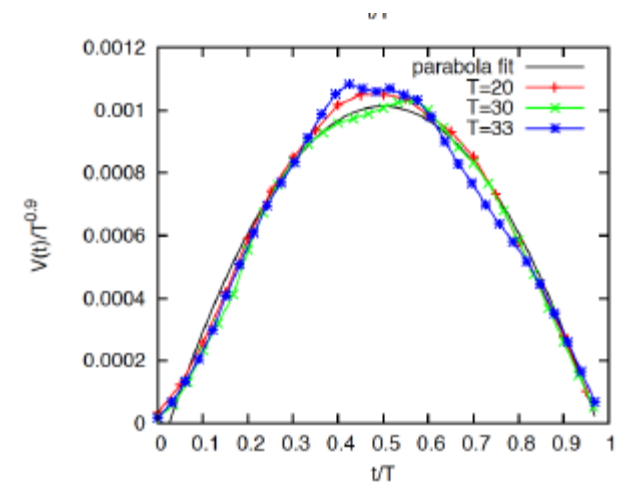
Mean Field Theory
for $\varepsilon = 0$



Simulations: raw data

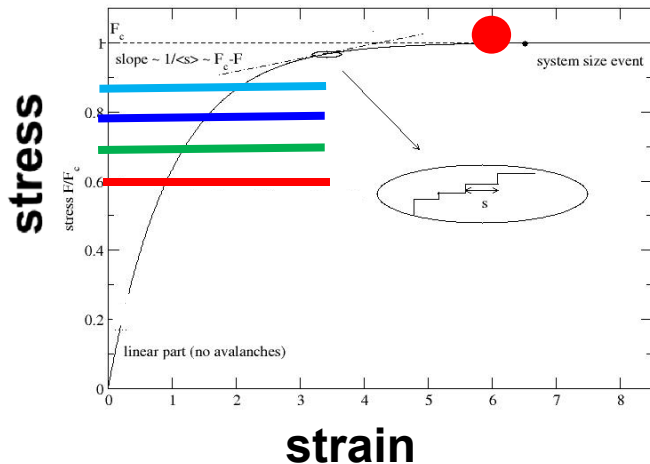


Collapse

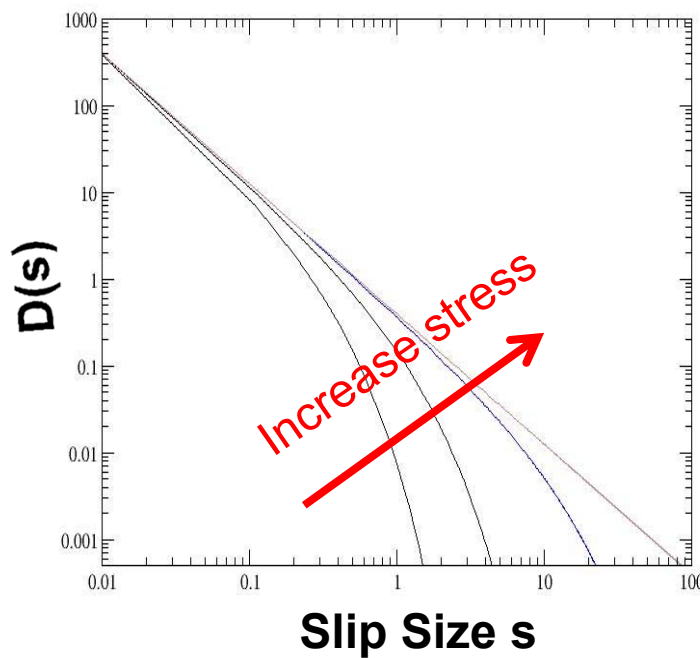


Georgios Tsekenis: Collapse $V(t) \sim T^{1-1/\sigma v z} f(t/T)$

Binning in Stress: Scaling Collapse (PRL 2012)



Mean Field Theory (MFT)

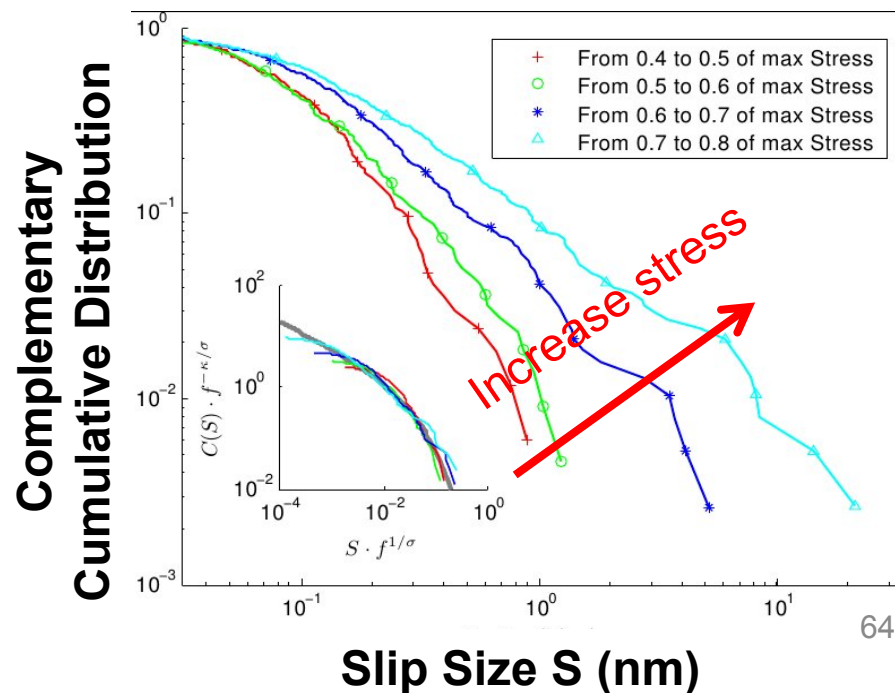


MFT Prediction for EXPONENTS
and scaling FUNCTION agree with
Experiments:

$$D(S) \sim 1/s^\kappa D(s (F - F_c)^{1/\sigma})$$

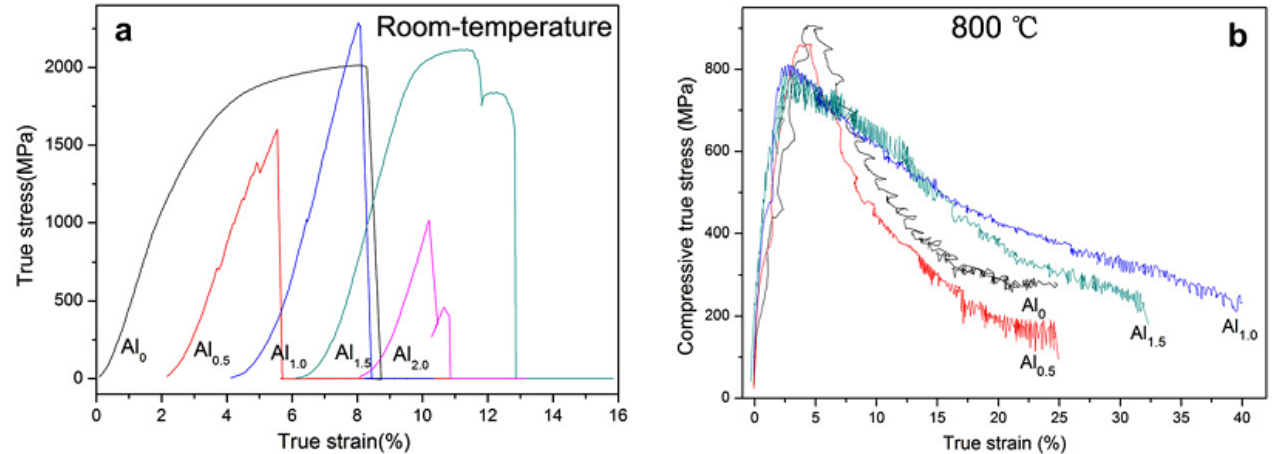
✓ with $\kappa = 1.5$ and $\sigma = 2$

Experiments on nanopillars

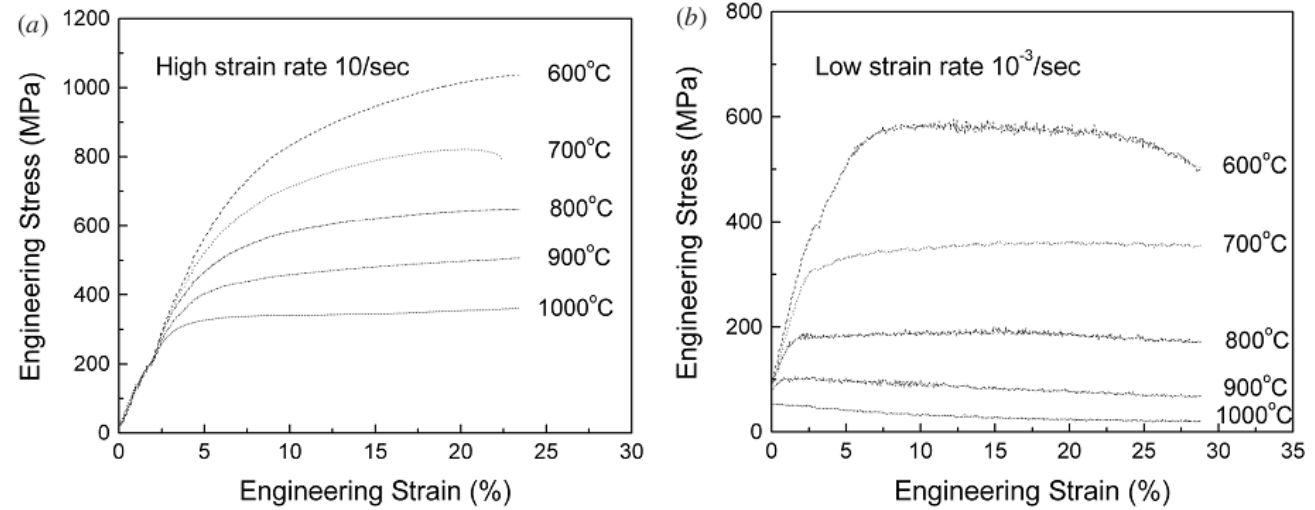


Serration in HEAs

$\text{Al}_x\text{CoCrFeNiTi}$



$\text{Al}_{0.5}\text{CoCrCuFeNi}$



K. Zhang and Z. Fu, *Intermetallics*, 2012, 28, pp. 34-39.

C. J. Tong, M. R. Chen, J. W. Yeh, S. J. Lin, S. K. Chen, T. T. Shun, and S. Y. Chang, *Metallurgical and Materials Transactions A*, 2005, 36(5), pp. 1263-1271.

Serration behavior of materials

Serration behavior: Inhomogeneous deformation in certain temperature and strain rate regimes appears in materials, e.g., Al-Li single crystal, Co₃Ti alloys (L12 ordered), Al-2Mg polycrystal, Mo-27 at.% Re alloy (disordered)

Mechanisms:

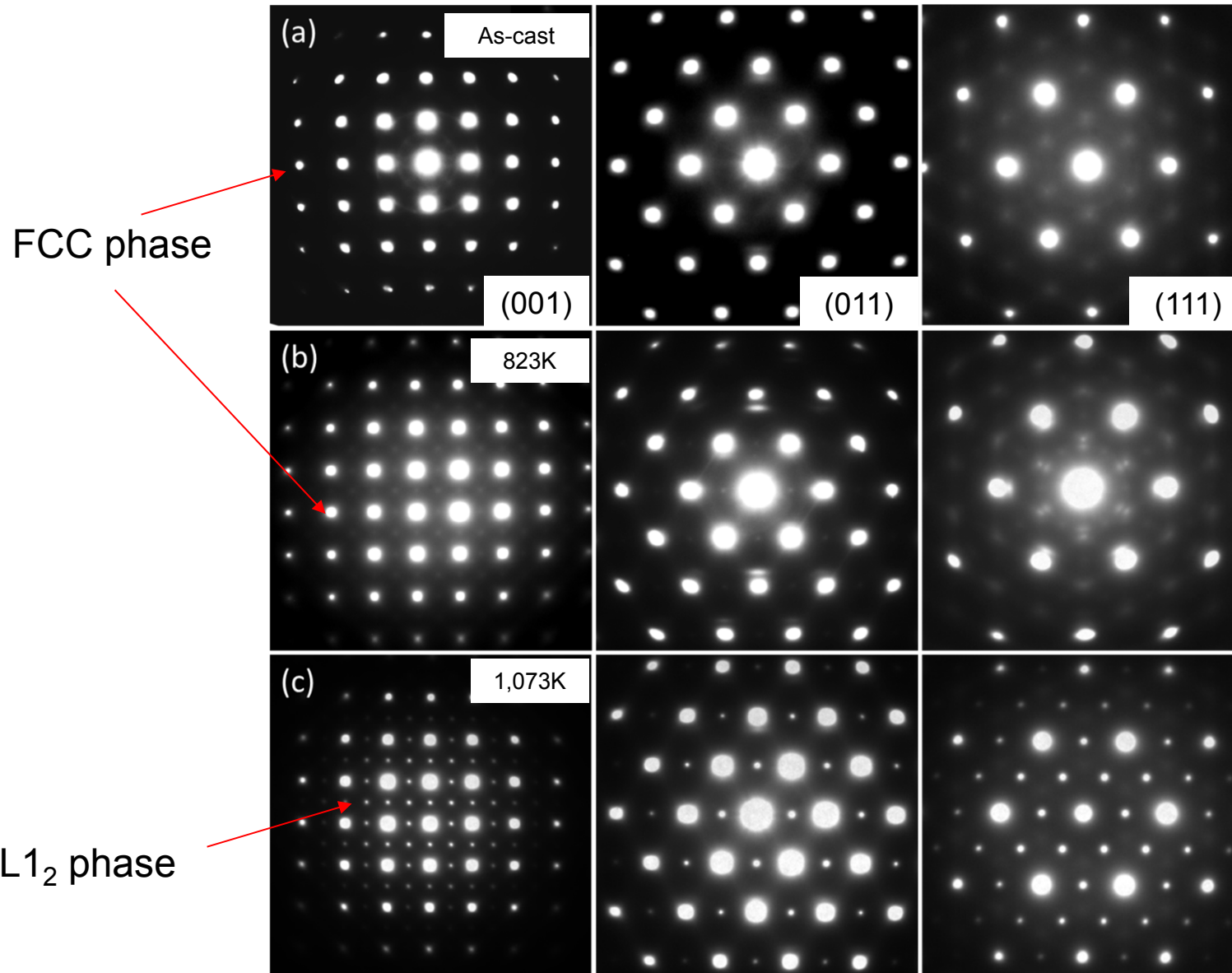
Strain induced martensitic transformation: MP35N alloy (multiphase cobalt alloy: 35 wt. Co, 35% wt. Ni, 20% wt. Cr, and 10% wt. Mo)

Deformation twinning: Mg–5Li–3Al–1.5Zn–2Re alloy

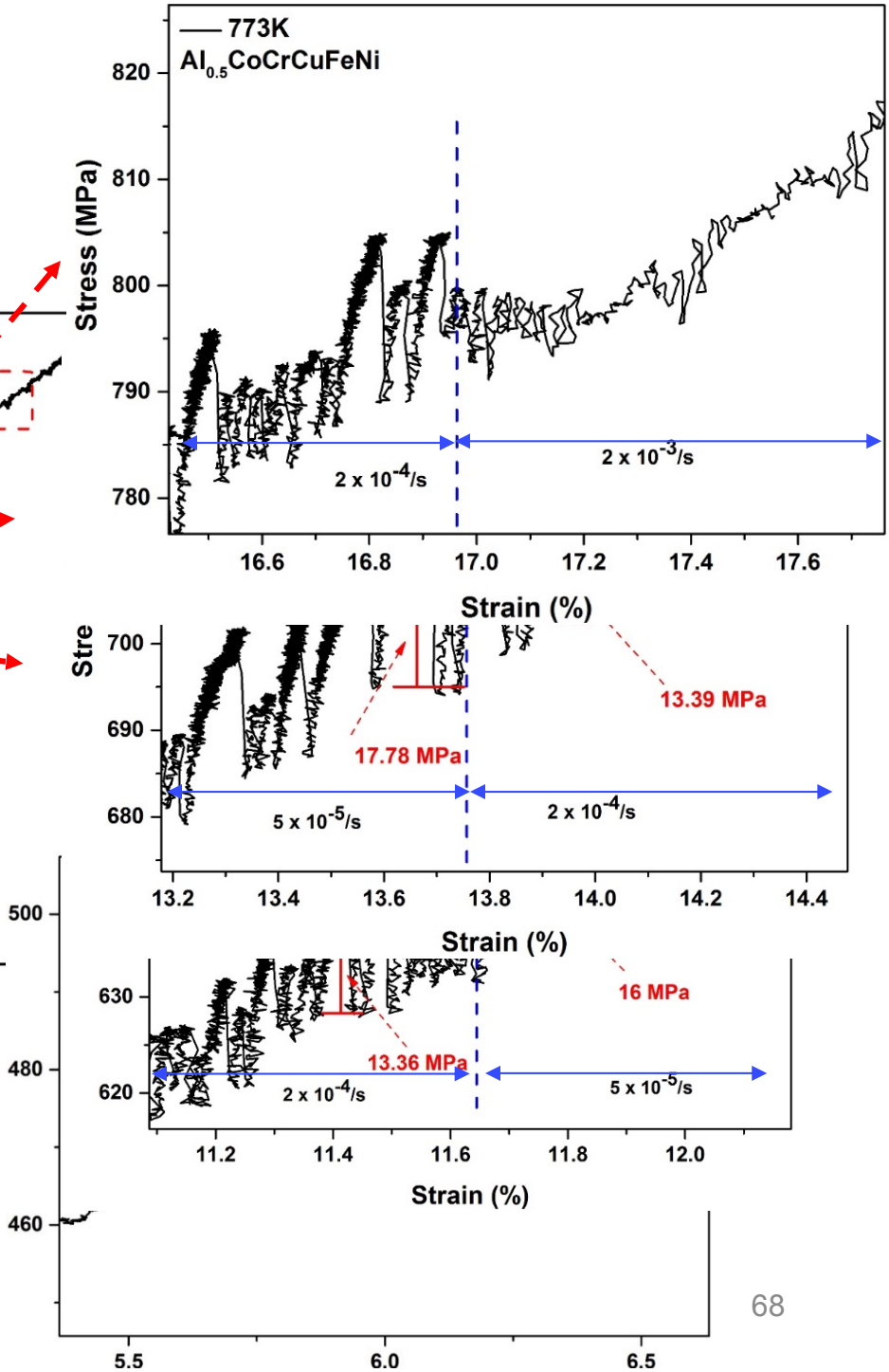
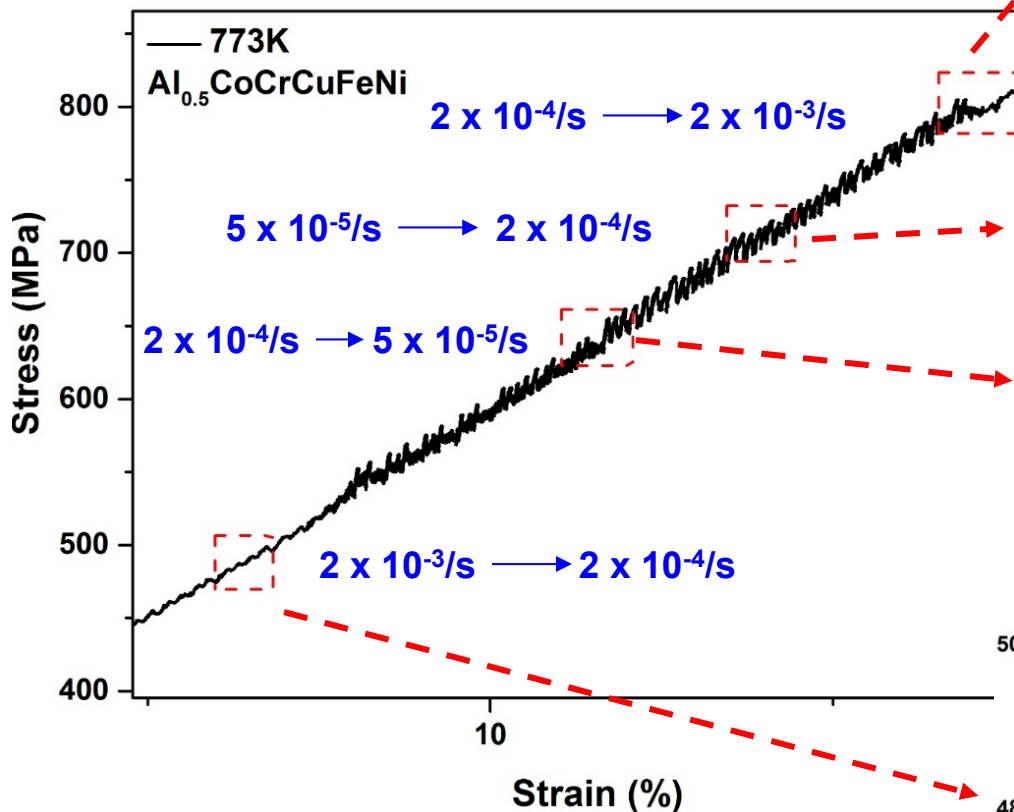
Portevin–Le Chatelier effect (PLC) of Solute-dislocation or dislocation-dislocation interaction: Very common in materials, like Al- and Ni-based alloys

1. B.H. Tian, Y.G. Zhang, C.Q. Chen, *Materials Science and Engineering A* 247 (1998) 263–269.
2. T. Takasugi, H. Honjo, Y. Kaneno, H. Inoue, *Acta Materialia* 50 (2002) 847–855.
3. K. Chihab, C. Fressengeas, *Materials Science and Engineering A* 356 (2003) 102-107.
4. X.J. Yu, K.S. Kumar, *Int. Journal of Refractory Metals and Hard Materials* 41 (2013) 329–338.
5. Reza Sharghi-Moshtaghin, Soroush Asgari, *Materials Science and Engineering A* 486 (2008) 376–380.
6. Rishi Pal Singh and Roger D. Doherty, *Metallurgical Transactions A* 23A (1992) 321-334.
7. T.Q. Li, Y.B. Liu, Z.Y. Cao, R.Z. Wu, M.L. Zhang, L.R. Cheng, D.M. Jiang, *Journal of Alloys and Compounds* 509 (2011) 7607–7610.
8. James Antonaglia, Xie Xie, Gregory Schwarz, Matthew Wraith, Junwei Qiao, Yong Zhang, Peter K. Liaw, Jonathan T. Uhl & Karin A. Dahmen, *Scientific Report*, 2014, 4, pp. 4382.

TEM results after compression tests at room temperature, 823K, and 1,073K with strain rate of $5 \times 10^{-5}/\text{s}$



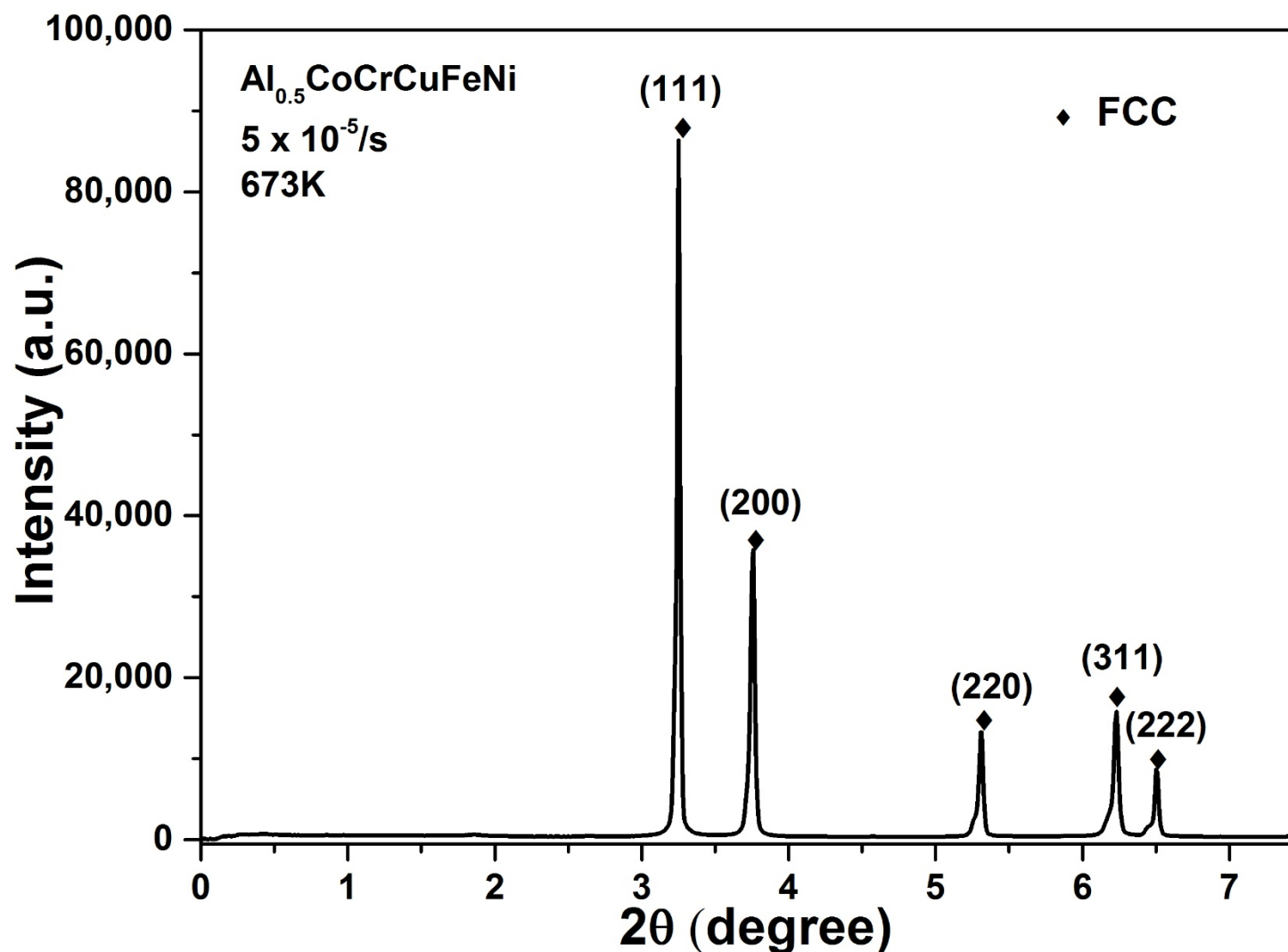
Changing strain rates during compression tests



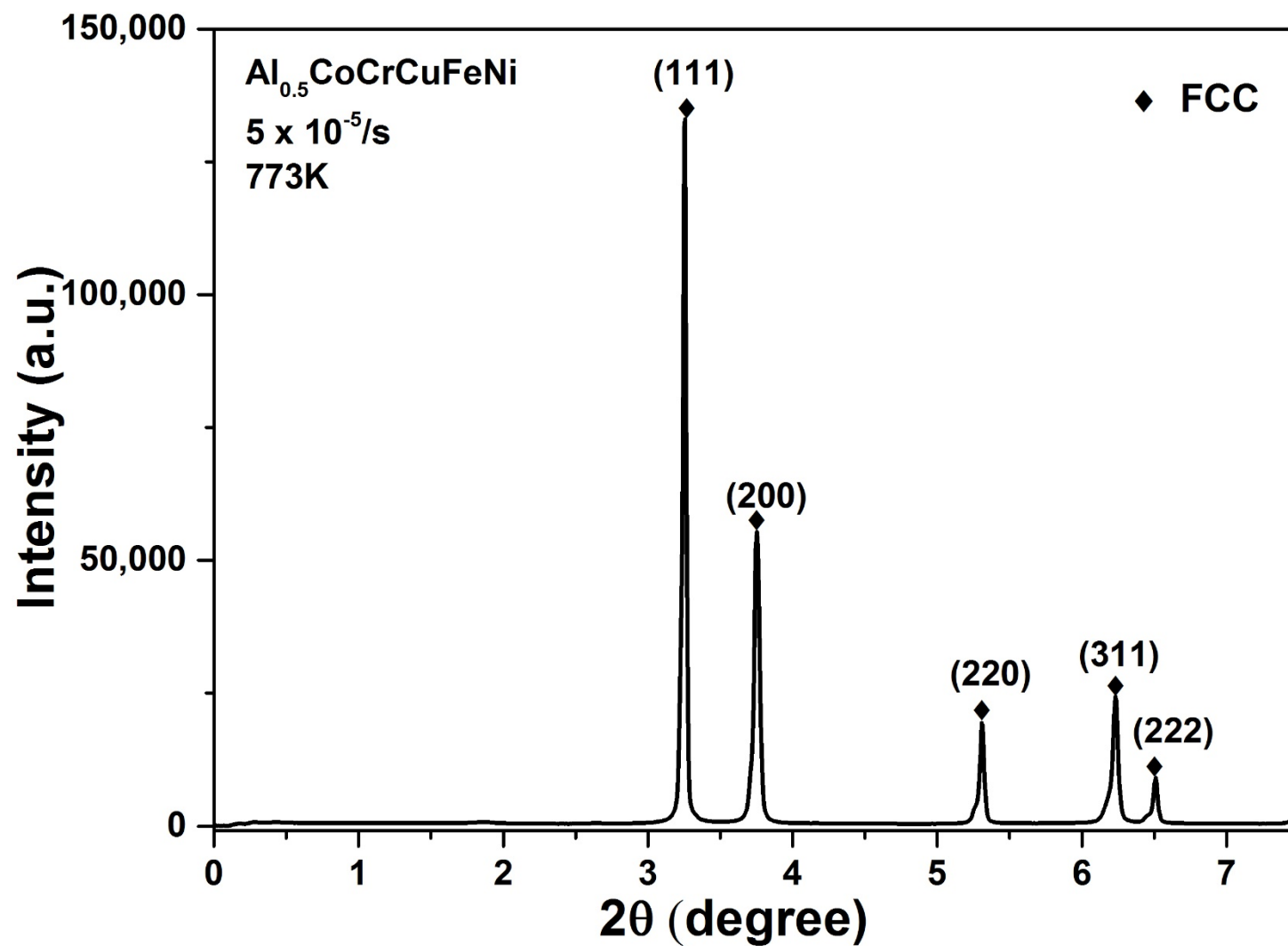
Characterization of Phases

Synchrotron diffraction results

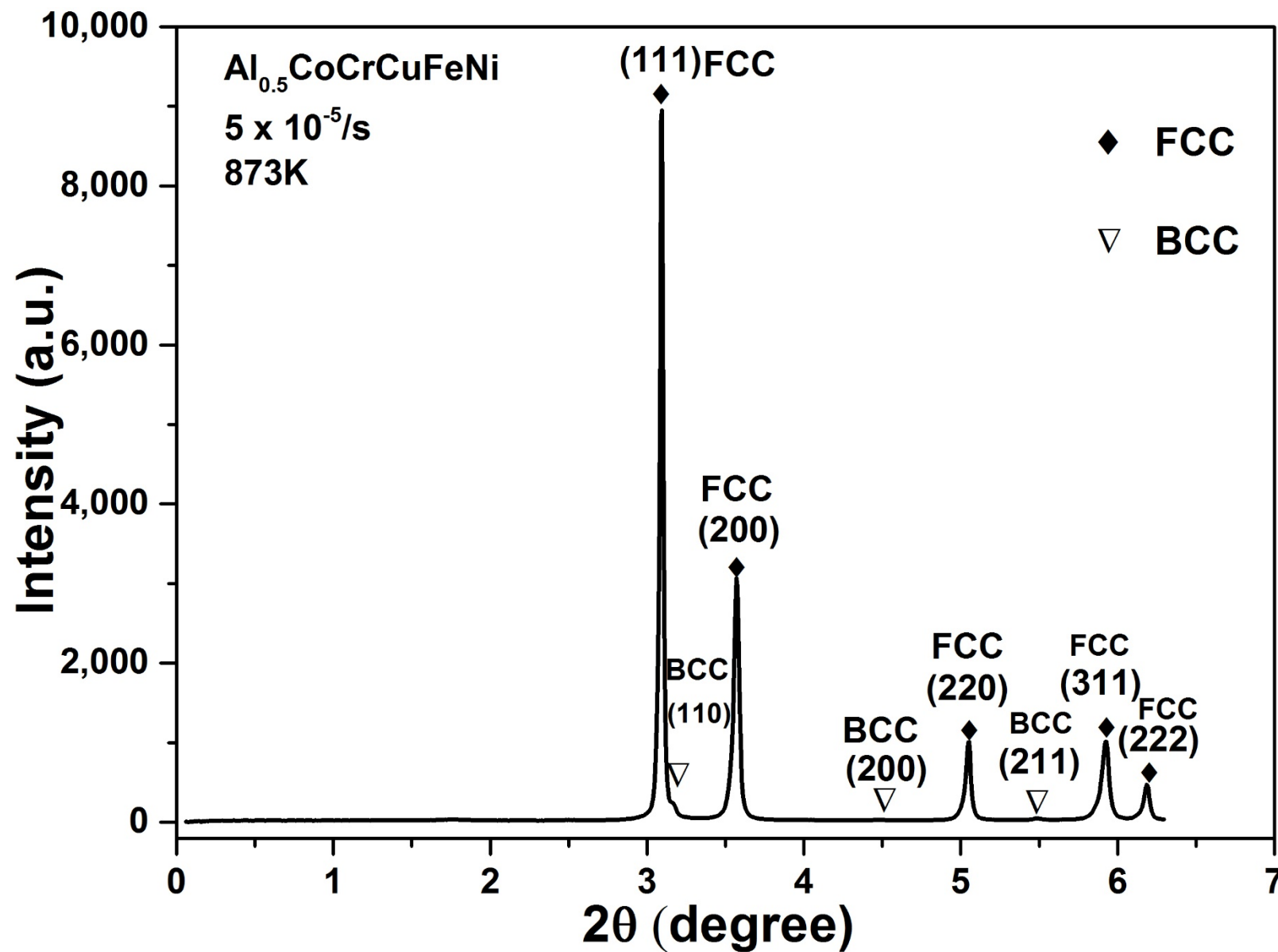
Diffraction pattern at strain rate of $5 \times 10^{-5}/\text{s}$ with temperature of 673K



Diffraction pattern at strain rate of $5 \times 10^{-5}/\text{s}$ with temperature of 773K

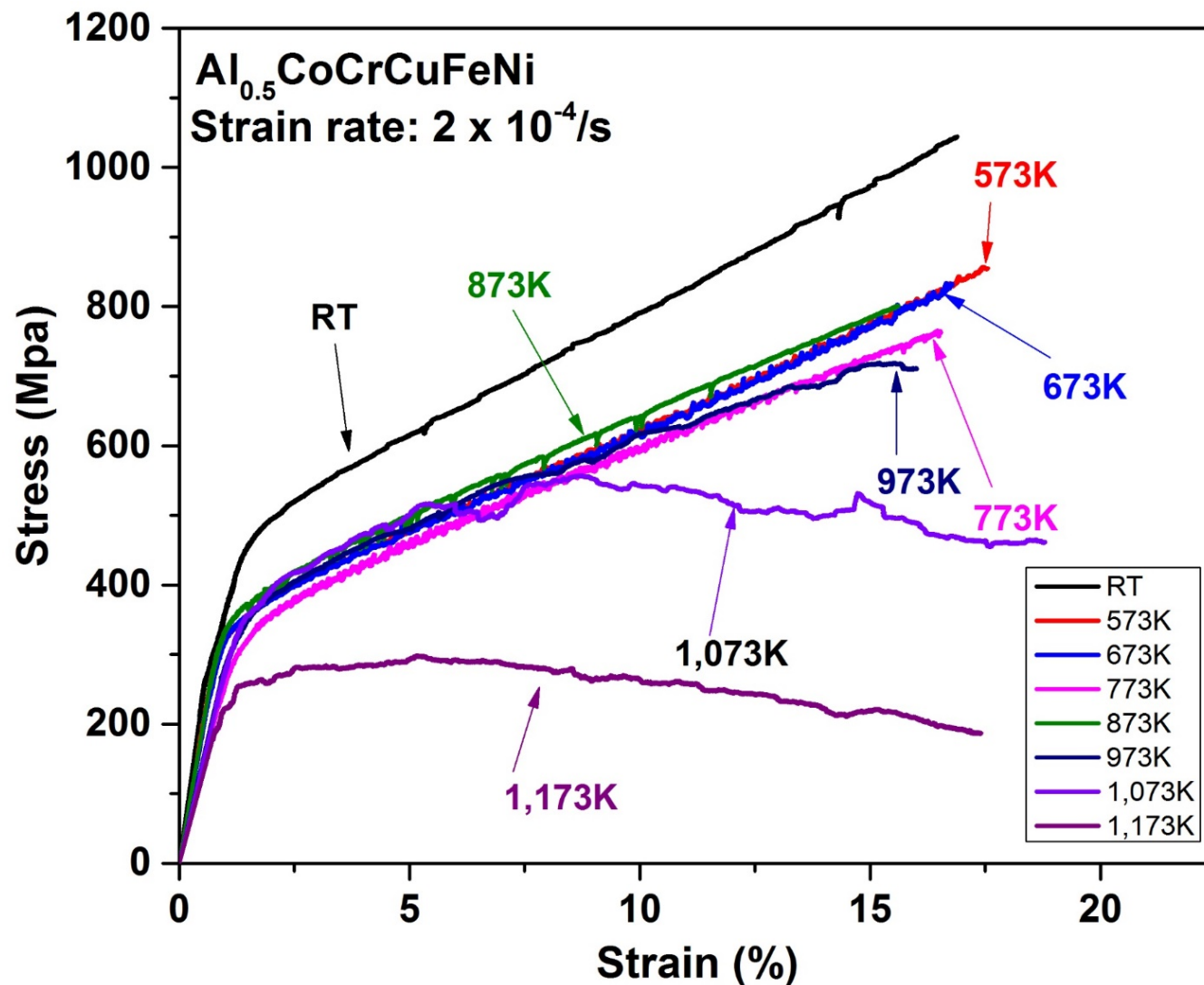


Diffraction pattern at strain rate of $5 \times 10^{-5}/\text{s}$ with temperature of 873K

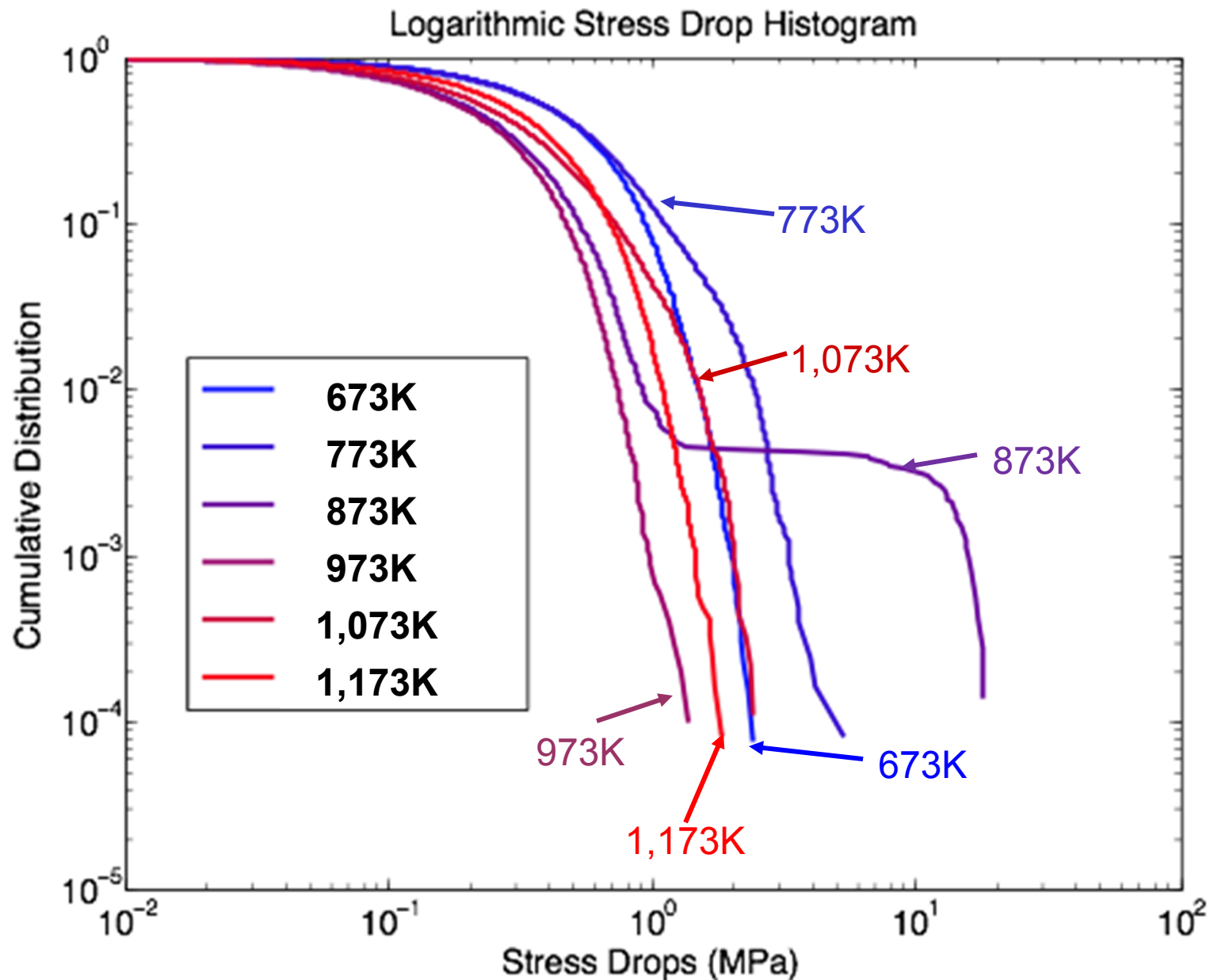


Characterization of Serration Behavior

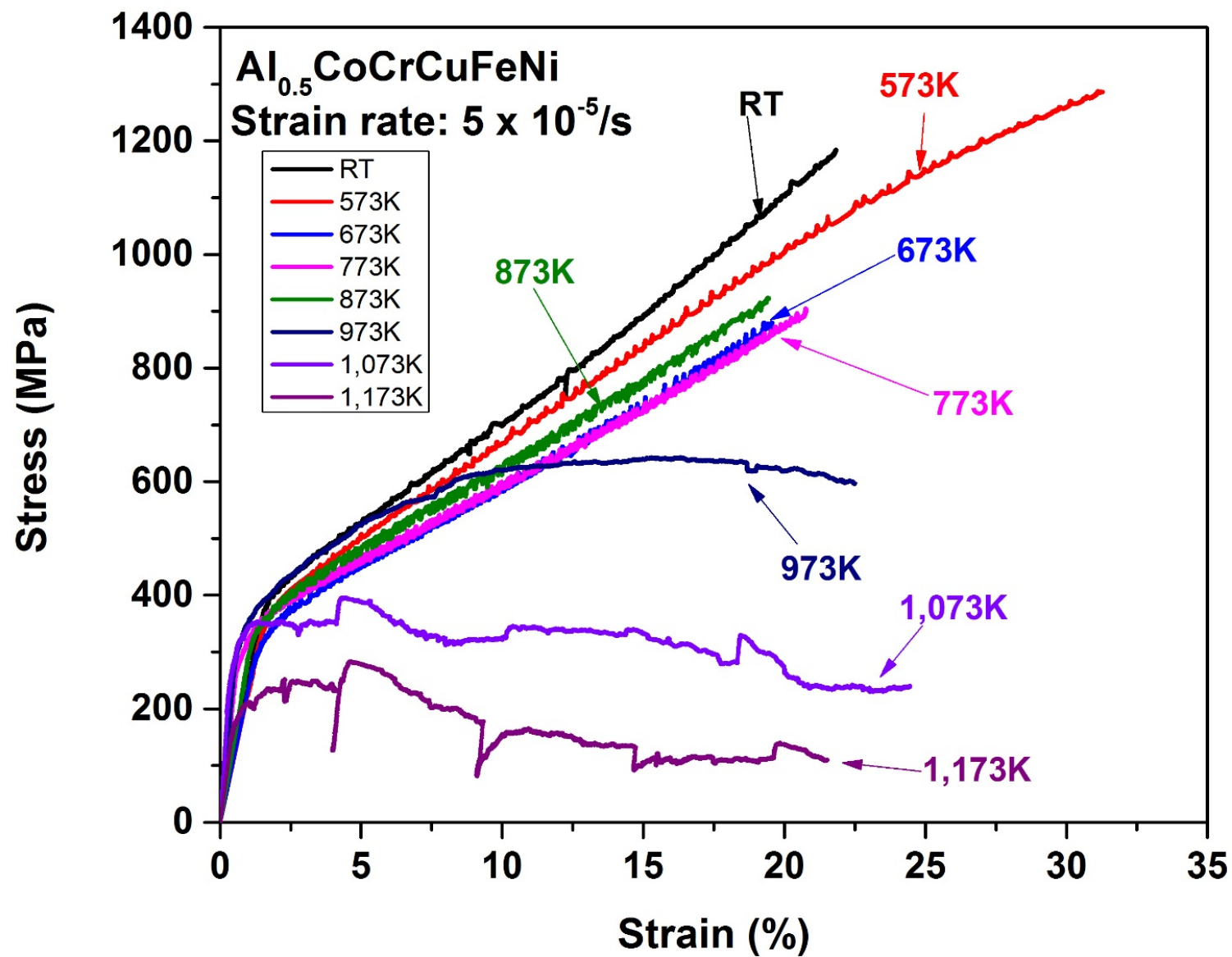
Stress-strain curve at strain rate of $2 \times 10^{-4}/\text{s}$



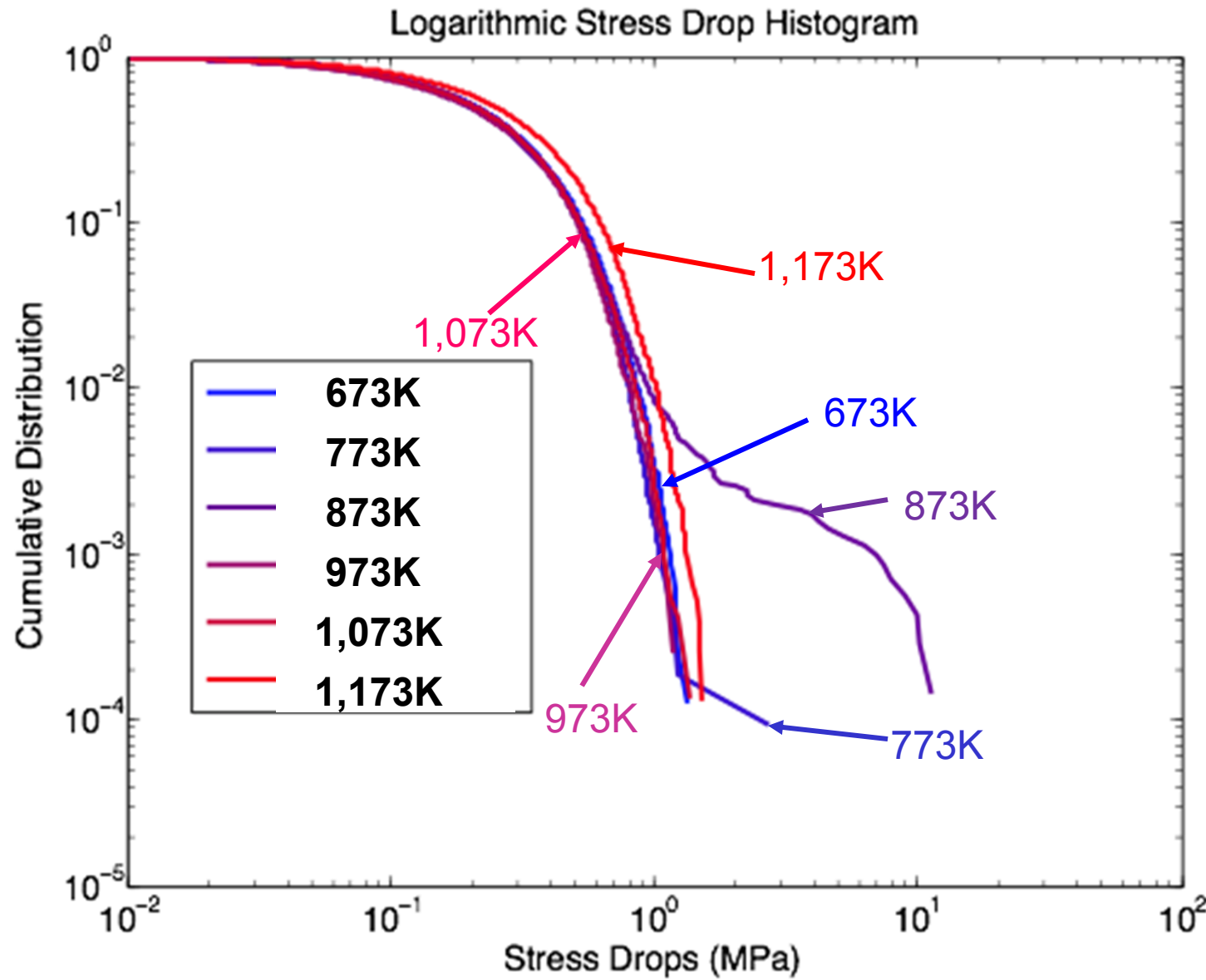
$2 \times 10^{-4}/\text{s}$



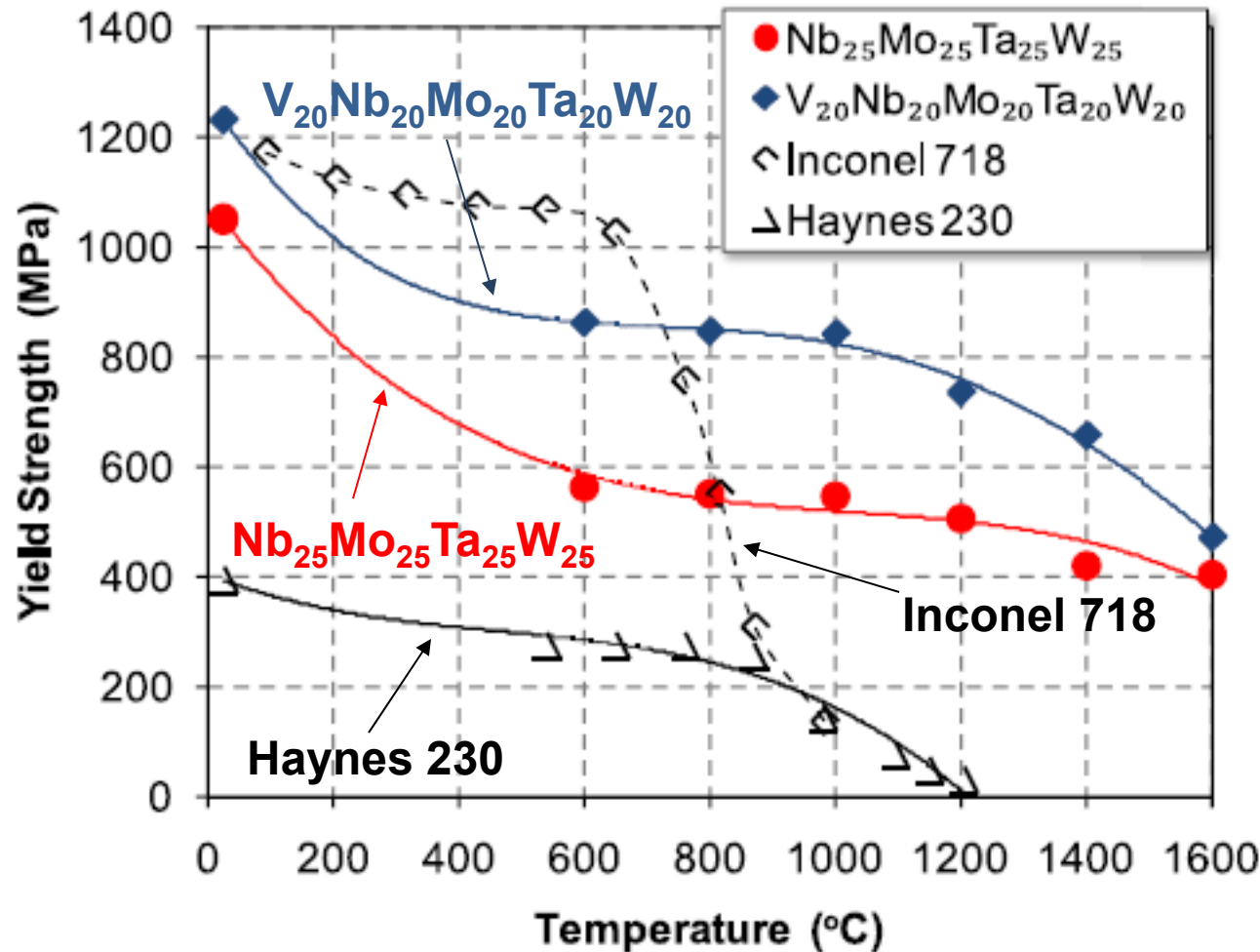
Stress-strain curve at strain rate of $5 \times 10^{-5}/\text{s}$



$5 \times 10^{-5}/\text{s}$



Refractory HEAs

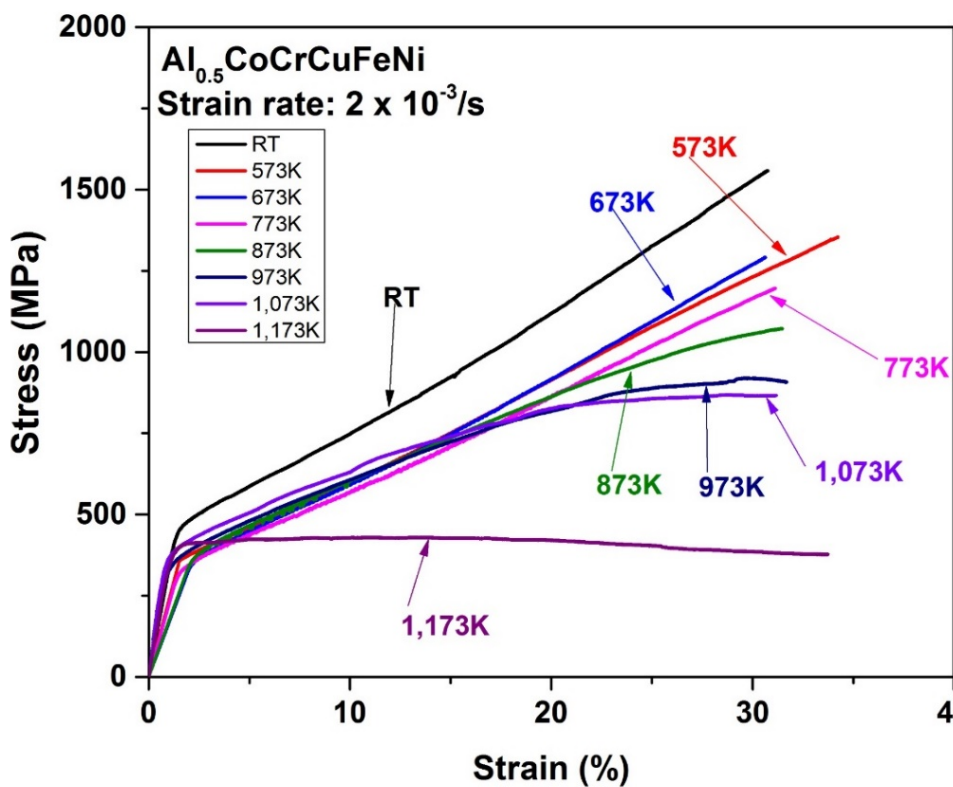


The temperature dependence of the yield stress of $\text{Nb}_{25}\text{Mo}_{25}\text{Ta}_{25}\text{W}_{25}$ and $\text{V}_{20}\text{Nb}_{20}\text{Mo}_{20}\text{Ta}_{20}\text{W}_{20}$ HEAs and two superalloys, Inconel 718 and Haynes 230

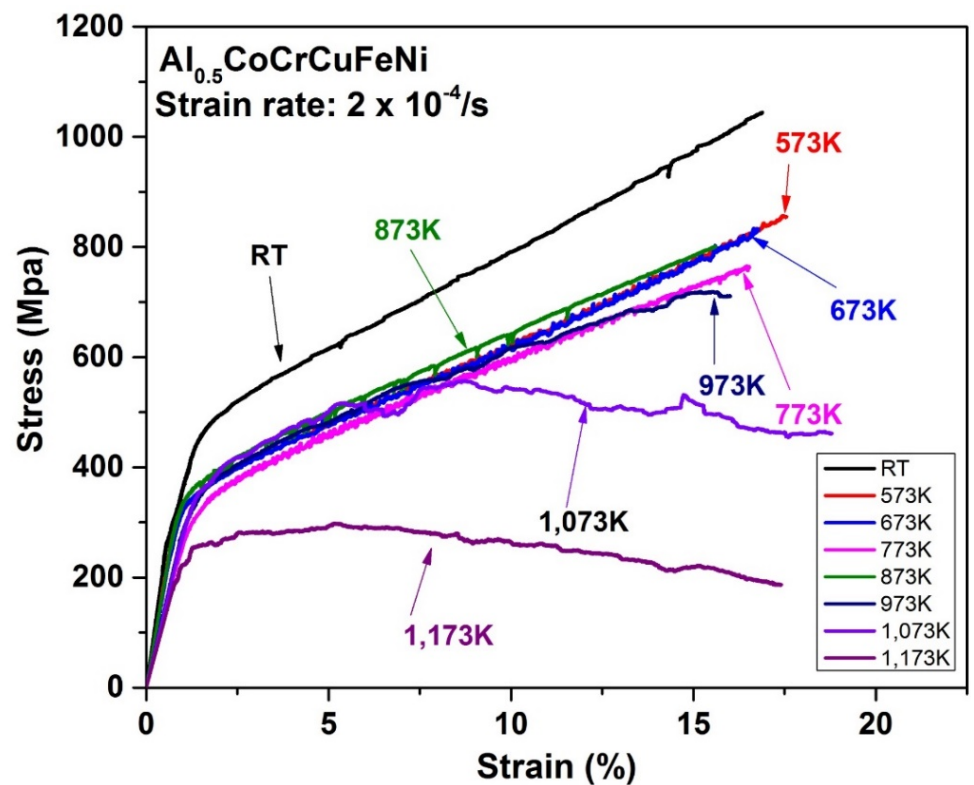
1. O.N. Senkov, G.B. Wilks, J.M. Scott, D.B. Miracle, "Mechanical properties of $\text{Nb}_{25}\text{Mo}_{25}\text{Ta}_{25}\text{W}_{25}$ and $\text{V}_{20}\text{Nb}_{20}\text{Mo}_{20}\text{Ta}_{20}\text{W}_{20}$ refractory high entropy alloys", *Intermetallics*, 2011, 19, pp. 9, p. 698.

Compression results and discussion

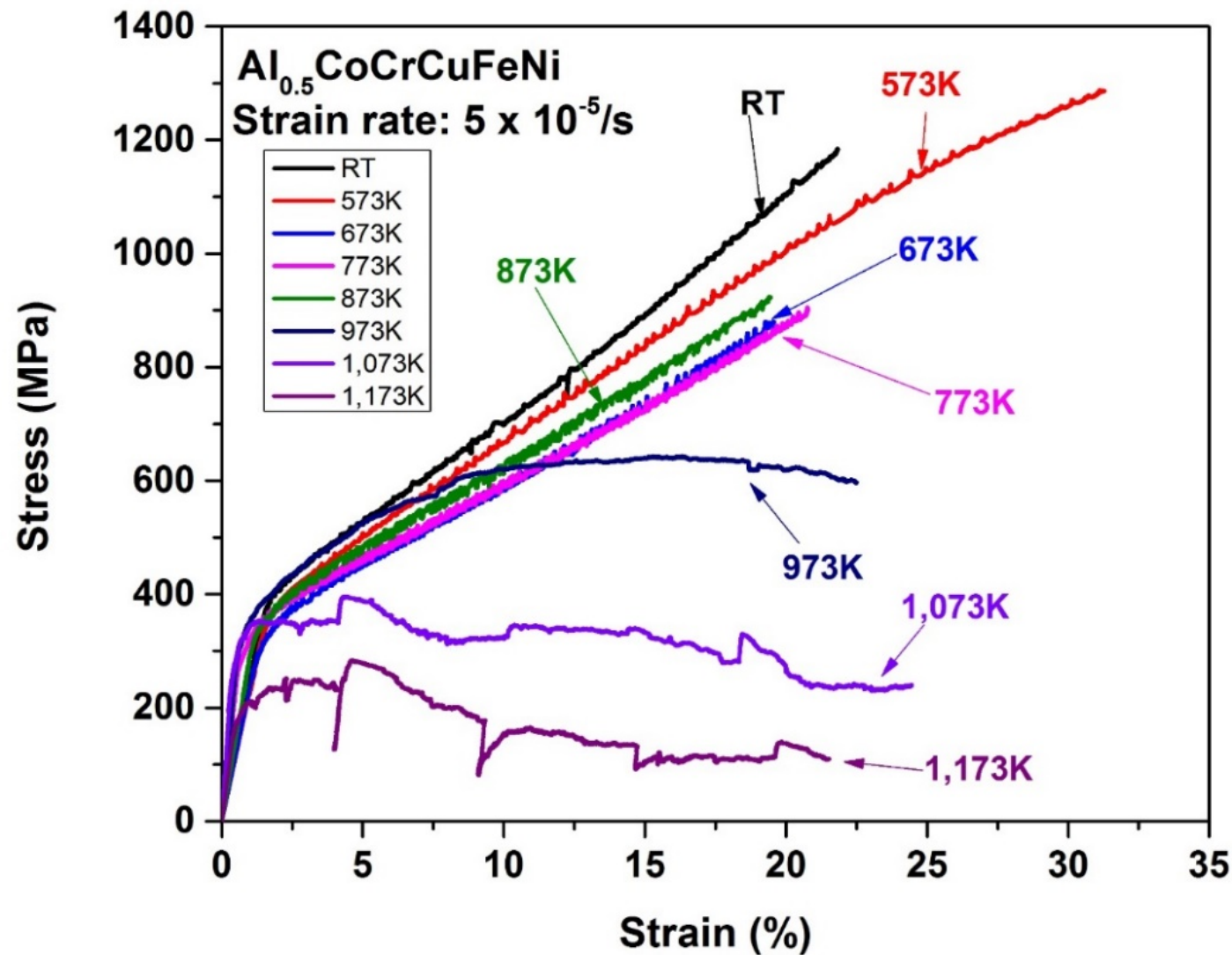
Strain rate: $2 \times 10^{-3}/\text{s}$



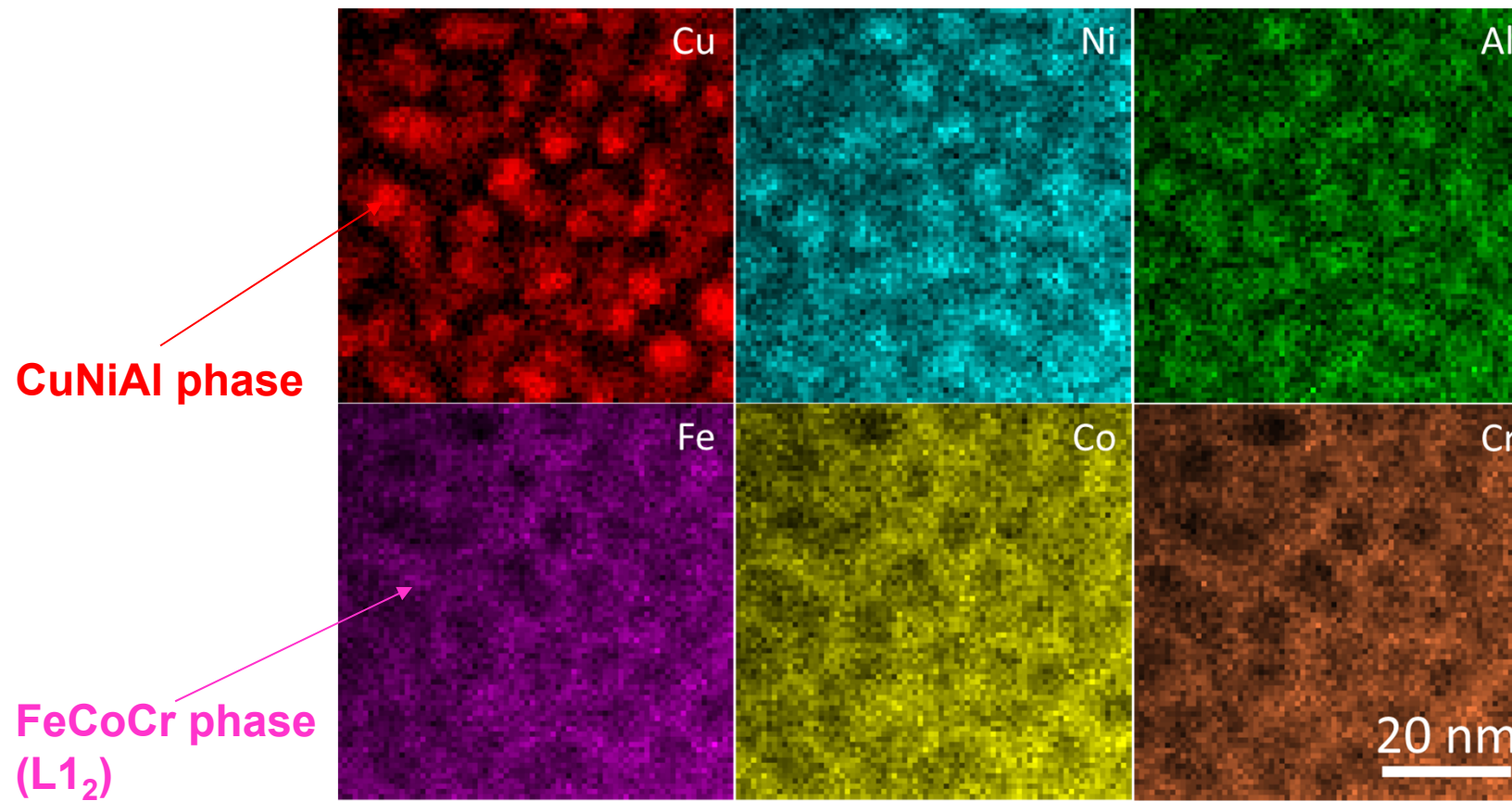
$2 \times 10^{-4}/\text{s}$



Strain rate: $5 \times 10^{-5}/\text{s}$

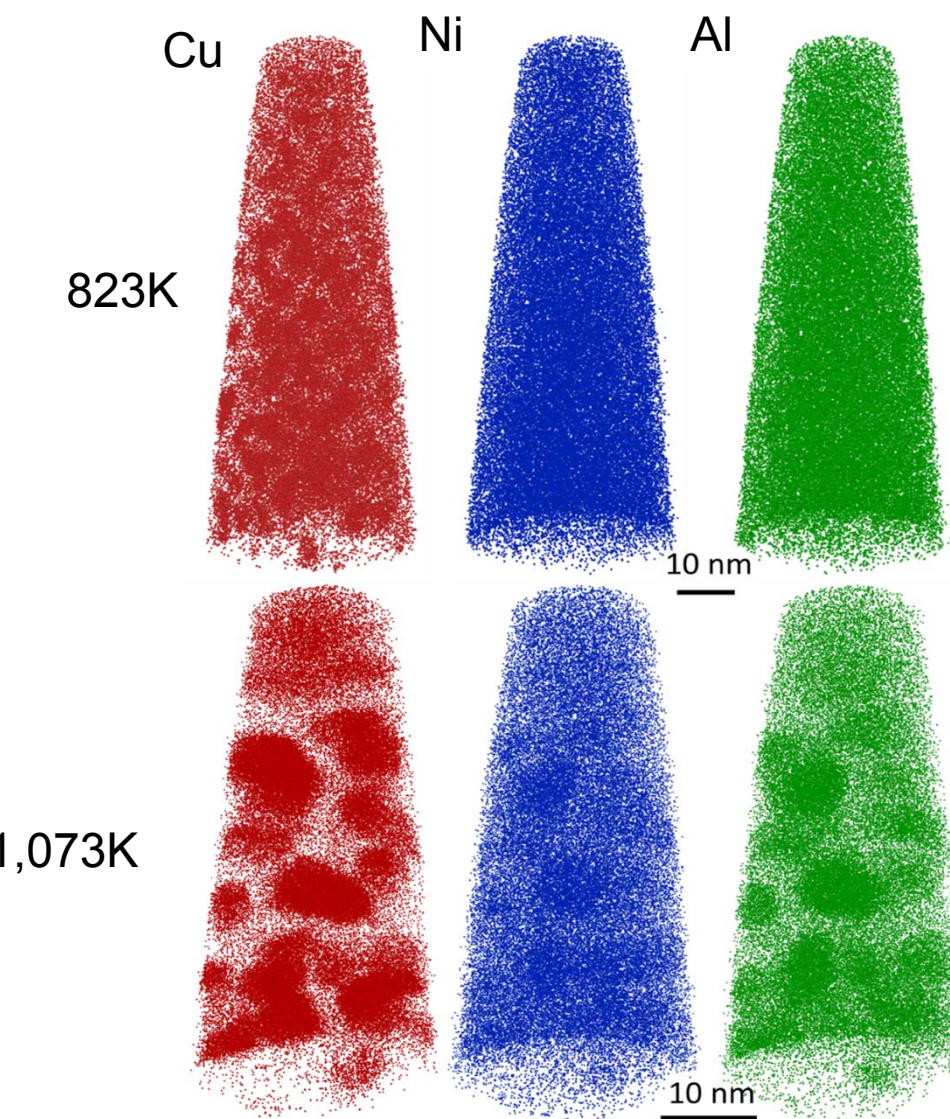


Energy dispersive spectroscopy (EDS) mapping of each elements



Scanning transmission electron microscopy energy-dispersive X-ray spectroscopy (STEM-EDS) mapping of the matrix phase in the sample compressed at 1,073K with strain rate of $5 \times 10^{-5}/\text{s}$

Reconstructed three-dimensional (3D) atom probe tomography (APT) after compression tests at the strain rate of $5 \times 10^{-5}/\text{s}$ with temperatures of 823K, and 1,073K



3D APT chemical mappings of the tested sample at 823K and 1,073K. The decomposition of the solid-solution phase into a NiAl phase can be seen with increasing annealing temperature.